Urban flood analyses in sloping areas with 3Di modelling

A case study of Banholt and Mheer, the Netherlands

Master's thesis

By
Margot Leicher

6 March 2016

Urban flood analyses in sloping areas with 3Di modelling

A case study of Banholt and Mheer, the Netherlands

This thesis is carried out in partial fulfilment of the requirements for the degree Master of Science in Water Science and Management at Utrecht University, faculty of Geosciences.

Cover Figure: aerial flood map of the Dalestraat, Banholt.

Author:
A.M. Leicher margotleicher@gmail.com

Supervisors:
Prof. dr. ir. M.F.P. Bierkens Utrecht University
Ir. M.A. Hoff Nelen & Schuurmans

Date: 6 March 2016

Utrecht University

Nelen & Schuurmans

Acknowledgements

This thesis is the result of my graduation research for the Master Water Science and Management at Utrecht University, faculty of Geosciences, and with that also the final product of my graduation internship at Nelen & Schuurmans. I cannot describe how much I have learnt during the past months. For that I am thankful to all the employees of Nelen & Schuurmans. In special I thank Alexander Hoff for his supervision, constructive feedback and for giving me the opportunity to be part of the project team for the pilot project Banholt - Mheer. Also, I thank Lizzy Meijer for helping me with the development of the 3Di model and all the coffee breaks.

Furthermore, I would like to thank the Municipality of Eijsden-Margraten and the Roer & Overmaas Water Authority. In special Dennis Spronk (Municipality Eijsden-Margraten), Marc Strookman (Roer & Overmaas Water Authority) and Helena Pavelková (Roer & Overmaas Water Authority) for sharing their knowledge of the research area and their feedback on the model performance.

I am also thankful to Marc Bierkens, my university supervisor, for his valuable feedback on my research proposal and the content of this thesis.

And of course, a special thanks to my family and friends for their support and endless believe in me. I would like to dedicate this work to my father, who unfortunately passed away just before I started with this research. Because I know that he would have loved the subject, but most of all because he taught me to be passionate about work and life.

Margot Leicher
Amsterdam, February 2016

‘‘. . . essentially, all models are wrong, but some are useful.’’ - George E. P. Box

Summary

During extreme rainfall the limited storage and discharge capacity of sewer systems can result in temporary accumulation of water on street level. The acceptance of this temporary accumulation is decreasing, while public and political concern about urban flooding is increasing (van Luijtelaar et al. 2008; RIONED Foundation 2013).

The purpose of this research is to evaluate the suitability of 3Di modelling for urban pluvial flood analyses in sloping areas. To this end a case study is performed in the villages of Banholt and Mheer in the south of Limburg. In the research area, a large part of the rain falling during extreme rainfall events becomes surface runoff. Still, interception and infiltration are hydrological processes that should be included during urban flood analyses. Also, from the model results it can be concluded that the magnitude of flooding has a strong relationship with rainfall intensity.

The analysis, conducted with a hydrodynamic 3Di flood model, provides insight in the flood prone locations, and the magnitude and causes of flooding at these locations. Added value of 3Di can be found in the possibility to include both 1D sewer flow and 2D surface flow simultaneously. Inclusion of both systems, and their interaction, is of added value because most flood locations in the research area appeared to be flood prone due to a contribution of both systems.

The subgrid method of 3Di makes it possible to include the whole contributing catchments in the model without too much loss of calculation speed. Including these whole catchments showed that rural runoff and open channel flow contribute to flooding in the research area, and is therefore of added value in the urban flood analysis. Also, with the subgrid method 3Di can account for various functional land use types at a small spatial scale. This way, 3Di can account for spatial variation within a research area.

After model simulation flood maps can be plotted of each desired time step during model simulation. These flood maps are of high-resolution because of the high spatial resolution 3Di can cope with, which is of added value for the urban drainage managers. Also, from these maps the largest contributing overland flow pathways can be derived. Insight in these pathways is required to assess the causes of flooding.

3Di modelling contributes to analysing the causes of pluvial flooding by its accurate two-dimensional surface runoff routing, and the interaction between 1D sewer flow and 2D surface flow. However, with the current model performance the volume and speed of rural surface runoff are significantly overestimated. To improve the contribution of the current 3Di model for the urban flood analysis in the area, model calibration and validation is recommended.

Based on the lessons learned during this research, recommendations for future improvements of the 3Di model Banholt-Mheer and the 3Di modelling toolbox in general are given. Improvement of the 3Di model for Banholt and Mheer is related to calibration and validation of the model. To improve the performance of the 3Di modelling toolbox in sloping areas, future research should focus on the consequences of the subgrid technique in sloping areas compared to flat ones.

Key words: Urban flood analysis; 3Di modelling; 1D-2D dual drainage model; sloping areas; extreme rainfall.

Table of Content

Acknowledgements i
Summary iii
List of Figures vii
List of Tables ix
1. Introduction 11
1.1 Background 11
1.2 Problem definition 11
1.3 Research aim and research questions 12
1.4 Relevance of the research 12
1.5 Thesis outline 13
2. Theoretical background 14
2.1 Urban catchment hydrology 14
2.2 Urban flood modelling 17
3. Methodology 22
3.1 Model development 23
3.2 Model validation 25
3.3 Rainfall scenario development 25
3.4 Urban flood analysis 26
4. Results 27
4.1 Model validation 27
4.2 Scenario analysis 27
4.3 Urban flood analysis 28
5. Discussion 46
5.1 Model performance and assumptions 46
5.2 Model calibration and validation 48
5.3 Research scope and limitations 48
6. Conclusion & recommendations 50
6.1 Conclusion 50
6.2 Recommendations 51
References 52
Appendices 55
A. Site description 55
B. Subgrid layers 59
B.1 DEM layer 59
B.2 Friction layer 59

B.3 Infiltration layer 62
B.4 Interception layer 62
C. 1D elements 64
C.1 Sewer system 64
C.2 Surface water structures 64
C.3 Boundary pumps 65
D. Calculation grid 67
E. Model validation 69
E.1 Rainfall scenario 69
E.2 Model results, observations and expert judgement 69
F. Extreme rainfall scenarios 80
F.1 Rainfall scenario 1 80
F.2 Rainfall scenario 2 80

List of Figures

Figure 2-1: Stages of sewer surcharge (Schmitt et al. 2004). 15
Figure 2-2: Flooding due to a pressure height that exceeds the surface level (van Luijtelaar 2014). 16
Figure 2-3: Schematization of urban drainage physics (Chang et al. 2015). 16
Figure 2-4: A cross-section can either increase or decrease with increasing depth (Nelen & Schuurmans 2016). 18
Figure 2-5: A DEM layer (grey pixels) and a quadtree calculation grid (blue layer) (van 't Veld 2015). 19
Figure 2-6: (a) A cross-section of one calculation cell with DEM pixels. (b) The V-h relationship derived initial to model simulation. 20
Figure 2-7: (a) The domains used to calculate the velocity between two calculation cells with a different resolution; (b) the pressure gradient stencil for different resolution calculation cells for the calculation of water levels (Stelling 2012). 20
Figure 2-8: The three types of flow interaction possible between the 1D and 2D components of the model. 21
Figure 3-1: The conceptual model of the research set up shows that the theoretical background is input for the case study, which provides input for the discussion, conclusion and recommendations. 22
Figure 3-2: Topographic location of the research area in the Netherlands. 22
Figure 3-3: DEM subgrid layer of the research area. 23
Figure 3-4: Total urban drainage system of Banholt and Mheer, including the contributing catchments of the Banholtergrub (above) and Horstergrub (below) streams. 24
Figure 3-5: Temporal distribution of rainfall scenario 1 with 56.8 mm of total rain fallen in 1 hour 25
Figure 3-6: Temporal distribution of rainfall scenario 2 with 100 mm of total rain fallen in 2 hours. 26
Figure 4-1: The urban locations where flooding emerged during simulation of rainfall scenario 1 and 2. 28
Figure 4-2: Urban drainage system around the Dorpsstraat flood location in Mheer. 29
Figure 4-3: Flood map of the Dorpsstraat after 1 hour of model simulation during rainfall scenario 1. 30
Figure 4-4: Flood map of the Dorpsstraat after 2 hours of model simulation during rainfall scenario 2. 30
Figure 4-5: The DEM shows the vulnerable location of the Dorpsstraat in the valley of the Horstergrub stream. . 31
Figure 4-6: Surface flow pathways show the three areas that contribute to flooding at the Dorpsstraat. 32
Figure 4-7: Storm water sewer discharge from the Duivenstraat to the Dorpsstraat during scenario 1. 32
Figure 4-8: Storm water sewer discharge from the Noorbeekerweg to the Dorpsstraat during scenario 1. 33
Figure 4-9: Urban drainage system around the Steegstraat flood location in Mheer. 33
Figure 4-10: Flood map at the Steegstraat after 45 minutes of model simulation during rainfall scenario 1. 34
Figure 4-11: Flood map at the Steegstraat after 2 hours of model simulation during rainfall scenario 2. 35
Figure 4-12: DEM of the gently sloping Steegstraat parallel to the Horstergrub stream. 35
Figure 4-13: Overland flow pathways from the Steegstraat (orange circle) and upslope rural area (red circle). ... 36
Figure 4-14: Flow pathways indicate the area that contributes rural runoff to the Steegstraat flood location. 37
Figure 4-15: Urban drainage system around the Dalestraat in Banholt. 37
Figure 4-16: Flood map at the Dalestraat after 45 minutes of model simulation during rainfall scenario 1. 38
Figure 4-17: Flood map at the Dalestraat after 2 hours of model simulation during rainfall scenario 2. 39
Figure 4-18: DEM shows the vulnerable location of the Dalestraat in the valley of the Banholtergrub stream. 39
Figure 4-19: Contributing surface runoff from the Bergstraat (red circle), Banholtergrub stream (pink circle) and Dalestraat/Sint Gerlachusstraat (orange circle). 40
Figure 4-20: Storm sewer discharge from upslope at the Dalestraat to the flood location during scenario 1. 40
Figure 4-21: Storm sewer discharge from upslope at the Dalestraat to the flood location during scenario 2. 41
Figure 4-22: Urban drainage system around the Pastoor Engelenstraat in Banholt. 42
Figure 4-23: Flood map at the Pastoor Engelenstraat after 45 minutes of model simulation during scenario 1. ... 43
Figure 4-24: Flood map at the Pastoor Engelenstraat after 2 hours of model simulation during scenario 2. 43
Figure 4-25: Plot of the DEM shows the local depression at the Pastoor Engelenstraat in Banholt. 44
Figure 4-26: Discharge through the outlet at the Pastoor Engelenstraat during rainfall scenario 1. 44
Figure 4-27: Overland flow pathways that contribute to flooding at the Pastoor Engelenstraat (red circle). 45
Figure 5-1: Water levels in flat and sloping areas with corresponding cross-section depths (Δh). 47
Figure A-1: Land use map of the research area. 55
Figure A-2: Surface water system with the Horstergrub (below) and Banholtergrub stream (above). 56
Figure A-3: Overview of sub-catchments draining to the water storage buffers in the research area. 57
Figure A-4: Photographs show the incorporation of the water storage buffers in the landscape. 57
Figure A-5: A closing valve at a buffer outlet (left) and a culvert incorporated in the landscape (right). 57

Figure A-6: Sewer system of Banholt and Mheer. 58
Figure B-1: The impact of various friction values on the water level rise in storage buffer Terhorst. 60
Figure B-2: Friction subgrid layer. 61
Figure B-3: Infiltration subgrid layer. 62
Figure B-4: Interception layer. 63
Figure C-1: Schematization of a culvert and outlet of a water storage buffer in 3Di. 65
Figure C-2: A buffer outlet (left) is translated into an orifice with a rectangular cross-section. 65
Figure C-3: locations of the downstream boundary conditions used in the 3Di model. 66
Figure D-1: Calculation grid of the entire research area. 67
Figure D-2: Close up of the calculation grid in North-Banholt (left) and at storage buffer 'het Struikgewas' (right). 68
Figure E-1: Temporal rainfall scenario of 18 August 2011, extracted from the Dutch national rainfall radar. 69
Figure E-2: Flood locations that emerged during model simulation of the rainfall event of 18 August 2011. 70
Figure E-3: Map marking the flood location at the Dorpsstraat in Mheer ranging between the two pins. 70
Figure E-4: Photographs of flooding at the crossroad with the Horstergrub stream (left) and at restaurant Taverne de Smidse. 71
Figure E-5: Flood map of the Dorpsstraat flood location after simulation of the rainfall event of 18 August 2011. 71
Figure E-6: Map marking the flood location and photographs of flooding at the Steegstraat in Mheer. 72
Figure E-7: Flood map of the Steegstraat flood location after simulation of the rainfall event of 18 August 2011. 72
Figure E-8: Map marking the flood location at the Dalestraat in Banholt. 73
Figure E-9: Flood map of the Dalestraat flood location after simulation of the rainfall event of 18 August 2011. .. 73
Figure E-10: Map marking the flood location at the Pastoor Engelenstraat in Banholt. 74
Figure E-11: Flood map of the Pastoor Engelenstraat after simulation of the rainfall event of 18 August 2011. ... 74
Figure E-12: Map marking the Herkenradergrubbe flood location and photographs available for validation. 75
Figure E-13: Flood map of the Herkenradergrubbe after simulation of the rainfall event of 18 August 2011. 76
Figure E-14: The sloping driveway at the Burgemeester Beckersweg 43, Mheer (Google 2009). 76
Figure E-15: Map showing the locations where flooding occurs in local depressions adjacent to buildings. 77
Figure E-16: The entrance of Dorpsstraat 7 in Mheer forms a local depression (Google 2009). 77
Figure E-17: Flood map at the Michiels Kessenichstraat 13, Mheer shows flooding at the sloping driveway. 78
Figure E-18: Different locations of measuring the water level and the retaining height of buffer Peerdsgracht. 78

List of Tables

Table 2-1: Topics covered in the theoretical background. 14
Table 4-1: Overview of observed and simulated average water depths on 18 August 2011. 27
Table 4-2: Interception, infiltration and runoff fluxes calculated after simulation of the extreme rainfall scenarios. 27
Table 4-3: Flood depths and durations at the Dorpsstraat corresponding to rainfall scenario 1 and 2. 29
Table 4-4: Dimensions of the culverts through which the Horstergrub stream passes the Dorpsstraat. 31
Table 4-5: Dimensions of the storm drains of which the discharge is plotted in the Figures 4-7 and 4-8. 32
Table 4-6: Flood depths and durations at the Steegstraat corresponding to rainfall scenario 1 and 2. 34
Table 4-7: Flood depths and durations at the Dalestraat corresponding to rainfall scenario 1 and 2. 38
Table 4-8: Dimensions of the storm water pipe corresponding to the Figures 4-20 and 4-21. 41
Table 4-9: Flood depths and durations at the Pastoor Engelenstraat corresponding to both rainfall scenarios. ... 42
Table 4-10: Dimensions of the storm water outlet that drains towards the Banholtergrub. 45
Table B-1: Conversion values used to retrieve the friction, infiltration and interception subgrid layers. 61
Table C-1: Overview of the 1D model elements and the required input parameters. 64
Table E-1: Interception, infiltration and runoff fluxes calculated after model simulation of 18 August 2011. 69
Table E-2: Calculated maximum water levels and overflow durations at the water storage buffers. 79

1. Introduction

1.1 Background

Since 1950, there has been an increase in both the occurrence and intensity of extreme downpours in the Netherlands (van Oldenborgh & Lenderink 2014). The most extreme, officially recorded, events are all from the last fifteen years (RIONED Foundation 2013). The Royal Netherlands Meteorological Institute (KNMI) defines 50 millimetres of rain per day, or more, as extreme rainfall (van Oldenborgh & Lenderink 2014). Extreme storm events can either be of short duration with high intensity, or of a longer duration with a more moderate intensity (Lenderink et al. 2011). Based on a trend analysis, van Oldenborgh & Lenderink (2014) concluded that the number of days with at least 50 millimetres of rain per day occur twice as often nowadays compared to 1950. Moreover, as a consequence of climate change, extreme storm events are expected to increase even more in: intensity, amount of rainfall during one event, occurrence and possibly also in size of affected area in the future (KNMI 2014).

Urban pluvial flooding has drawn increased attention globally in recent years. This is caused by threats of climate change, ongoing urbanization and urban densification (e.g., Chen & Liu 2014; Schmitt et al. 2004; Spekkers 2015; Zhang & Pan 2014). In the Netherlands, the increased occurrence and future threats of extreme precipitation are a cause for concern among municipalities.

Dutch sewer systems are usually designed with the capacity to fully collect and discharge the rain water of an event with a return period of two years,[1] without the occurrence of flooding (RIONED Foundation 2006). However, during storm events that exceed the design amount of rainfall, not all the water can be discharged through and stored in the sewer system. Consequently, the limited storage and discharge capacities of the sewer system result in temporary accumulation of water on street level (van Luijtelaar et al. 2008). The acceptance of this temporary accumulation is decreasing, while public and political concern about urban flooding is increasing. So, even though urban drainage systems are not designed to cope with water amounts associated with extreme events, an extensive amount of water in the streets or flooding is not always accepted (van Luijtelaar et al. 2008; RIONED Foundation 2013).

Depending on the event, extreme rainfall can cause severe problems by e.g. obstructing traffic, damage to buildings or wastewater that is flowing out of the sewer through manholes (RIONED Foundation 2015). Spekkers (2015) elaborates with a number of severe damage events how serious the consequences of extreme precipitation can be. In Copenhagen for example, home insurers paid out more than 800 million euros[2] as a result of an extreme event in July 2011 (Garne et al. 2013). In the Netherlands, the direct damage to households, industries and agriculture of one extreme storm event in the autumn of 1998 was estimated around 410 million euros[3] (Jak & Kok 2000).

1.2 Problem definition

During excessive rainfall, surface runoff is often a determining factor for the location and significance of flooding (van Luijtelaar 2014; Mark et al. 2004). Yet, during the design of a sewer system, hydrodynamic surface flow and its interaction with the sewer system is generally not taken into account (RIONED Foundation 2009).[4] Consequently, surface runoff dynamics are often oversimplified, which might result in water hindrance at unexpected locations (Chang et al. 2015; Kluck & van Luijtelaar 2010).

[1] This refers to a storm event with 19,8 millimetres rain falling in 1 hour of rainfall, with a maximum intensity of 110 l s^{-1} ha^{-1} (RIONED Foundation 2004).
[2] 2011 value
[3] 1998 value
[4] Sewer systems are usually designed with use of the NWRW inflow model, which translates rainfall into runoff based on the types of paved surface draining towards the sewer (RIONED Foundation 2004). Additionally, when surcharge in the sewer system exceeds the surface level, this is modelled as a temporary water column on top of the manhole.

Sloping areas, such as the Dutch region South Limburg are prone to flooding. Water flow velocities at both surface level and in sewer systems are higher in sloping areas compared to flat grounds. This results in a lower storage capacity and more discharge in sloping areas. As a result, accumulated ponding in sloping areas tend to result in larger damages (RIONED Foundation 2009).

About twenty per cent of measures taken by Dutch municipalities to reduce flooding were not effective at hindsight (van Luijtelaar et al. 2008; RIONED Foundation 2013). RIONED explains this is due to a limited availability of instruments that can predict both the magnitude of flooding, and the impact of possible measures. In 2009 RIONED stated that existing sewer models could not adequately simulate the hydraulic behaviour of storm water in the total urban drainage system[5] during extreme storm events (RIONED Foundation 2009). Understanding of the hydraulic behaviour of storm water in the total urban drainage system is needed for the development of solutions that effectively reduce urban flood risk (e.g. Lipeme Kouyi et al. 2009; Sto. Domingo et al. 2010). To achieve this, models require detailed information about the surface system and the connection between the sewer and surface system (RIONED Foundation 2009).

Recent computational developments resulted in cheaper and more extensive computation possibilities. Additionally, modern survey techniques have become available, which allow for easier and cheaper collection of high quality input data. Together, these two developments resulted in more advanced predictive numerical flood modelling possibilities (Alkema 2007). The 3Di modelling toolbox is one of these possibilities. 3Di is a hydrodynamic numerical modelling toolbox under development since 2009 (3Di consortium 2014). The 3Di toolbox can be used for issues related to water management, flood risk management and urban flooding. A 3Di model can be developed in such a manner that it accounts for both surface and sewer flow simultaneously.

The 3Di modelling toolbox can contribute to increased understanding of the hydraulic behaviour of storm water in urban drainage systems during extreme events. Subsequently, this knowledge can be used as decision support for urban flood risk management (Dahm et al. 2014; Lipeme Kouyi et al. 2009). Yet, urban flood analyses in sloping areas, with a model accounting for both surface and sewer flow, are not conducted with 3Di before.

1.3 Research aim and research questions

The purpose of this research is to evaluate the suitability of 3Di modelling for urban pluvial flood analyses in sloping areas. For this purpose, a case study is performed in the villages Banholt and Mheer. Also, this research only focusses on extreme storm events with a short duration and high rainfall intensity.

Research questions

The main research question is:

What is the hydraulic behaviour of storm water in sloping areas during extreme rainfall, and how can the 3Di modelling toolbox contribute to assess the causes of urban flooding?

To answer the main research question, the following sub questions are answered:

1. What hydrological and hydraulic processes play a role during extreme storm events?
2. How does 3Di account for these processes?
3. What are the urban flood locations in the research area?
4. What is the magnitude of flooding at these locations?
5. What are the causes of flooding at these locations?
6. What are the contributing overland flow pathways at these locations?

1.4 Relevance of the research

Urban drainage managers have a desire to increase their knowledge about the behaviour of storm water during extreme storm events. More understanding of the hydraulic processes involved in flooding contributes to more effective decision making on urban flood risk (Dahm et al. 2014). High-resolution high-speed flood modelling tools, such as the 3Di toolbox, are useful to obtain this desired

[5] The total urban drainage system comprises of the sewer and surface system, and their interaction.

insight (Chang et al. 2015; Dahm et al. 2014; van Luijtelaar 2014). Moreover, for urban flood analyses the models should include both the surface and sewer system. Therefore, in this research a 3Di model is developed with a connection between the sewer system, taken into account as one-dimensional (1D) flow, and the surface system, taken into account as two-dimensional (2D) flow. In the literature this is known as dual drainage modelling (Djordjevic et al. 1999).

However, hydrodynamic 1D-2D dual drainage modelling is relatively new. As a result, the number of case studies and researches on this topic is limited. According to ten Veldhuis (2010) examples of calibrated 1D-2D dual drainage models cannot be found in the literature, because these models require extensive computational efforts and have a large data requirement (Aronica & Lanza 2005; Zoppou 2001). Furthermore, a lack of calibration data results in limited validation possibilities (Leandro et al. 2009). Consequently, it will take time before 1D-2D dual drainage models obtain sufficient reliability of application (ten Veldhuis 2010).

Scientifically, this research contributes to the application of 1D-2D dual drainage modelling with 3Di for urban flood analyses in moderate to steeply sloping watersheds. 3Di is already successfully in use, or under development for urban areas in the Netherlands - e.g. Amsterdam, The Hague and Rotterdam. However, it's validated applicability in moderate to steeply sloping watersheds with inclusion of the interaction between surface and sewer flow is currently non-existent. This limited experience with 1D-2D dual drainage 3Di modelling in sloping areas, and a lack of calibration data are major challenges, yet also an opportunity to contribute to the confidence of 3Di as a suitable support-decision tool for urban drainage managers in sloping areas.

In the long term, urban drainage managers aim at effective flood risk management within their management area. Since the purpose of this research is to analyse how 3Di can contribute to this aim, the research is also of societal relevance.

1.5 Thesis outline

This thesis continues with the required theoretical background in Chapter 2, which is the result of a literature research and provides an answer to research sub question 1 and 2. Then, Chapter 3 contains the methodological approach of this research, including the development of the 3Di model. Subsequently, Chapter 4 presents the model results, which covers the definition of the flood locations and the magnitude and causes of flooding at each urban flood location. Or in other words, Chapter 4 presents the answers to research sub questions 3 to 6. Chapter 5 contains a discussion about the model performance, assumptions, and model calibration and validation requirements. Additionally, the research scope and limitations are discussed. Finally, combining all these chapters, the main research question is answered in Chapter 6. In addition to the conclusion, this chapter also provides recommendations for future research, both for this specific case study and the 3Di toolbox in general. The appendices included at the end of the report provide more information about the model development including the input data used, modelling choices and assumptions made, and the development of the rainfall input scenarios. They also provide the results of the model validation, based on the historical rainfall event of 18 August 2011.

2. Theoretical background

This literature research is executed to gain the required knowledge in urban catchment hydrology during extreme storm events, including the storm water hydraulics at the surface and in the sewer system. Additionally, understanding of hydrodynamic flood modelling, and 3Di in specific, is required for this research. Table 2-1 one gives an overview of the topics covered in this chapter.

Table 2-1: Topics covered in the theoretical background.

Urban catchment hydrology	Urban flood modelling
Surface system: • *Interception* • *Infiltration* • *Surface runoff* Sewer system: • *Surcharge* • *Flooding*	Hydrodynamic numerical modelling 3Di toolbox: • *Shallow water equations* • *Subgrid and quadtree technique* • *Rainfall-runoff distribution* • *Runoff routing* • *1D-2D flow interaction* • *1D structures*

2.1 Urban catchment hydrology

2.1.1 Surface system

Ponding can occur at surface level when the amount of rainfall exceeds the absorbing and discharge capacities of a catchment. When raining, water drops can either be: (1) intercepted, (2) infiltrate or (3) become surface runoff (Dingman 2008).

Interception

Interception is the part of precipitation that is kept by vegetation and other structures on the earth's surface and will eventually be subjected to evaporation (Dingman 2008; NHV 2002). The amount of interception depends on features such as land use and vegetation type. Gerrits (2010) explains that the role of interception in the hydrological cycle is relatively constant in time due to various types of interception storage. Furthermore, interception is known to be small on impervious surfaces and larger on pervious surfaces (Boyd et al. 1993).

Since interception subsequently evaporates, storm events influence the interception capacity of an area temporarily (Gerrits 2010). So, when analysing a single storm event, the actual interception capacity will depend on previous rainfall.

Infiltration

The second possibility is that the rainwater infiltrates. After it infiltrates it can either percolate to the deep groundwater, or become subsurface flow in the unsaturated zone.

The infiltration rate depends on the effects of gravity and pressure forces acting on water arriving at the surface (Dingman 2008). In turn, the following factors determine the gravity and pressure forces:

- Either the rate at which rain arrives on the surface or the depth of ponding at the surface.
- The saturated hydraulic conductivity of the soil.
- The initial moisture content of the soil.
- The slope and roughness of the soil surface.
- The chemical characteristics of the soil surface.
- The physical and chemical properties of water.

According to Nassif & Wilson (1975) the correlation between infiltration capacity and steady-state infiltration is strong for soils with a high permeability, e.g. course sand, and low for soils with a low permeability, e.g. clay. Additionally, the steeper the slope and the smoother the surface of a permeable surface, the lower the infiltration rate (Fox & Bryan 1999; Nassif & Wilson 1975).

Surface runoff
When rainwater is not intercepted nor infiltrated, it becomes surface runoff. There are two well-known processes associated with runoff: Dunnian overland flow and Hortonian overland flow (Dingman 2008). Dunnian overland flow occurs when the soil is saturated from below. Generally, this occurs in humid areas with high groundwater tables. Hortonian overland flow refers to surface runoff that occurs on a surface that is either impermeable or saturated from above, which occurs when the rainfall intensity exceeds the saturated hydraulic conductivity of the soil. Hortonian overland flow is more likely to occur in moderate to steeply sloping catchments with deep groundwater tables.

Geology, topology and land cover determine the rates and paths of movement of water as it travels downslope (Dingman 2008). Additionally, surface runoff is also impacted by the rainfall intensity (van Dijk 2011).

Surface runoff is usually turbulent or quasi-turbulent. Runoff rates increase with increasing slope, and decrease with increasing roughness (Battany & Grismer 2000; Dingman 1984). The impact of steeper slopes on the increase in surface runoff can be explained by the reduction of initial interception storage, the decrease in infiltration, and increase of overland flow velocities (Ebrahimian et al. 2012; Huang et al. 2006). The minimum water depth of runoff decreases with increasing slope (Zhan & Huang 2004).

2.1.2 Sewer system
The primary functions of sewer systems are the collection and discharge of wastewater and storm water. There are two types of gravity sewer systems to fulfil this task, combined and separated sewers. In a combined sewer, both wastewater and storm water are collected and discharged by one and the same sewer. A separated sewer system refers to a situation with two separated systems, one for wastewater and one for storm water (TU Delft 2008).

All sewer systems have a limited storage and discharge capacity (Chang et al. 2015). Under normal circumstances, sewer systems in sloping areas have a smaller storage capacity and a higher discharge capacity to the wastewater treatment plant and external overflows, than sewer systems in flat areas (RIONED Foundation 2006). When the amount of surface runoff exceeds the storage and discharge capacity of the sewer system, this can result in either surcharge or flooding conditions.

Surcharge
Surcharge is defined as *"a condition in which wastewater and/or surface water is held under pressure within a gravity drain or sewer system, but does not escape to the surface to cause flooding"* (Schmitt et al. 2004, p.301). This means that the water level in a manhole can rise up, and range, between the pipe crown and the surface level of the manhole (Figure 2-1).

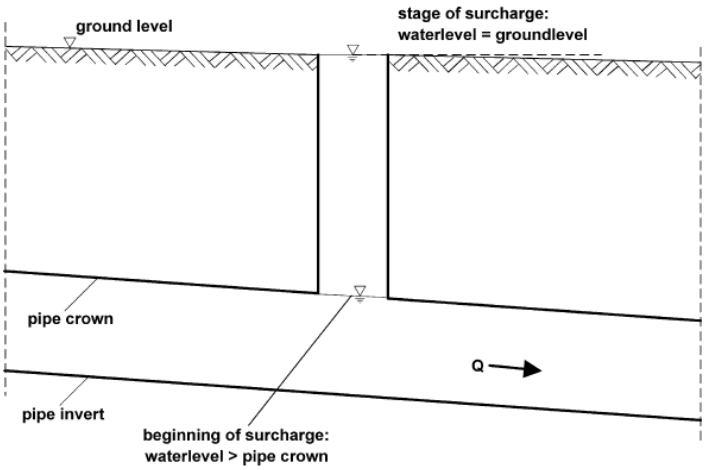

Figure 2-1: Stages of sewer surcharge (Schmitt et al. 2004).

Flooding
Schmitt et al. (2004, p.301) define flooding as the *"condition where wastewater and/or surface water escapes from or cannot enter a drain or sewer system and either remains on the surface or enters buildings".* Continued surcharge conditions may lead to a water level rise close or equal to surface

level, which prevents water from entering the sewer system. Or more severe, when the surcharge level exceeds the surface level, water escapes from the sewer system.

Flooding may occur at different stages of surcharge depending on the type of drainage system, general drainage design characteristics as well as specific local constraints (RIONED Foundation 2013; Schmitt et al. 2004). Also, upstream surcharge or flooding conditions can produce flooding downstream when the inlet level of a manhole lies below the pressure height, as illustrated in Figure 2-2 (Schmitt et al. 2004; van Luijtelaar 2014).

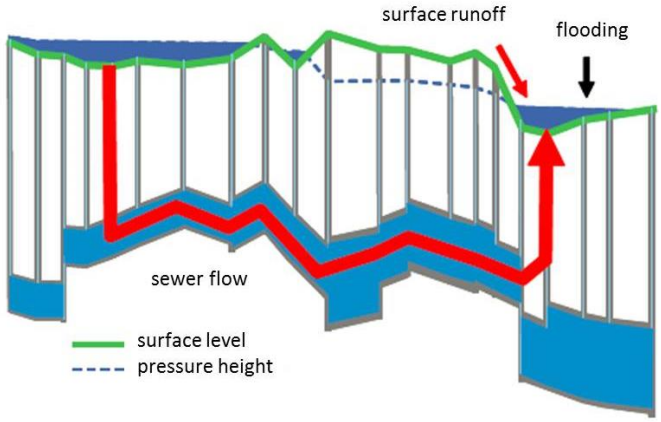

Figure 2-2: Flooding due to a pressure height that exceeds the surface level (van Luijtelaar 2014).

2.1.3 Interaction between surface and sewer system

As the flood definition given by Schmitt et al. describes, water can either not enter or escapes from a sewer system, meaning that there is an interaction between the flows at and below the surface. Figure 2-3 shows various flows that can occur as soon as rainwater starts to flow over the surface. In the figure roofs drain directly to the storm sewer, this is not necessarily always the case. It is also possible that roofs drain to the surface. At the surface, rainwater starts as overland flow before it enters the sewer system through drainage inlets. It is possible that part of the water flows past a sewer inlet due to high flow velocities, or because of extended surcharge (Mark et al. 2004). In addition, water can flow out of the sewer downslope when the pressure height exceeds the surface level. This causes either an increase in surface runoff, or an increase in flood depth in case of a depression at the outflow location. The paths of overland flow are influenced by manmade facilities such as drainage systems, roads and buildings (Hsu et al. 2000).

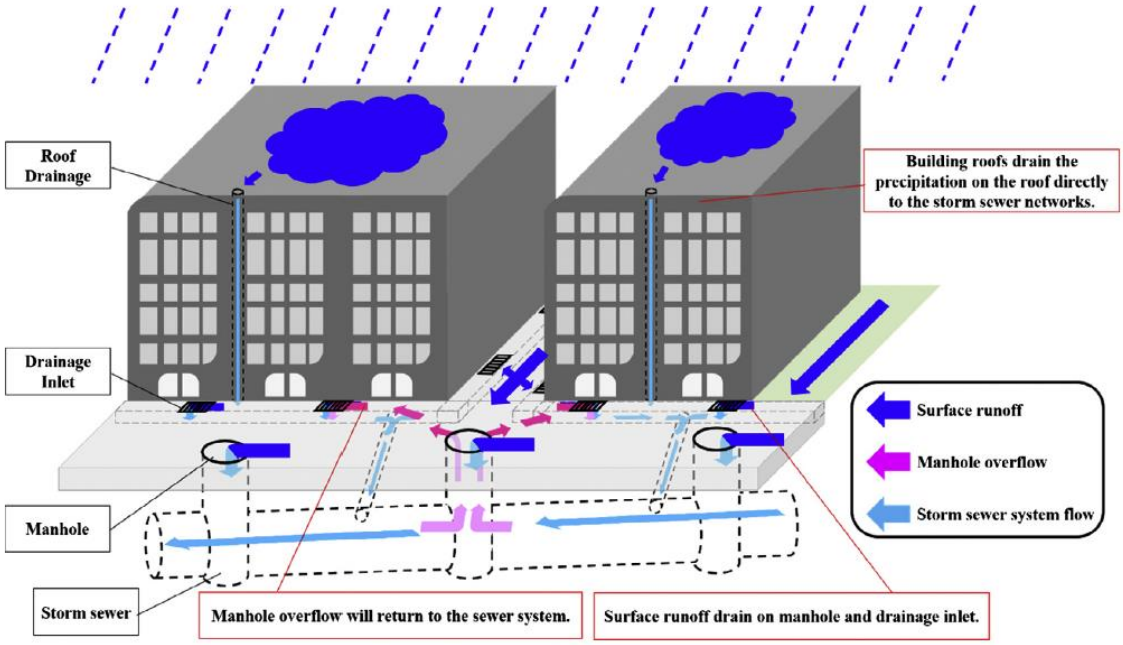

Figure 2-3: Schematization of urban drainage physics (Chang et al. 2015).

According to Mark et al. (2004) flood durations depend on the inlet capacity of the sewer, the drainage capacity of the pipe system, and the infiltration and evaporation rates in the contributing catchment. The effect of evaporation is neglected in this research, as frequently applied in flood analyses, since the rate of evaporation is very low (Butler & Davies 2011; Ochoa-Rodriguez et al. 2013).

2.2 Urban flood modelling

Urban flood models can vary to a great extent, ranging from simple to more sophisticated approaches. Which tool or program to use depends on various aspects, such as the aim of the research, the purpose of the model and the data availability. Broadly there are three different types of models regularly used for urban flood analyses (van Dijk 2011):

- Surface analysis tools based on a geographic information system (GIS).
- 1D-1D dual drainage models.[6]
- 1D-2D dual drainage models (3Di). [7]

For a quick analysis on urban flooding with a limited data availability and few computational efforts a GIS based surface model can be used (see e.g. Chen et al. 2009; Zhang & Pan 2014). In this case, the sewer system is taken into account as an abstraction flux from the surface based model.

Yet, to simulate flooding in a more realistic manner, the sewer and surface system need to be coupled (van Dijk 2011; Mark & Parkinson 2005; Schmitt et al. 2004). Van Dijk (2011) stresses that the interaction between, and hence inclusion of, both the sewer system and surface system is especially important in sloping areas with a downhill flat area.

When flooding is only minor and the surface water stays within pre-defined flow paths, e.g. curb boundaries, a 1D-1D dual drainage model can provide acceptable results (Allitt et al. 2009; ten Veldhuis 2010).

However, when runoff is not confined to street profiles, for example during more extensive flooding or in sloping areas, the 1D-1D dual drainage approach is inaccurate (Mark et al. 2004; ten Veldhuis 2010). In such situations, a model that routes surface runoff two-dimensionally will contribute to the accuracy of the results (see e.g. Aronica & Lanza 2005; Hsu et al. 2000; Maksimović et al. 2009).

2.2.1 Hydrodynamic numerical modelling

Model simulations are based on physical equations, features of an area - such as elevation and roughness - and external forces such as storm events (Al-Sabhan et al. 2003; Bates & De Roo 2000; de Moel & Aerts 2011; Stelling 2012). Hydrologic or hydrodynamic[8] models are required to quantify water flow as a function of topography (Alkema 2007). These models are based on the conservation of mass (continuity), conservation of momentum and conservation of energy. Hydrologic models usually satisfy the conservation of mass only, while hydrodynamic models solve the conservation of both mass and momentum (Zoppou 2001). The systems of interest during hydrodynamic modelling are often complex, which prevents a solution of the governing equations analytically. Therefore these problems are solved numerically.

To account for the occurring water flows during extreme rainfall, flood simulation models should accurately describe the hydraulic phenomena of surcharged and flooded sewer systems, by describing at least (Schmitt et al. 2004):

- The transition from free flow to pressurized flow in the sewer pipes.
- The water level rise in a manhole until surface level and water escaping from the sewer.
- The occurrence of surface runoff during surface flooding.
- The interaction between pressurized sewer flow and surface runoff.

[6] In a 1D-1D dual drainage model both sewer and surface flows are represented by flow in one dimension
[7] In a 1D-2D dual drainage model the sewer system is represented by flow in one dimension, and the surface system by flow in two dimensions.
[8] Hydrodynamic modelling is also known as hydraulic modelling.

2.2.2 3Di modelling toolbox

As previously described, scholars emphasize the added value of hydrodynamic 1D-2D dual drainage modelling for urban flood analyses. However, they also emphasize the larger data requirements and larger computational efforts. 3Di is a modelling toolbox that combines innovative modelling techniques to overcome these boundaries (Dahm et al. 2014). Consequently, 3Di calculations can contain both a high level of detail and fast calculation speed (3Di consortium 2014).

Shallow water equations

In 3Di, flow routing is done by numerically solving the shallow water equations of Saint Venant. Flood modelling of inviscid water with a shallow depth of flow compared to its width, and a relatively small bottom slope can be done using these shallow water equations (Alkema 2007). The shallow water equations consist of the continuity equation and the momentum equation in one or two directions.

The following set of equations is used to calculate 2D surface flow:

$$\frac{\partial h}{\partial t} + u\frac{\partial h}{\partial x} + v\frac{\partial h}{\partial y} = 0 \qquad continuity\ equation$$

$$\frac{\partial u}{\partial t} + u\frac{\partial u}{\partial x} + v\frac{\partial u}{\partial y} + g\frac{\partial \zeta}{\partial x} + \frac{c_f}{h}u\|u\| = 0 \qquad momentum\ equation\ in\ x-direction$$

$$\frac{\partial v}{\partial t} + u\frac{\partial v}{\partial x} + v\frac{\partial v}{\partial y} + g\frac{\partial \zeta}{\partial y} + \frac{c_f}{h}v\|u\| = 0 \qquad momentum\ equation\ in\ y-direction$$

Where h is the water depth determined by $h=\zeta-e$, ζ the water level above plane of reference, e bottom elevation above plane of reference, u and v the depth averaged velocities in x and y direction, $\|u\|$ the velocity magnitude, and c_f the dimensionless friction function for which both Manning or Chézy can be used (Stelling 2012; van 't Veld 2015).

To simulate sewer flow it is assumed that the sewer system consists of a set of interconnected branches where flow is governed by the continuity and momentum equations representing 1D flow:

$$\frac{\partial A}{\partial t} + \frac{\partial Au}{\partial x} = 0 \qquad continuity\ equation$$

$$\frac{\partial u}{\partial t} + u\frac{\partial u}{\partial x} = -g\frac{\partial \eta}{\partial x} - \gamma u \qquad momentum\ equation\ in\ x-direction$$

Where t is the time, x is the spatial position in a local coordinate system, u is the unknown depth and width averaged water velocity, η is the unknown pressure representing either the free surface or the piezometric head when the flow is pressurized, A is the cross-sectional area, g is the gravitational acceleration, and γ is any nonnegative and possibly nonlinear friction coefficient (Casulli & Stelling 2013).

Numerical simulation of unsteady flows is a challenging task. Implementation of a Newton iteration ensures the conservation of mass while solving this unsteady nonlinear system. In a sewer system, where the width of a flow profile can decrease with increasing depth (Figure 2-4) a double iteration is required to ensure the conservation of volume (Nested-Newton iteration). See Casulli (2009); Casulli & Stelling (2013); Nelen & Schuurmans (2016) for more information.

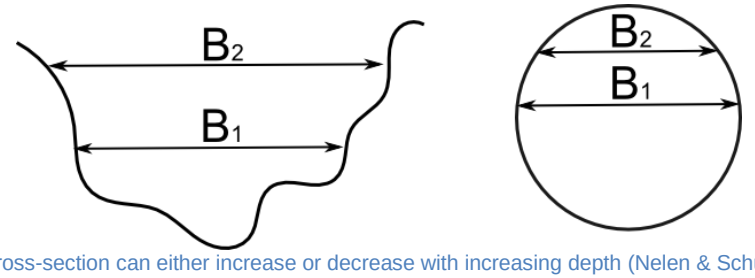

Figure 2-4: A cross-section can either increase or decrease with increasing depth (Nelen & Schuurmans 2016).

Subgrid and quadtree technique

A bathymetry raster, or digital elevation map (DEM), and friction raster are used to solve the shallow water equations for 2D surface flow, and to calculate the associated water levels and flow velocities. For the calculation of water levels and flow velocities fine grid pixels are clustered into larger calculation cells, this is the so called subgrid technique (Figure 2-5). At least four DEM cells are linked to one calculation grid cell, which is valid under the assumption that the water level could be averaged over one calculation cell. Due to this subgrid method 3Di can use high resolution bathymetry and roughness effects in a limited amount of calculation cells while solving the continuity and momentum equations (Volp et al. 2013). This has large advantages for the accuracy and computation time of 3Di model simulations (Stelling 2012).

Within a model area, some locations require more detail than other locations. For example, in a polder, a levee requires more detail than the relative flat polder area. Also, cities require a higher spatial detail than rural areas (Niemczynowicz 1999). This can be achieved with calculation grid refinement. The structure of a calculation grid with refinement is based on quadtrees. A quadtree is a data structure based on a tree that divides a 2D region into squares with groups of four. Each of these squares could individually be divided again in groups of four, creating a hierarchical system with different resolutions. This is illustrated by the blue layer in Figure 2-5 which represents a calculation grid with two different resolutions. For every refinement step, the resolution of the calculation cell becomes twice as high along the cell border.

For example, in Figure 2-5, one calculation grid cell is linked to 4 or 16 DEM, which reduces the number of calculation cells from 32 to 5 (van 't Veld 2015). 3Di is the only 2D flow model that uses the subgrid and quadtree technique. Most models use the resolution size of the information layer for the computations, e.g. SOBEK and Delft3D.

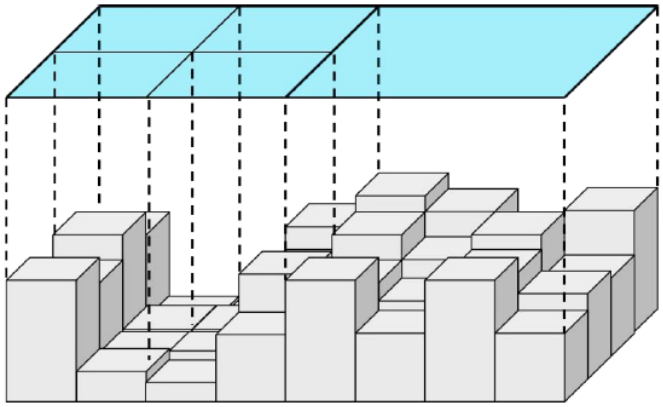

Figure 2-5: A DEM layer (grey pixels) and a quadtree calculation grid (blue layer) (van 't Veld 2015).

Rainfall-runoff distribution

In an urban 3Di model infiltration can be extracted during model simulations by adding an infiltration subgrid layer. The amount of infiltration possible per subgrid pixel is calculated by multiplying the maximum infiltration capacity of the soil with a permeability factor based on land use. The infiltration capacity is constant in time. Hence, the amount of infiltration depends only on water availability and not on the level of soil saturation. During a storm event infiltration is extracted over an area with a similar spatial extent as the rainfall input scenario. During the dry periods of model simulation, infiltration is only extracted from wet subgrid pixels[9].

Urban 3Di models can currently not account for interception by insertion of an interception subgrid layer. Yet, interception can be initially extracted from the rainfall event. The total amount of interception can be calculated with an interception subgrid layer, which is derived from a land use map. This way, the detailed land use information available is used to determine the interception capacity.

[9] Wet pixels refer to subgrid pixels where the water level is higher than the bathymetry of that pixel.

Runoff routing

Initial to the model simulation 3Di derives volume tables based on the DEM (Figure 2-6a), from which a nonlinear volume - water level (V-h) relationship is derived for each calculation cell (Figure 2-6b). With this method detailed bathymetry information is used while solving the 2D shallow water equations (Dahm et al. 2014). Use of these volume tables significantly reduces the simulation time since they are derived in advance and easily accessible during the model run.

With use of the V-h relationship one water level is calculated per calculation cell. This means that the DEM cells within one calculation cell have the same calculated water level, even when this is physically impossible. To calculate the water level, a pressure gradient stencil is used as drawn in the quadtrees of Figure 2-7b. So, for the calculation of water levels the centres of the calculation cells are used.

The DEM pixels along the border of the calculation cell determine whether flow between two adjacent calculation cells is possible. If the water level in a calculation cell is higher than the bathymetry of one pixel at the border, water starts to flow to the adjacent calculation cell. The calculation of velocity between two calculation cells is based on the structure described by the shaded cells in Figure 2-7a. A quarter of the larger neighbouring calculation cell and half of the smaller neighbouring calculation cell are used for the velocity calculation between these cells.

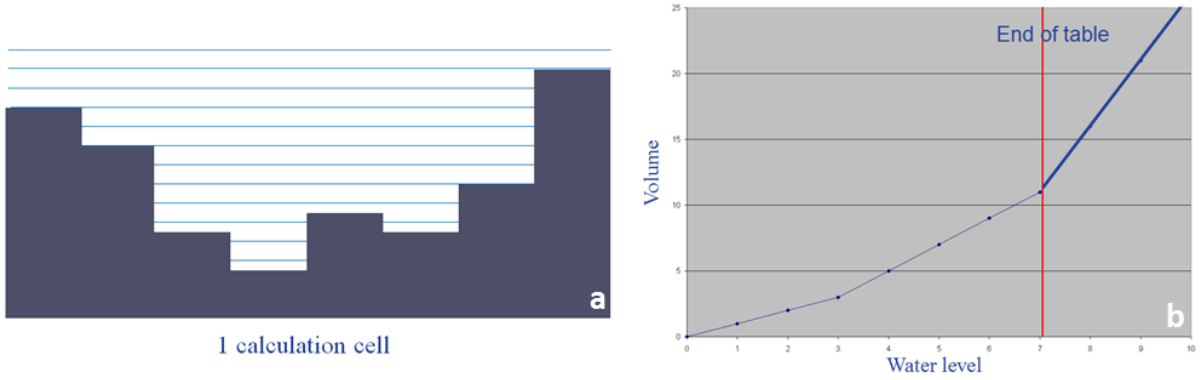

Figure 2-6: (a) A cross-section of one calculation cell with DEM pixels. (b) The V-h relationship derived initial to model simulation.

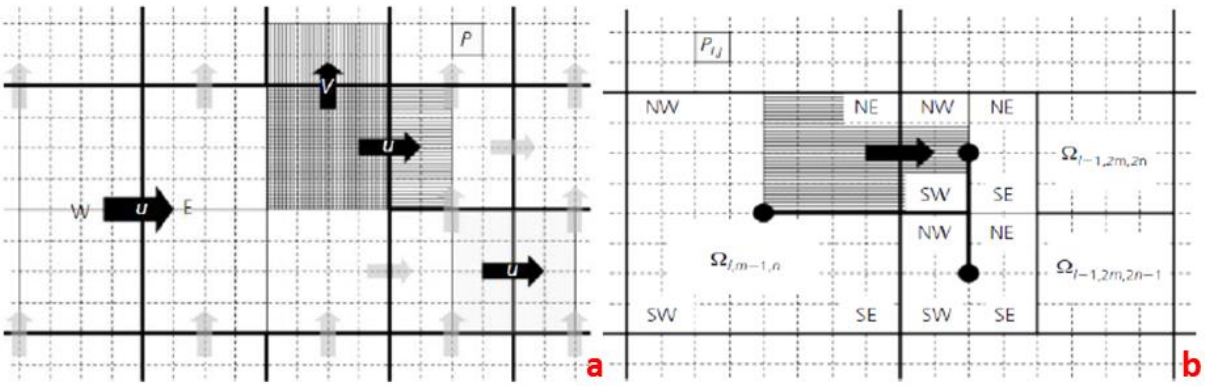

Figure 2-7: (a) The domains used to calculate the velocity between two calculation cells with a different resolution; (b) the pressure gradient stencil for different resolution calculation cells for the calculation of water levels (Stelling 2012).

1D-2D flow interaction

To account for flow exchange between the 2D and 1D flow components of the 3Di model, a connection is required. Numerically this is achieved in solving the continuity equation (Nelen & Schuurmans 2016). In the model, the two components are linked via the centre of the 2D calculation cell and the manholes of the 1D system that are located within that calculation cell.

To each manhole a connection type is assigned. In total there are three types of connection possible: isolated, connected and embedded (Figure 2-8). To elaborate:

- When the connection is isolated there is no flow exchange between the surface and sewer system.
- With a connected manhole setting, water can flow into the sewer when the water level in the calculation cell exceeds both the drainage and water level in the manhole. There is also flow exchange from the sewer to the surface when the water level in the manhole exceeds the surface level of the corresponding DEM pixel. With this setting, the water level in the calculation cell and the water level in the manhole can differ.
- With an embedded connection water from the sewer has a free outflow to the surface system and vice versa. In this situation the water levels in the calculation cell and manhole are equal.

In the illustrations of Figure 2-8 only one manhole is present in a calculation cell. In a model multiple manholes per calculation cell are possible, and each can be given its own connection setting.

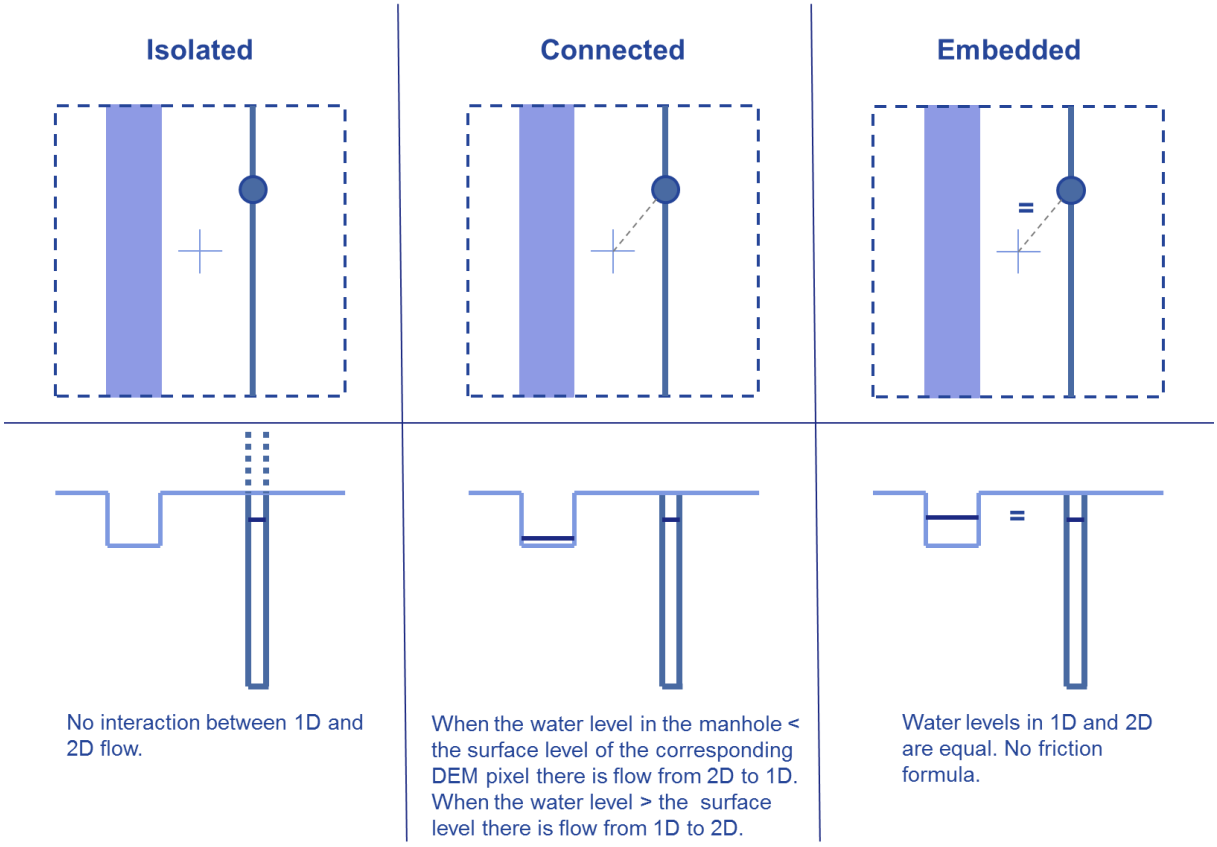

Figure 2-8: The three types of flow interaction possible between the 1D and 2D components of the model.

1D structures

Sewer and surface water structures, such as orifices, culverts and short weirs, can all be calculated with the same formula, by adjustment of the flow-through profiles and discharge coefficients. At these structures the depth average velocity assumption no longer holds, therefore rules of thumb are applied. The formulas used for flow calculations at these structures are the submerged and unsubmerged forms of the short weir formula:

$$Q_i = mB\frac{2}{3}\sqrt{\frac{2}{3}g}\,H_i^{\frac{3}{2}} \quad \text{and} \quad Q_i = mA_i\sqrt{2g\left(\tilde{H}-h_i\right)}$$

In which m is a discharge coefficient depending on the flow direction, $\tilde{H}$ is the energy head and B is the width (Nelen & Schuurmans 2016).

3. Methodology

Figure 3-1 shows a conceptual model of the research set up. This research comprises of:

- A literature study that provided in the theoretical background.
- The case study Banholt - Mheer. The case study Banholt - Mheer is subdivided into: (1) model development, (2) model validation, (3) rainfall scenario development and (4) results.
- A discussion about the research results, which result in a research conclusion and recommendations for the case study specific and the 3Di toolbox in general.

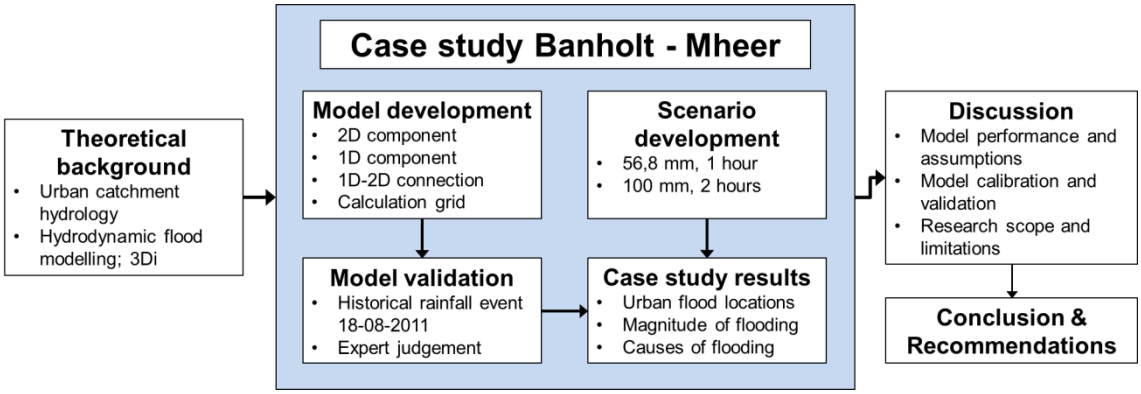

Figure 3-1: The conceptual model of the research set up shows that the theoretical background is input for the case study, which provides input for the discussion, conclusion and recommendations.

The research area (Figure 3-2) is located in the Municipality of Eijsden-Margraten and within the management area of the Roer & Overmaas Water Authority. The research area comprises the two watersheds of the Banholtergrub and Horstergrub streams, in which the villages Banholt and Mheer are located. Topographically, the area is characterized by high elevations and considerable relief (Figure 3-3).

The surface water system in the area is of ephemeral character. Therefore, the water authority constructed fifteen water storage buffers to increase the storage capacity of the surface water system. Still, due to historical extreme storm events urban flooding occurred. A more extensive site description is given in Appendix A.

Figure 3-2: Topographic location of the research area in the Netherlands.

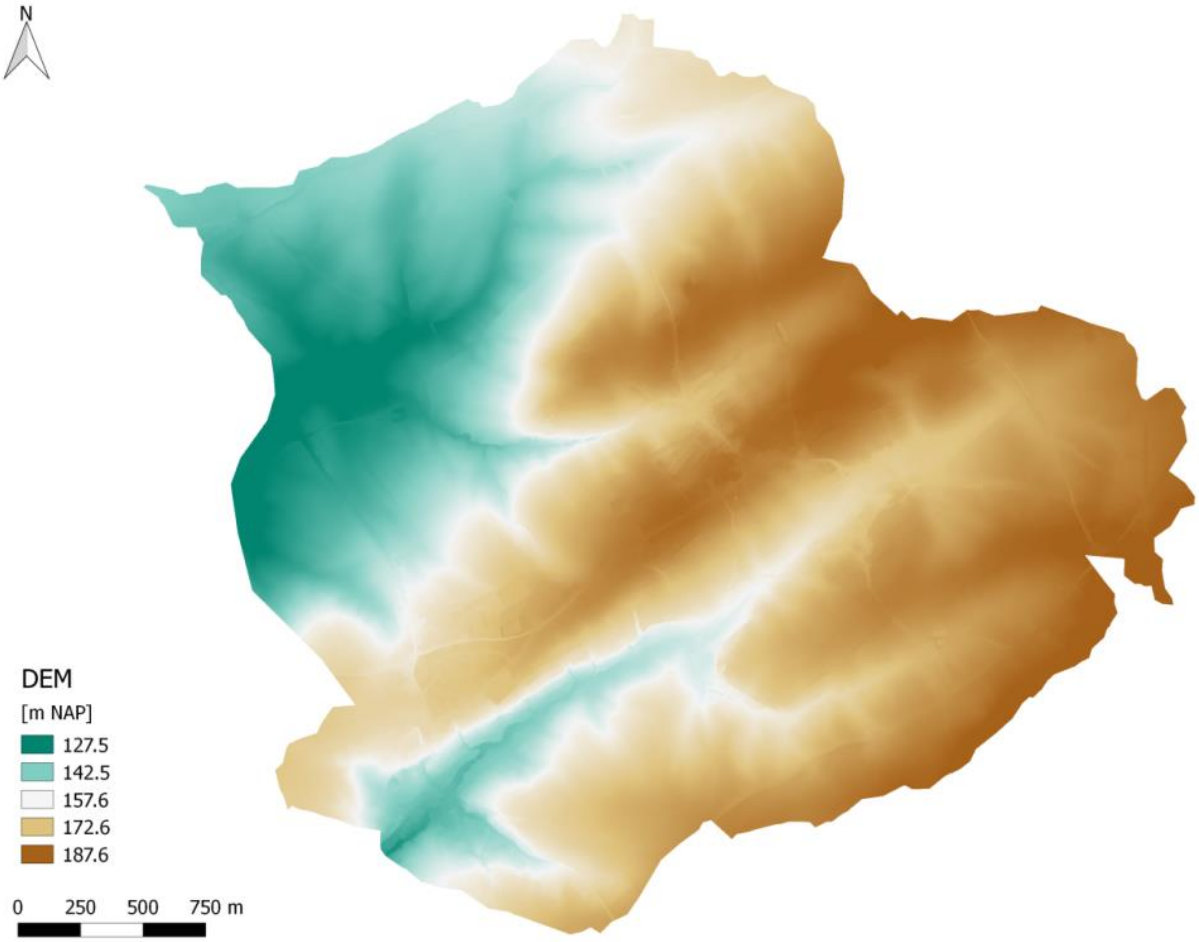

Figure 3-3: DEM subgrid layer of the research area.

3.1 Model development

The integrated 3Di model consists of two main components: the 2D flow component and the 1D flow component. Combined, these two components represent the total urban drainage system of the area (Figure 3-4).

In this research hydrodynamic surface flow and its interaction with the sewer system is taken into account. This means that in the model rain falls directly on the 2D surface, where it can infiltrate into the subsurface, or flow towards the sewer or surface water streams. When the sewer system becomes surcharged water cannot enter the sewer and remains surface runoff. Additionally, if water escapes from the sewer it will become surface runoff again. This way, the flow paths of the rainwater are not predefined.

Considering the aim of this research, the model is developed for short extreme storm scenarios. Consequently, the model should be able to simulate the quick flow processes that occur due to extreme storm events. During model development, the following starting points are used:

- Evapotranspiration and groundwater flow are not taken into account in this study.
- The surface water streams and water storage buffers are included in the 2D flow component.
- The wastewater load is neglected in this analysis.
- At the beginning of an extreme storm scenario, there is no initial water level at the surface, in the channels or in the sewer present.
- All the rainfall that enters the model starts as 2D overland flow, including the building roofs that actually drain directly to the wastewater sewer.
- Downstream in the catchments there is free outflow from the model.

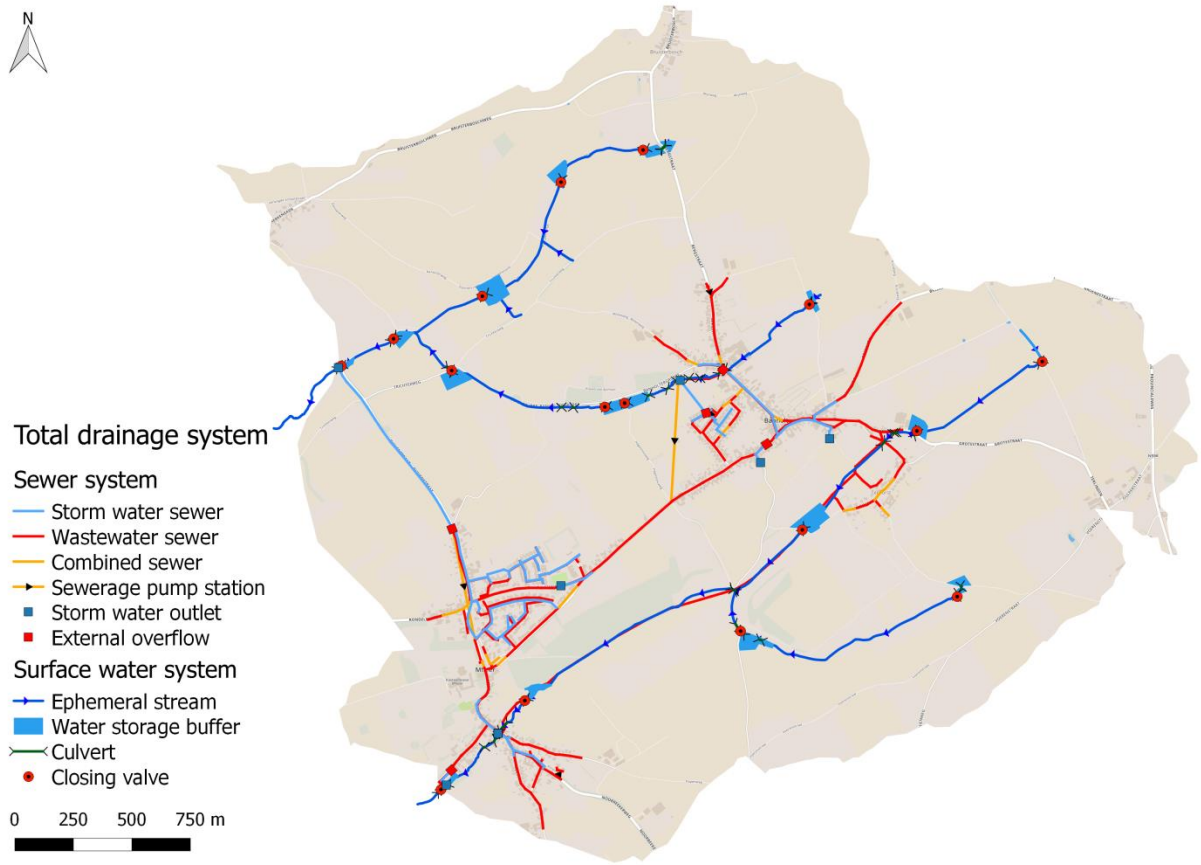

Figure 3-4: Total urban drainage system of Banholt and Mheer, including the contributing catchments of the Banholtergrub (above) and Horstergrub (below) streams.

2D flow component

The 2D flow component represents both surface runoff and open channel flow. This component consists of three subgrid layers with a spatial resolution of 0.25 m^2:

- DEM layer (Figure 3-3)
- Infiltration layer
- Friction layer

Appendix B explains the derivation of these subgrid layers from the available data sources. Including the assumptions and alterations that are made before the subgrid layers are used in this research.

1D flow component

The 1D flow component includes the sewer system and the surface water structures. In total the model consist of the following 1D elements:

- Manholes
- Pipelines
- External overflows
- Storm water outlets
- Orifices
- Sewerage pump stations

The required sewer and surface water system data is provided by the municipality and water authority respectively. Appendix C describes how this data is translated into the 1D component of the model.

1D-2D flow interaction
Flow between the two components is realized by assigning the following settings to the manholes:

- *Isolated:* all manholes from the wastewater system where there is no flow exchange with the surface.
- *Connected:* wastewater sewer manholes in case of incorrect sewer connections or surface water inlet connections, and all the storm water sewer manholes including the storm water outlets.
- *Embedded:* entry and exit points of the orifices and long culverts, i.e. the 1D surface water structures.

Calculation grid
The calculation grid consists of several resolutions, motivated in Appendix D. The largest calculation cells are 20 x 20 meters and the highest resolution is 5 x 5 meters. Calculation grid refinement is applied at the areas of interest during the analysis:

- The rainwater storage buffers.
- The urban areas of Banholt and Mheer.

3.2 Model validation

The model is validated using photographs and expert judgement of the municipality and water authority, of the rainfall event of 18 August 2011. Where possible, validation is based on a comparison of the flood depth and spatial extent of the flood observed in the photographs and calculated with the model. Expert judgement on the model performance is obtained during two work sessions, one with the municipality and one with the water authority. The model results of 18 August 2011, including the comparison with photographs and the expert judgement are included in Appendix E.

3.3 Rainfall scenario development

The model is used to analyse the hydraulic behaviour of storm water during extreme storm events to define the causes of urban flooding. For this purpose, two extreme rainfall scenarios are developed as model input (see Appendix F). The extreme scenarios are:

- Scenario 1: 56.8 millimetres of rainfall in one hour (Figure 3-5).
- Scenario 2: 100 millimetres of rainfall in two hours (Figure 3-6).

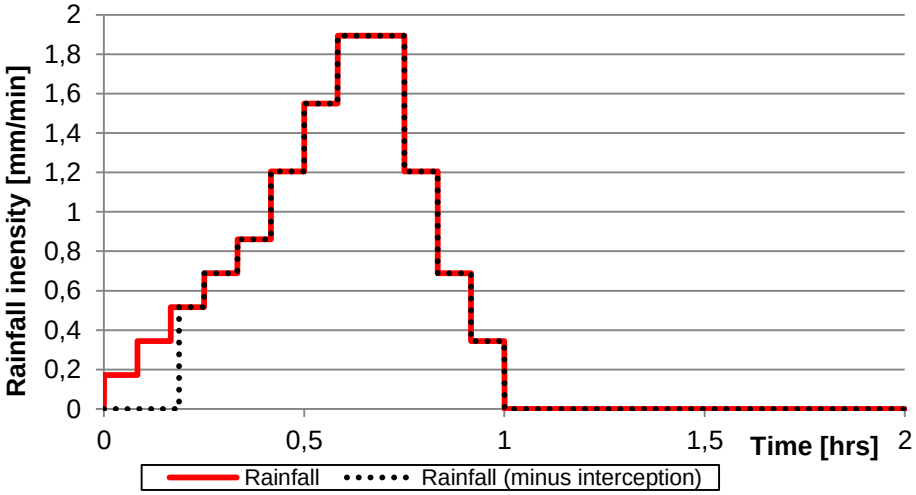

Figure 3-5: Temporal distribution of rainfall scenario 1 with 56.8 mm of total rain fallen in 1 hour.

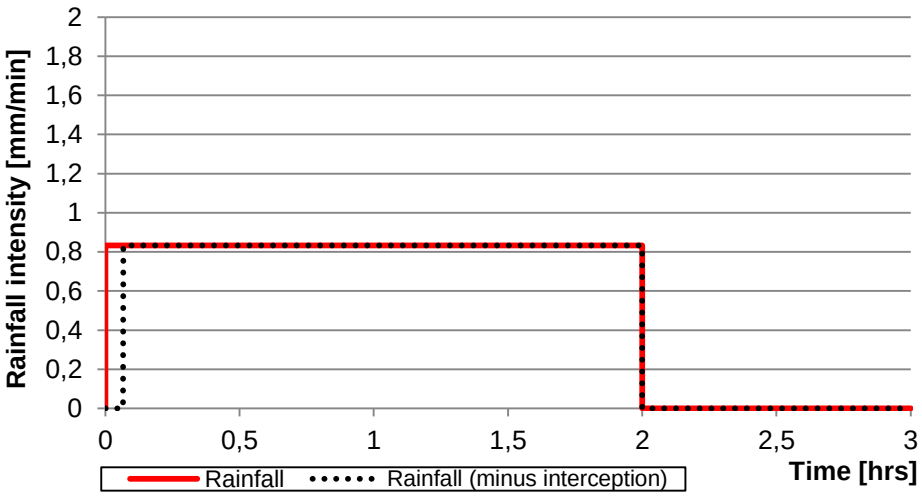

Figure 3-6: Temporal distribution of rainfall scenario 2 with 100 mm of total rain fallen in 2 hours.

3.4 Urban flood analysis

Finally, using these two extreme scenarios an urban flood analysis is performed for the research area. For this analysis the following 3Di results are used:

- Sewer results: with discharges and flow velocities in pipelines and water levels and volumes in manholes.
- Surface flood maps: plotted at least at every other fifteen minutes of model simulation.

The urban flood analysis is divided into: (1) determination of the flood locations and (2) the causes of flooding at each location.

The first step of the urban flood analysis is the definition of the urban flood locations based on the model results. All the locations where flooding emerged as a result of the rainfall scenarios, that are located within the villages of Banholt or Mheer, are defined as urban flood locations.

Secondly, the magnitude and causes of flooding at each of these locations are analysed by looking at the following aspects:

- The average maximum water depth and corresponding flood extent.
- The time to flood and flood duration.
- The cause of flooding and the role of sewer, surface and channel flow at each flood location.
- The contributing overland flow paths ways.

4. Results

The results presented in this chapter comprise of the model validation, scenario analysis and urban flood analysis. The scenario analysis gives the calculated interception, infiltration and runoff fluxes for extreme scenario 1 and 2. The results of the urban flood analysis are given per flood location to determine the flood depth, flood duration and causes of flooding caused by the two extreme rainfall scenarios.

4.1 Model validation

The validation showed deviations between observations and model results:

- The simulated flood extent and depth (Table 4-1).
- The model overestimated the water levels in, and overflows of the storage buffers significantly.
- The model overestimated inundation in local depressions near buildings.

The deviations between observed and calculated flood extent and depth can best be explained per flood location:

- *Dorpsstraat:* the simulated flood extent is also significantly larger in addition to the overestimation in flood depth.
- *Steegstraat:* The simulated flood depth is in the correct order of magnitude due to errors in runoff routing caused by the use of a V-h relationship per calculation cell.
- *Herkenradergrubbe*: part of the contributing runoff area is missing due to the research area boundary.

Table 4-1: Overview of observed and simulated average water depths on 18 August 2011.

Flood location	Observed flood depth [m]	Simulated flood depth [m]
Dorpsstraat, Mheer	0.10	0.20
Steegstraat, Mheer	0.05	0.06
Herkenradergrubbe	0.20	0.15

Despite the deviations between observations and simulation results, it is expected that the model performs well enough to analyse the suitability of 3Di for this urban flood analysis.

4.2 Scenario analysis

After model simulation, 60 per cent of the rain fallen during scenario 1 becomes runoff. During rainfall scenario 2, 50 per cent of the rain fallen becomes runoff (Table 4-2). These percentages represent a total average runoff value for the whole research area including both surface and sewer flow and temporary storage in the area and in the buffers. Runoff is calculated with use of a course waterbalance:

$$runoff = total\ rainfall - interception - infiltration.$$

Table 4-2: Interception, infiltration and runoff fluxes calculated after simulation of the extreme rainfall scenarios.

	Rainfall scenario 1		Rainfall scenario 2	
	Volume [m^3]	**Percentage [%]**	**Volume [m^3]**	**Percentage [%]**
Total rainfall	520048	100	929448	100
Interception	29648	6	29648	3
Infiltration	178450	34	434980	47
Runoff	311950	60	464820	50

Rainfall scenario 1, with a peak rainfall intensity of 1.89 mm/min produces a larger fraction of runoff than scenario 2, with a constant rainfall intensity of 0.83 mm/min. More rainwater infiltrates during rainfall scenario 2, which has a duration of 2 hours, than during rainfall scenario 1, with a duration of 1 hour. The total interception volume of 29648 m^3 is a fixed value in this reseach, so the higher the total amount of rainfall, the lower the percentage of the interception flux. Therefore, the percentage drops from 6 per cent during rainfall scenario 1 to 3 per cent during rainfall scenario 2. Interception is a relatively small flux compared to infiltration and runoff during both scenarios.

4.3 Urban flood analysis

Based on the simulation results of the two extreme rainfall scenarios, flooding occurred at four urban locations (Figure 4-1).

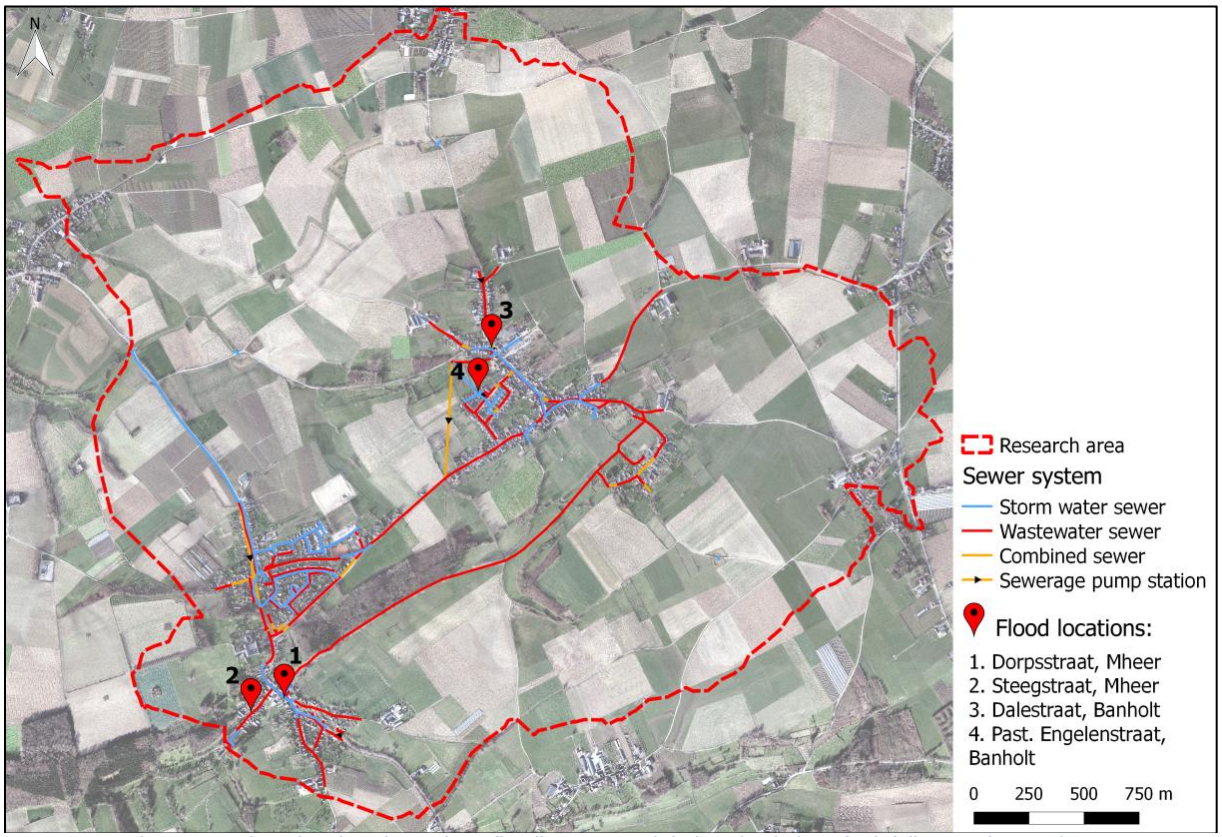

Figure 4-1: The urban locations where flooding emerged during simulation of rainfall scenario 1 and 2.

4.3.1 Location 1: Dorpsstraat, Mheer

The Dorpsstraat in Mheer crosses the valley of the Horstergrub stream and connects the two upslope urbanized parts of the village (Figure 4-2). Rainwater that falls in the upslope parts of Mheer drains towards the Dorpsstraat. Here it enters the Horstergrub stream through two storm water outlets. Also, the Horstergrub stream crosses the street underground at this flood location.

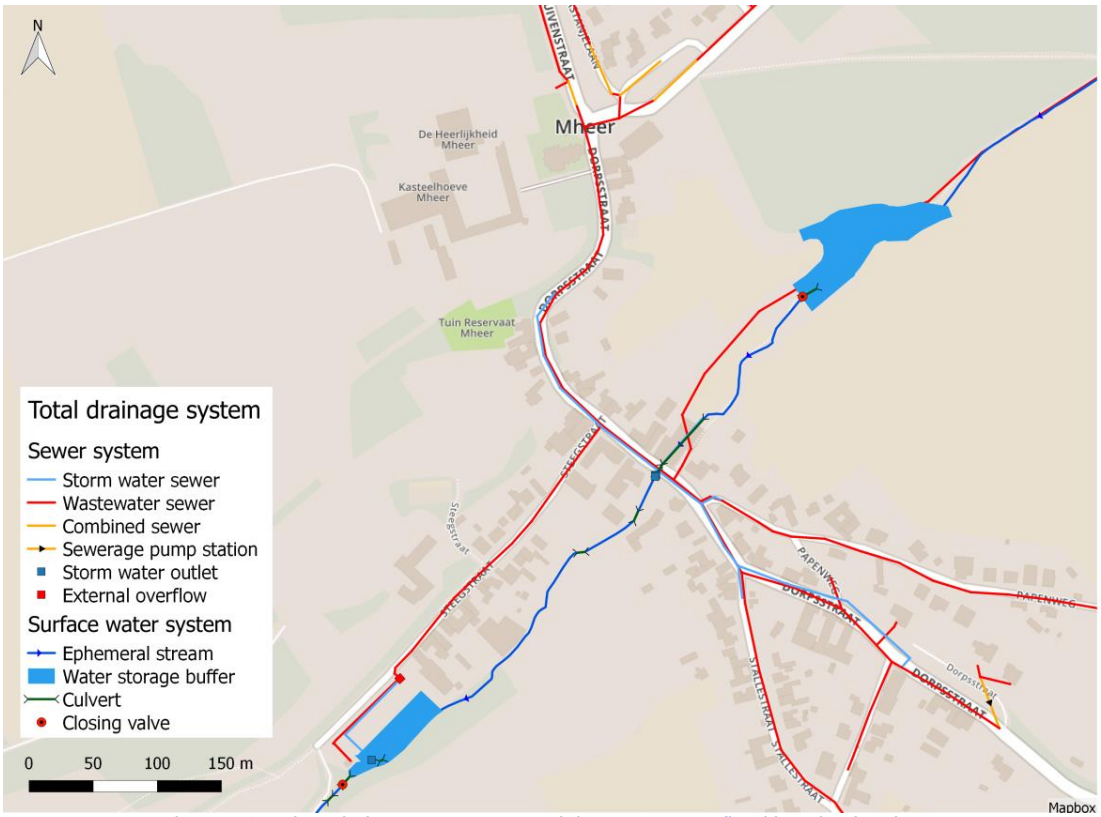

Figure 4-2: Urban drainage system around the Dorpsstraat flood location in Mheer.

Flood depth and duration

The maximum average flood depths that emerged at the Dorpsstraat caused by scenario 1 and 2 are given in Table 4-3. Both maximum water depths emerged at the end of the rainfall events, just before it becomes dry. Figure 4-3 and Figure 4-4 are flood maps that show the maximum flood extent at the Dorpsstraat during scenario 1 and 2 respectively. Considering the model performance, the flood depth at the Dorpsstraat is an overestimation (at least with a factor 2). Scenario 1 causes a larger flood depth and correspondingly a larger flood extent than rainfall scenario 2. The runoff towards the Dorpsstraat observed in the model simulation during scenario 1 is largest after 45 minutes of rainfall, which is just after the peak intensity of the storm event.

Correspondingly, the time to flood and flood duration of scenario 1 and 2 are given in Table 4-3. The time to flood refers to the time it takes before flooding in the street occurs, measured from the start of model simulation. The flood duration represents the time between the start and end of flooding, or in this case between the start of flooding and end of model simulation. At the end of the model simulations there is still water on the street, with an average depth of 15 centimetres during both scenarios, which means that the actual flood durations are longer, however unknown.

Table 4-3: Flood depths and durations at the Dorpsstraat corresponding to rainfall scenario 1 and 2.

	Maximum average flood depth [m]	Simulation time [min]	Time to flood [hrs]	Flood duration [hrs]	Water depth at the end of simulation [m]
Rainfall scenario 1	0.44	60	0:20	1:40	0.15
Rainfall scenario 2	0.40	120	0:08	2:52	0.15

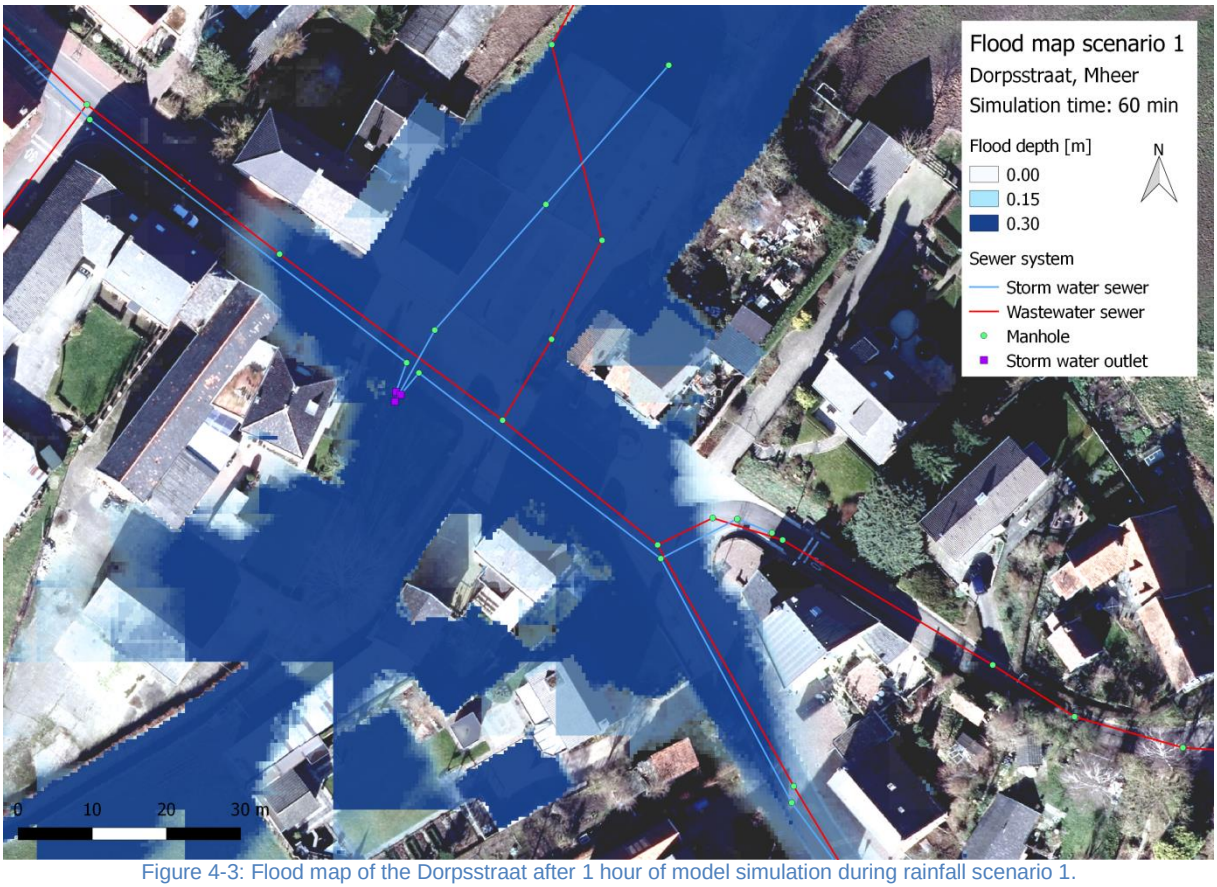

Figure 4-3: Flood map of the Dorpsstraat after 1 hour of model simulation during rainfall scenario 1.

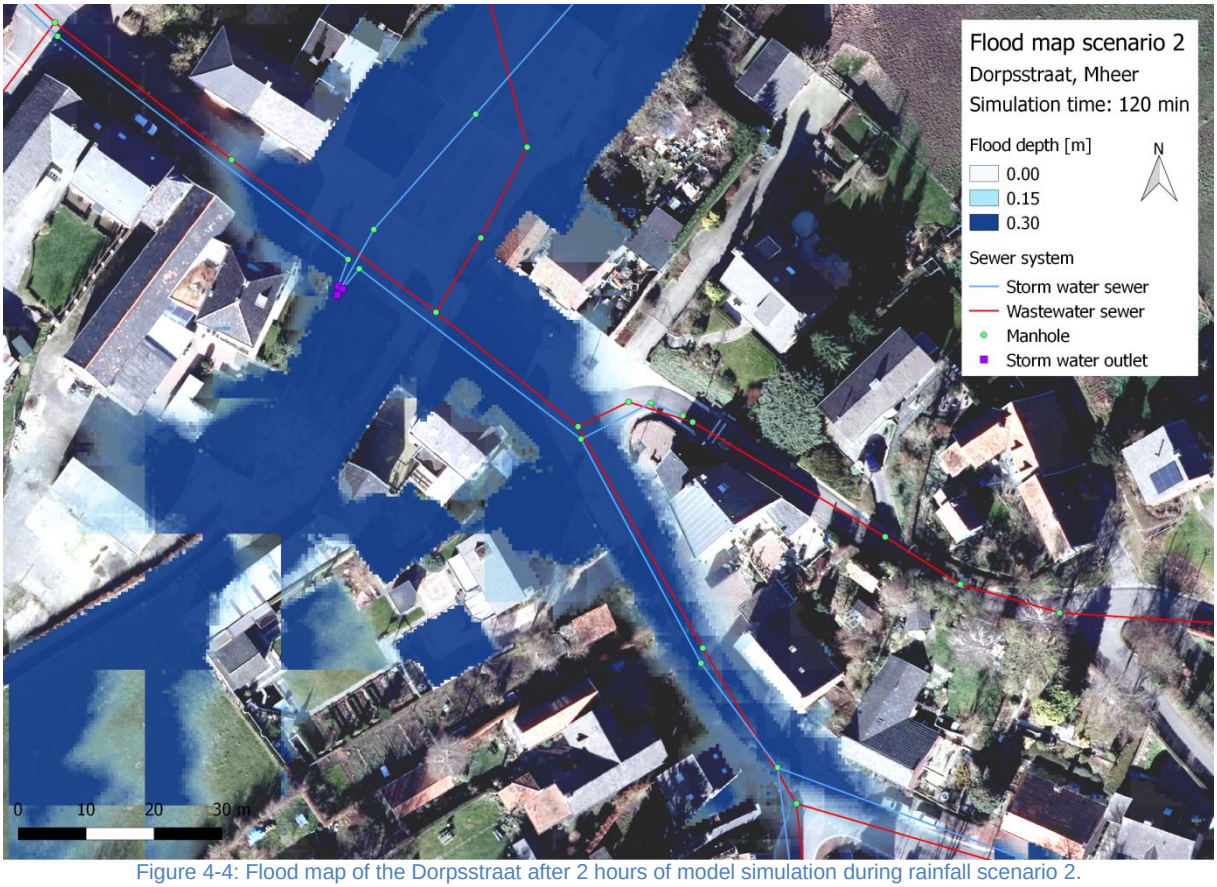

Figure 4-4: Flood map of the Dorpsstraat after 2 hours of model simulation during rainfall scenario 2.

Causes of flooding

The Dorpsstraat is prone to flooding because of its location in the valley of the Horstergrub stream (Figure 4-5). The Horstergrub stream, surface runoff from both upslope sides of Mheer and the storm water sewer system all drain towards the flood location at the Dorpsstraat. Therefore, they all play a role in the magnitude of flooding at the Dorpsstraat.

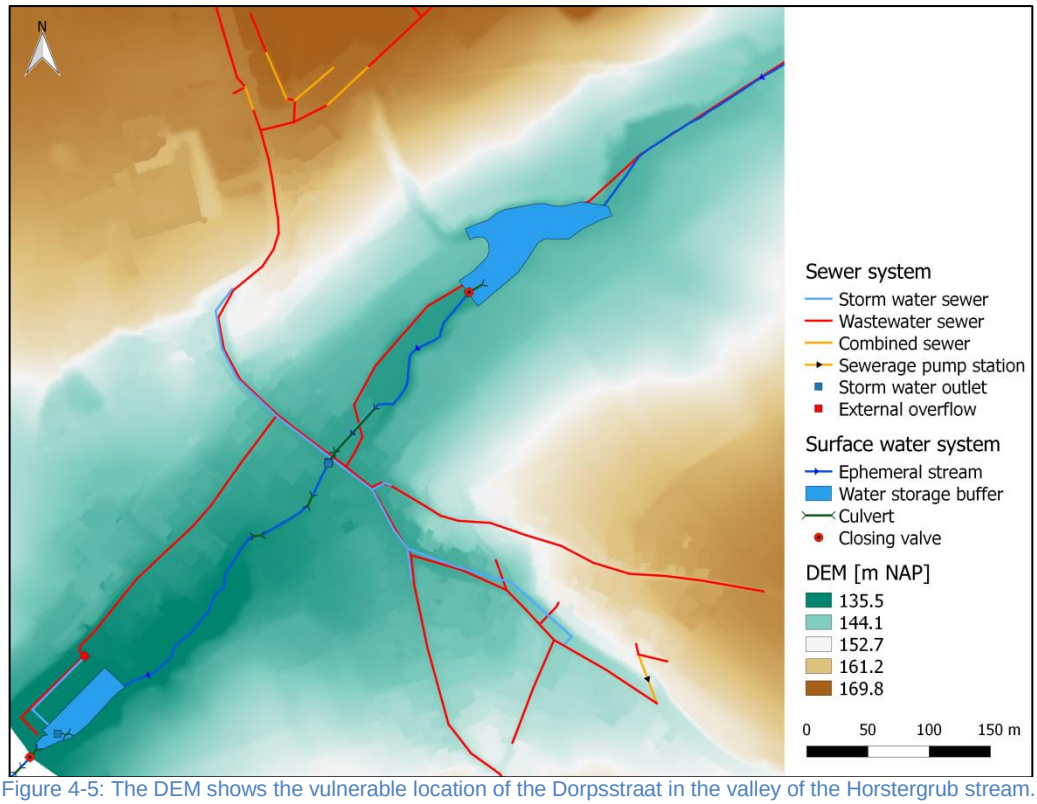

Figure 4-5: The DEM shows the vulnerable location of the Dorpsstraat in the valley of the Horstergrub stream.

Figure 4-6 shows with flow paths how water from the Duivenstraat direction (red circle), the Horstergrub stream (pink circle) and the Noorbeekerweg area (orange circle) flow towards the Dorpsstraat. Quantification of these surface flows is difficult. However, based on comparison of all the flood maps, the order of contributing magnitude of the flows is:

- Water from the Horstergrub stream, which starts about 3 kilometres upstream, so the contributing area from the Horstergrub is larger than shown in Figure 4-6.
- Runoff from the Noorbeekerweg, including the Papenweg and Stallestraat. Here runoff from both urbanized and rural area contributes to flooding at the Dorpsstraat. Most of the water comes from the Noorbeekerweg.
- Runoff from the Duivenstraat direction. Here only urban runoff towards the Dorpsstraat occurs. Compared to the amount of water from the Horstergrub stream and Noorbeekerweg area the contributing surface runoff from this area seems relatively small.

The Horstergrub stream passes the Dorpsstraat through a set of concrete culverts underground over a total length of 58.8 meters. The dimensions of the culverts are given in Table 4-4. When the Horstergrub stream discharge exceeds the culvert's capacity, water will flow alongside buildings towards the Dorpsstraat. Based on the flood maps of this location (Figures 4-3 and 4-4) one can observe that this is the case during both scenarios. However, model validation learned that surface runoff, especially rural surface runoff, is overestimated. Hence, this has to be taken into account during interpretation of the results.

Table 4-4: Dimensions of the culverts through which the Horstergrub stream passes the Dorpsstraat.

	Code	Length [m]	Area [m^2]	Invert level start point [m NAP]	Invert level end point [m NAP]
Culvert 1	_17100507-_17100508 _17100505-_17100508	47.73	0.19	136.90	137.69
Culvert 2	_17100505-_17100510	11.06	0.28	137.55	137.50

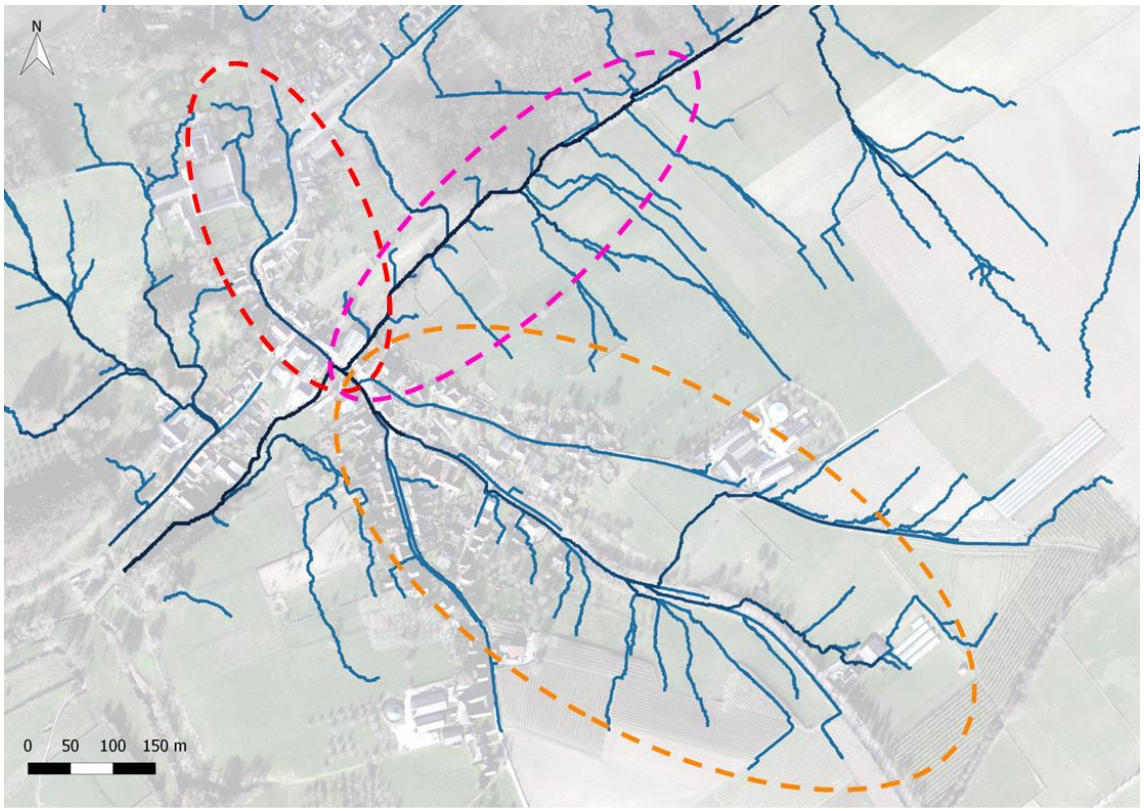

Figure 4-6: Surface flow pathways show the three areas that contribute to flooding at the Dorpsstraat.

Figure 4-7 shows the sewer discharges from the Duivenstraat and Figure 4-8 from the Noorbeekerweg towards the Dorpsstraat. The negative discharge from the Duivenstraat is a result of data input and does not have any consequences for the flow direction. These graphs show that the contribution of rainwater from the Noorbeekerweg area is larger than from the Duivenstraat. Table 4-5 gives the corresponding dimensions of these storm sewer pipelines.

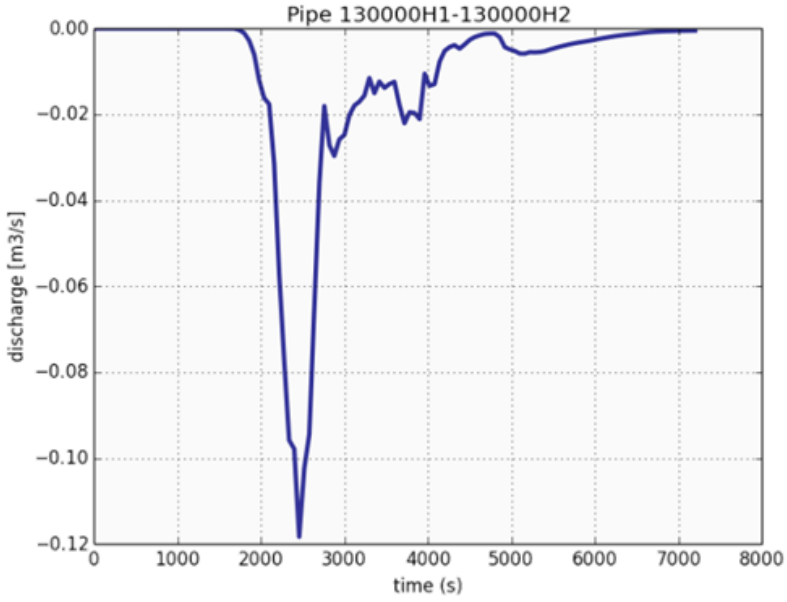

Figure 4-7: Storm water sewer discharge from the Duivenstraat to the Dorpsstraat during scenario 1.

Table 4-5: Dimensions of the storm drains of which the discharge is plotted in the Figures 4-7 and 4-8.

Code	Length [m]	Area [m^2]	Invert level start point [m NAP]	Invert level end point [m NAP]
_130000H1-_130000H2	53.89	0.08	138.98	137.57
_17100518-_17100497	28.06	0.07	142.22	141.37

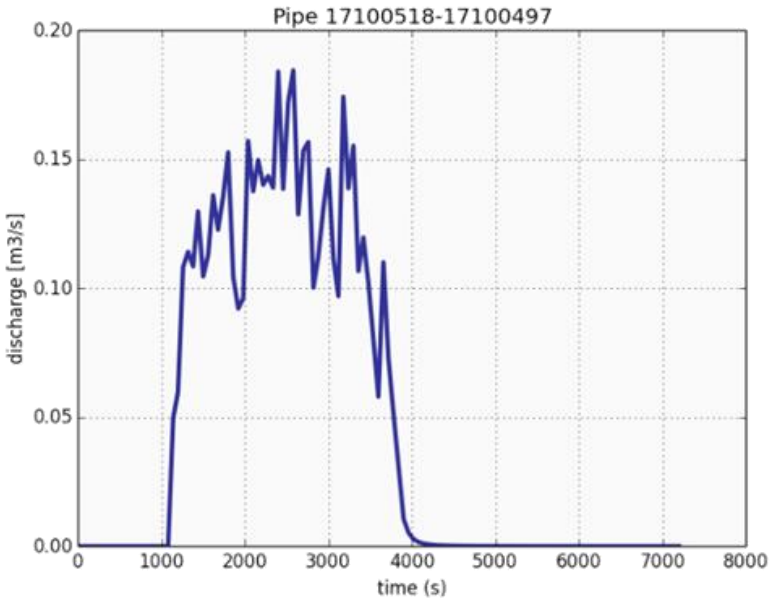

Figure 4-8: Storm water sewer discharge from the Noorbeekerweg to the Dorpsstraat during scenario 1.

At the Dorpsstraat, the discharge capacity of the storm water outlets is too small for the total amount of receiving rainwater. Especially runoff from the Horstergrub stream and the Noorbeekerweg area contribute to flooding at the Dorpsstraat.

4.3.2 Location 2: Steegstraat, Mheer

The Steegstraat in Mheer is a gently sloping street located parallel to the Horstergrub stream (Figure 4-9). There is no storm water sewer located at the Steegstraat. The wastewater sewerage pump station located at the end of the Steegstraat, pumps all the wastewater from Banholt and Mheer to the wastewater treatment plant.

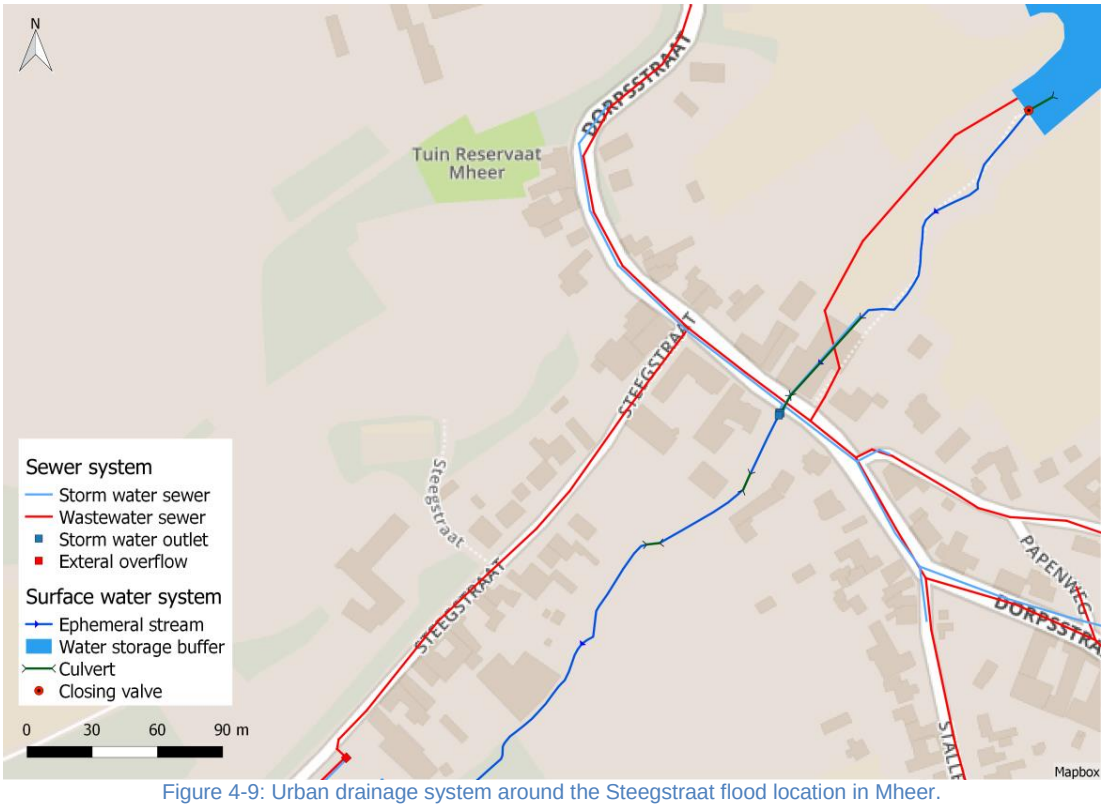

Figure 4-9: Urban drainage system around the Steegstraat flood location in Mheer.

Flood depth and duration

Table 4-6 shows the maximum average flood depths calculated at the Steegstraat during rainfall scenario 1 and 2. During scenario 1, the maximum water depth occurred directly after the peak rainfall intensity, which is after 45 minutes of rainfall. During scenario 2 the maximum flood depth emerged after 2 hours of constant rainfall. Moreover, the maximum depth caused by scenario 1 is larger than the maximum flood depth caused by scenario 2. The Figures 4-10 and 4-11 show the maximum spatial extent of the floods. As can be seen in these maps, flooding does not stay within the street profile but comes up to the front side of houses. Based on the model validation the calculated flood depths that emerge at the Steegstraat are in the correct order of magnitude.

Table 4-6: Flood depths and durations at the Steegstraat corresponding to rainfall scenario 1 and 2.

	Maximum average flood depth [m]	Simulation time [min]	Time to flood [hrs]	Flood duration [hrs]	Water depth at the end of simulation [m]
Rainfall scenario 1	0.09	45	0:15	1:45	0.01
Rainfall scenario 2	0.06	120	0:10	2:50	0.01

The times to flood and flood durations measured at the Steegstraat are given in Table 4-6. A flood depth of 1 centimetre at the end of model simulation is not considered as flooding. Therefore, the end of model simulation is also the end of flooding, which means that the given durations represent the total flood durations at the Steegstraat.

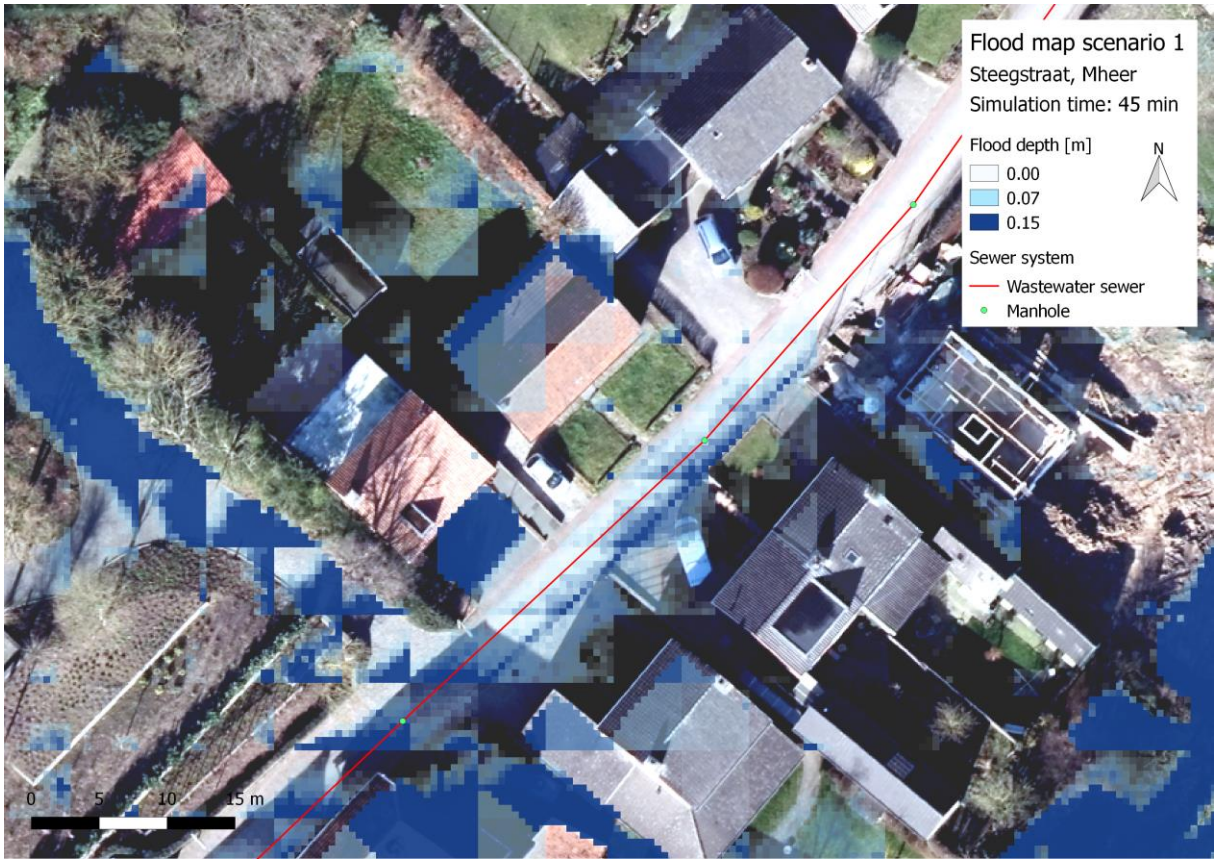

Figure 4-10: Flood map at the Steegstraat after 45 minutes of model simulation during rainfall scenario 1.

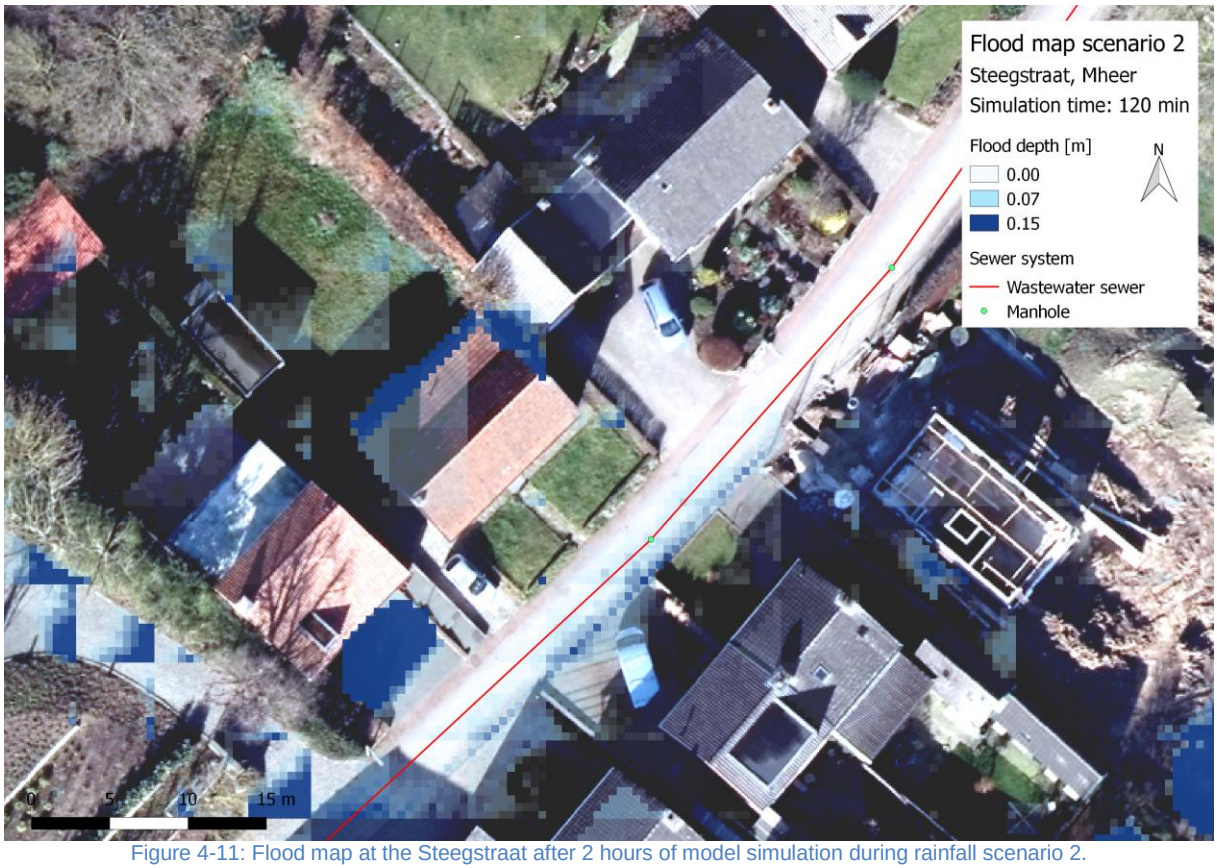

Figure 4-11: Flood map at the Steegstraat after 2 hours of model simulation during rainfall scenario 2.

Causes of flooding

The Steegstraat does not drain towards a storm water sewer. Moreover, the wastewater sewer cannot exchange flow with the surface, and only drains a small amount of upstream collected rainwater towards the sewerage pump station. Therefore, flooding at the Steegstraat is merely the result of surface runoff.

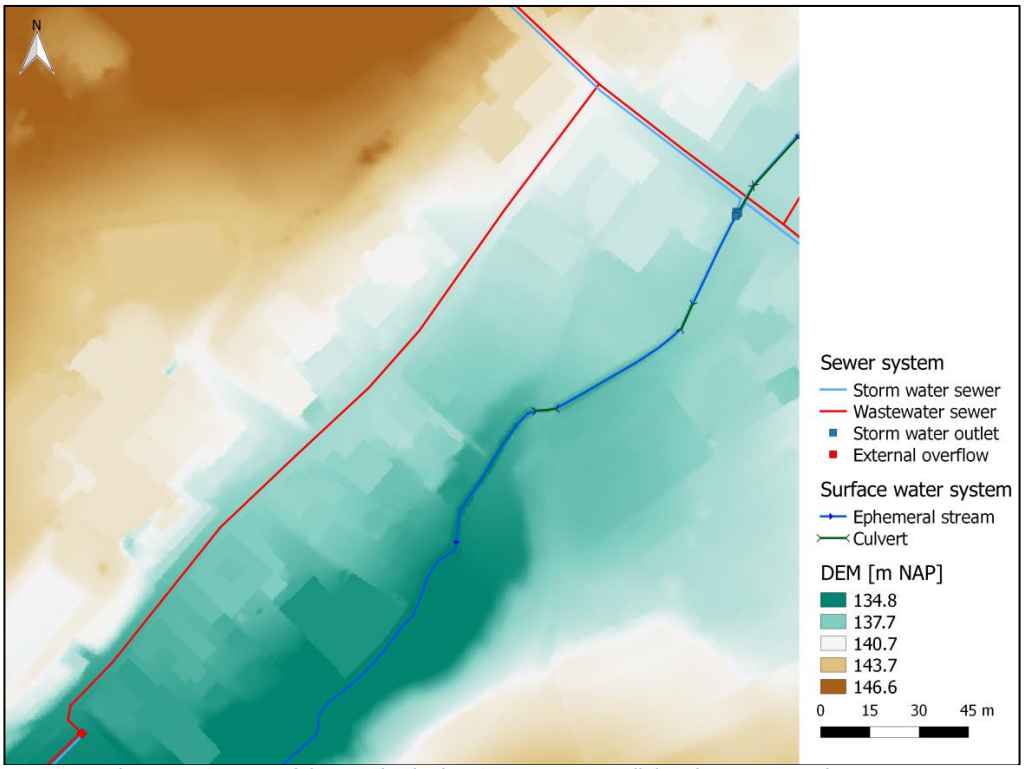

Figure 4-12: DEM of the gently sloping Steegstraat parallel to the Horstergrub stream.

Figure 4-12 shows a gently sloping Steegstraat where the houses at one side of the road (above) have a higher elevation level than the houses at the other side of the road (below). Moreover, the rural area above the Steegstraat is steeply sloped, perpendicular to the Steegstraat. Based on the DEM, flow paths are plotted to show where surface runoff could come from (Figure 4-13 and Figure 4-14). These flow paths show:

- Runoff from the Steegstraat itself towards the flood location (orange circle, Figure 4-13).
- Runoff from rural area upslope of the Steegstraat (red circles in Figures 4-13 and 4-14).

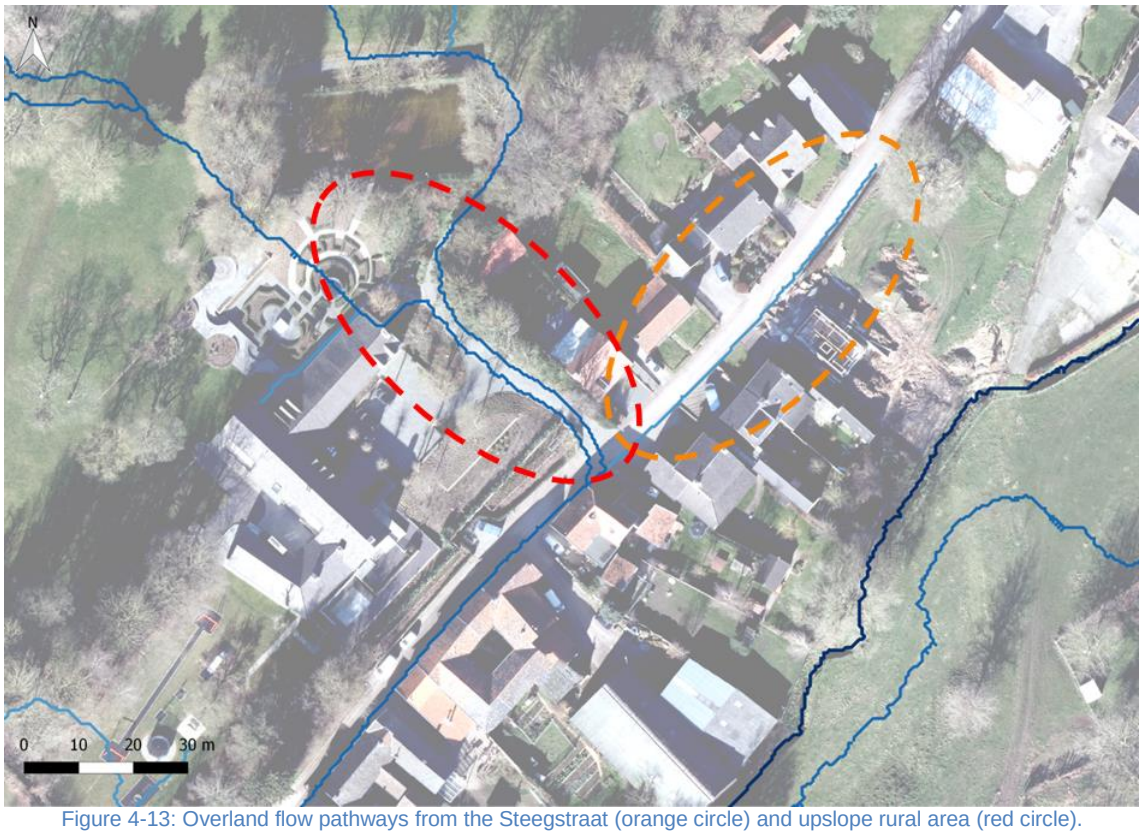

Figure 4-13: Overland flow pathways from the Steegstraat (orange circle) and upslope rural area (red circle).

The Steegstraat contributes to the emerging floods with urban runoff from the gently sloping street itself. Observing flood maps after model simulation confirms that there is no runoff from the Dorpsstraat towards the Steegstraat that could contribute to the emerging floods at the Steegstraat. Moreover, the upslope rural area contributes to flooding at the Steegstraat. This means that the amount of rainfall exceeds the interception and infiltration capacity of this area.

Quantification of these flows, to see how much each area contributes to flooding, is not possible based on the flood maps. Yet, by observing the flood maps the rural upslope area shows a higher contribution to flooding than urban runoff from the Steegstraat itself. It can be estimated that the rural runoff contributes about 90 per cent of the flooding at the Steegstraat. This results in a contribution of approximately 10 per cent by urban runoff from upslope in the Steegstraat.

Also, from the flood maps, Figure 4-10 and Figure 4-11, it can be observed that water coming from the rural area upslope, not only flows towards the flood location at the Steegstraat. It is also held upslope in local depressions, and it flows from the Steegstraat along the houses and towards the Horstergrub stream.

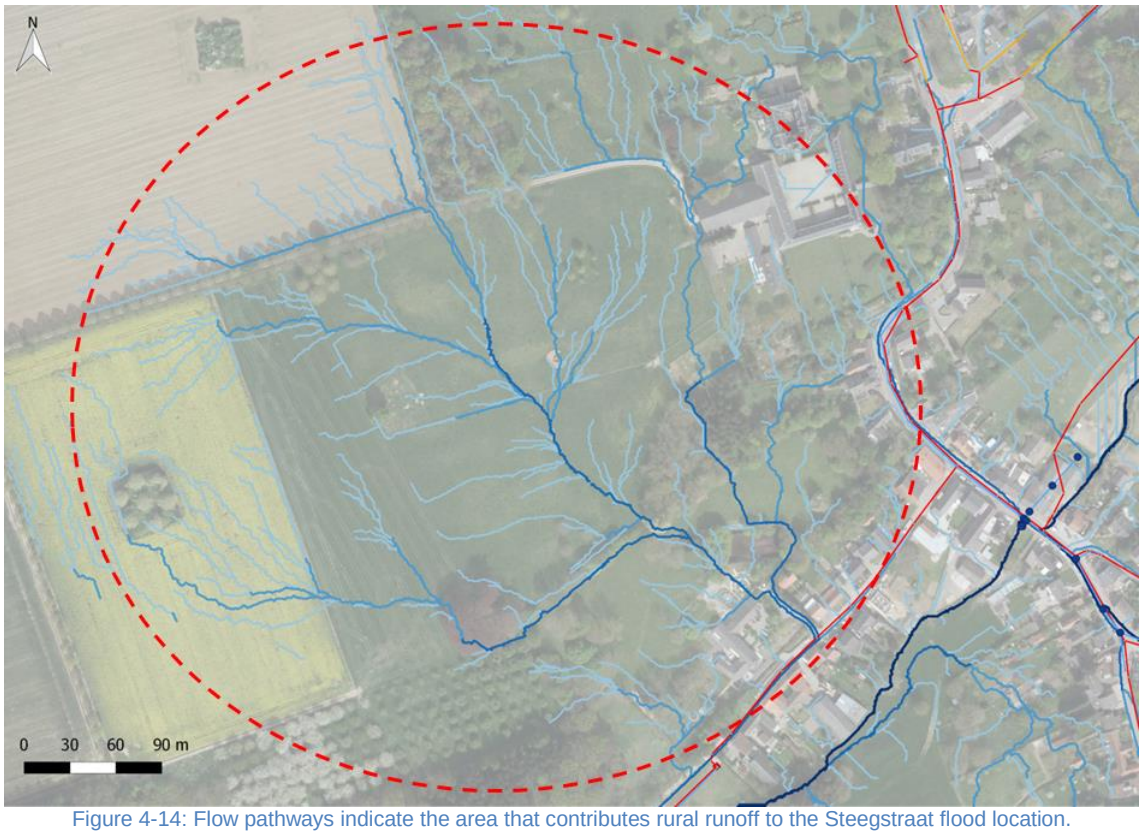

Figure 4-14: Flow pathways indicate the area that contributes rural runoff to the Steegstraat flood location.

4.3.3 Location 3: Dalestraat, Banholt

There is both a wastewater and a storm water sewer located at the Dalestraat. Here, not only the storm water sewer, but also the wastewater sewer drains part of the rainwater (Figure 4-15). The wastewater sewer drains 0.006 m^3/s from the flood location, which is only a minor flux during extreme storm events. Moreover, the Banholtergrub stream crosses Banholt at the Dalestraat.

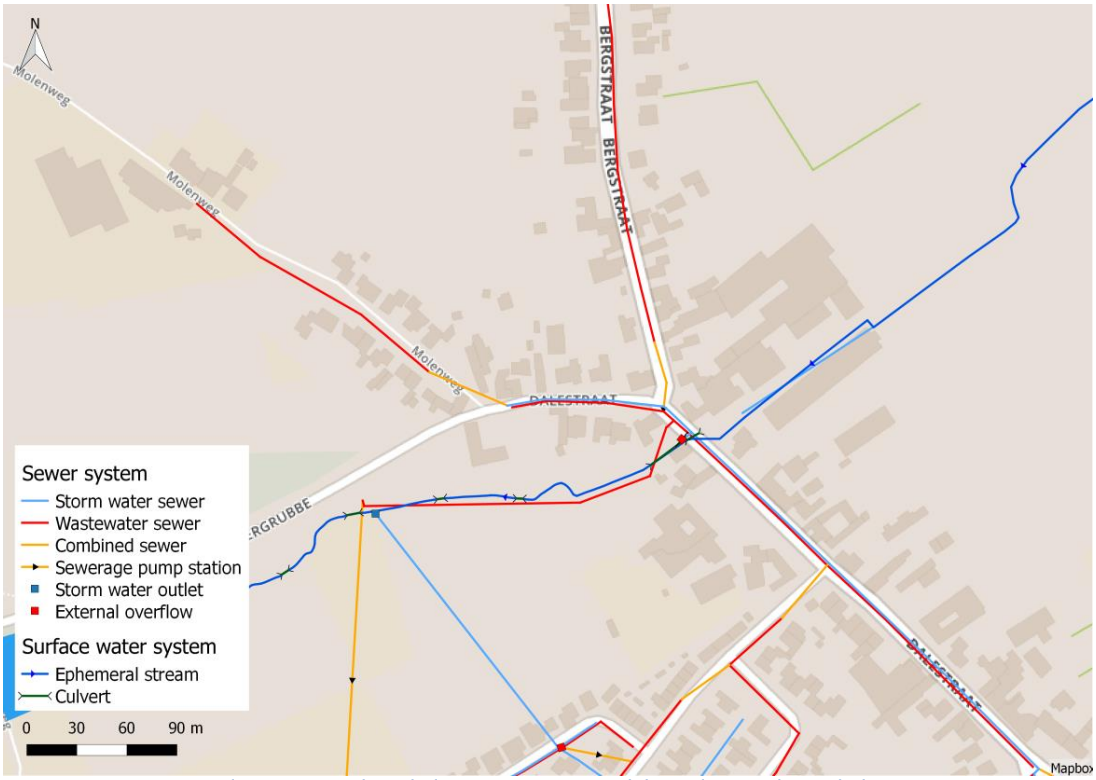

Figure 4-15: Urban drainage system around the Dalestraat in Banholt.

Flood depth and duration

The average maximum water depths calculated at the Dalestraat caused by the extreme rainfall scenarios are given in Table 4-7. The corresponding flood maps are given in the Figures 4-16 and 4-17. The maximum flood depth and extent caused by rainfall scenario 1 are larger then the flood depth and extent caused by scenario 2. In the flood map of rainfall scenario 2 (Figure 4-17) it is visible that flooding at the Dalestraat can be seperated in flooding left and right of the speedbump at the crossroad with the Bergstraat.

Table 4-7 also gives the times to flood and flood durations calculated at the Dalestraat. At the end of the model simulations there is still water left on the street during both scenarios. So, the flood duration only represents the time between the start of flooding and the end of the model simulation. The actual flood duration is longer, yet unknown.

Table 4-7: Flood depths and durations at the Dalestraat corresponding to rainfall scenario 1 and 2.

	Maximum average flood depth [m]	Simulation time [min]	Time to flood [hrs]	Flood duration [hrs]	Water depth at the end of simulation [m]
Rainfall scenario 1	0.35	45	0:19	1:41	0.09
Rainfall scenario 2	0.26	120	0:08	2:52	0.10

The external overflow located at the Dalestraat is not in operation during scenario 1 and 2. This means that with the starting points used during this research, this overflow does not contribute to flooding on street level.

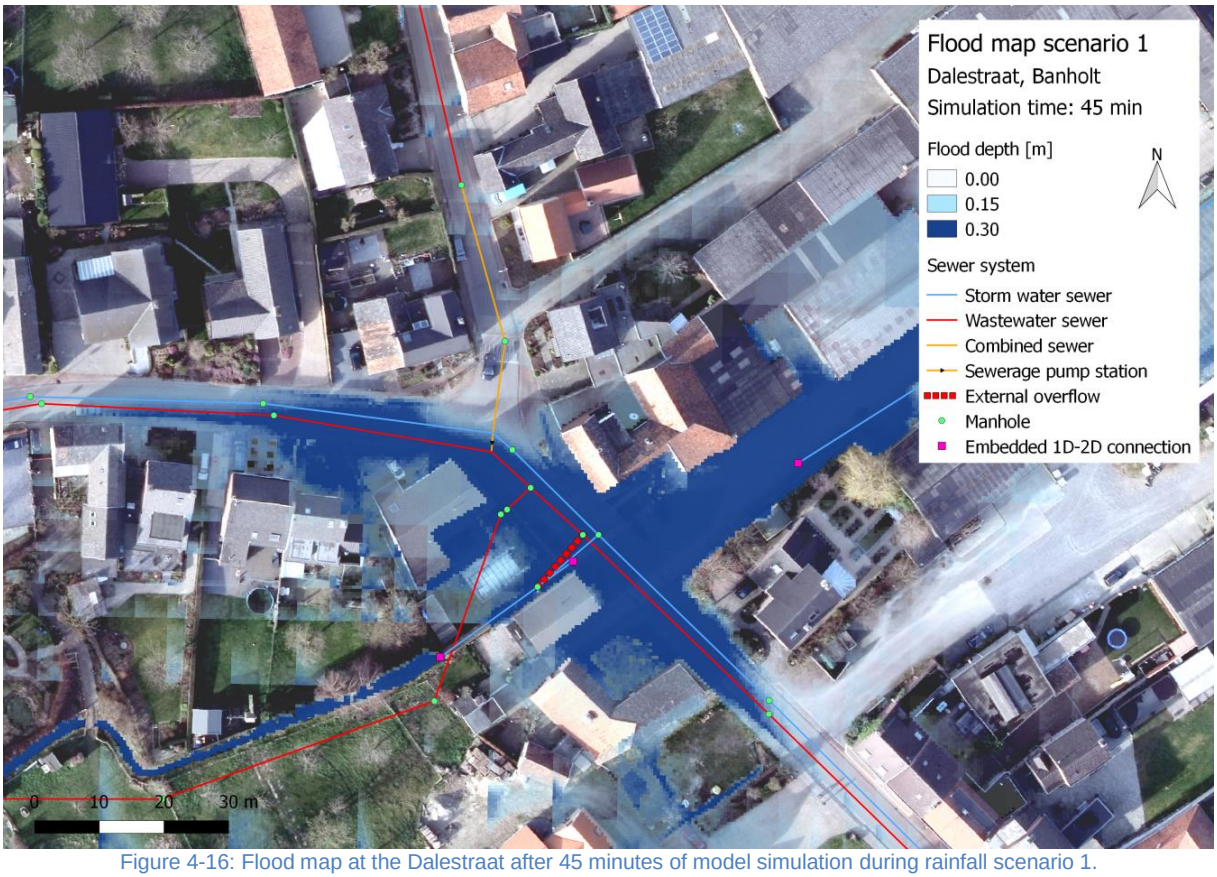

Figure 4-16: Flood map at the Dalestraat after 45 minutes of model simulation during rainfall scenario 1.

Figure 4-17: Flood map at the Dalestraat after 2 hours of model simulation during rainfall scenario 2.

Causes of flooding

Figure 4-18 shows a plot of the DEM around the Dalestraat flood location. The Dalestraat is located in the valley of the Banholtergrub stream. Also the Bergstraat area steeply slopes downwards to the flood location.

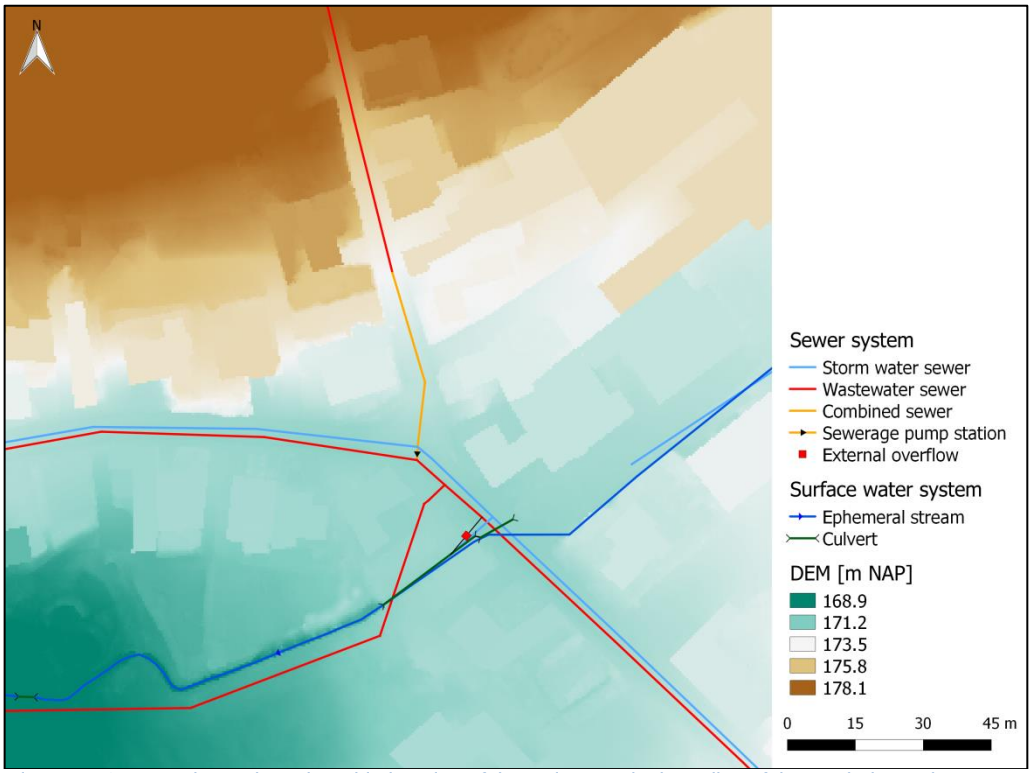

Figure 4-18: DEM shows the vulnerable location of the Dalestraat in the valley of the Banholtergrub stream.

The Dalestraat receives surface runoff from three different areas (Figure 4-19). The contribution of these areas in order of magnitude, retrieved from the various flood maps of scenario 1 and 2, is:

- Water from the Banholtergrub stream (pink circle).
- Urban runoff from the Dalestraat and Sint Gerlachusstraat (orange circle).
- Urban runoff from the upstream Bergstraat area (red circle).

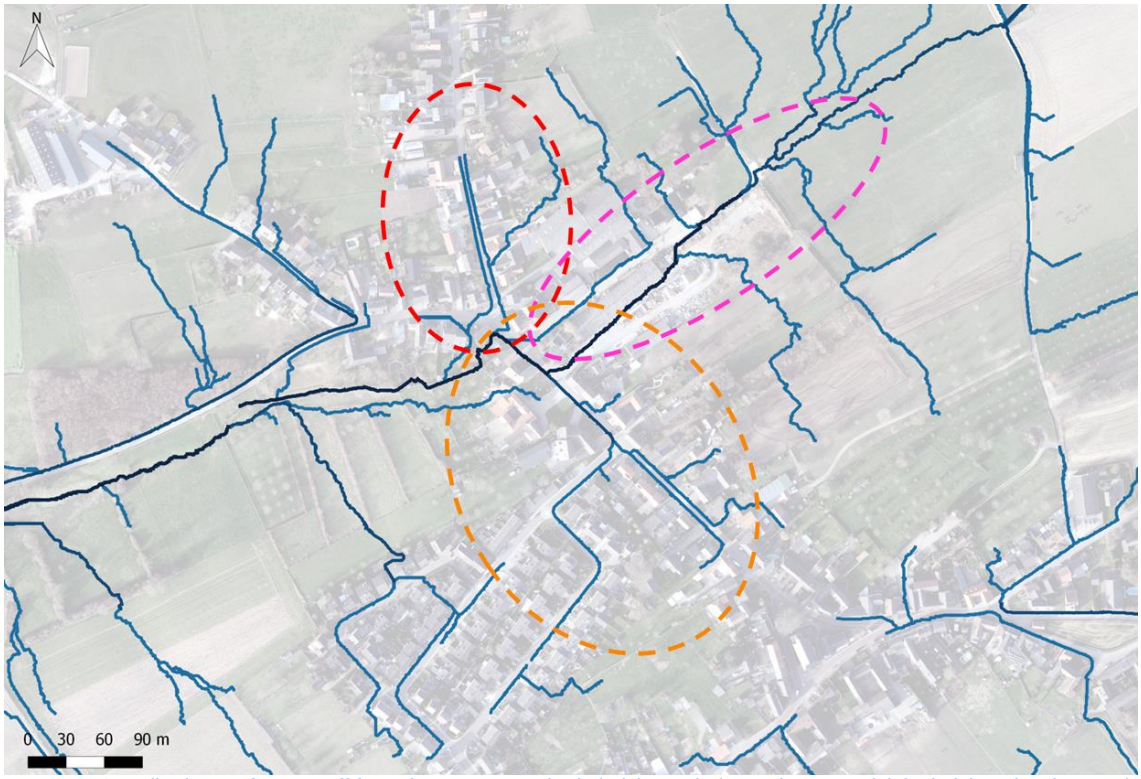

Figure 4-19: Contributing surface runoff from the Bergstraat (red circle), Banholtergrub stream (pink circle) and Dalestraat/Sint Gerlachusstraat (orange circle).

Runoff from The Banholtergrub stream crosses the village of Banholt at this flood location. In order to do so, the water first enters a concrete culvert to cross several buildings. This culvert has a total length of 92.8 meters and a rectangular cross-section of 1.0 x 0.3 meters (width x height). This culvert ends upslope of the Dalestraat. So, from here water flows over the Dalestraat and enters a concrete culvert again downslope, at the other side, of the Dalestraat. Consequently, part of the water in the street is water from the Banholtergrub stream, crossing the urban area.

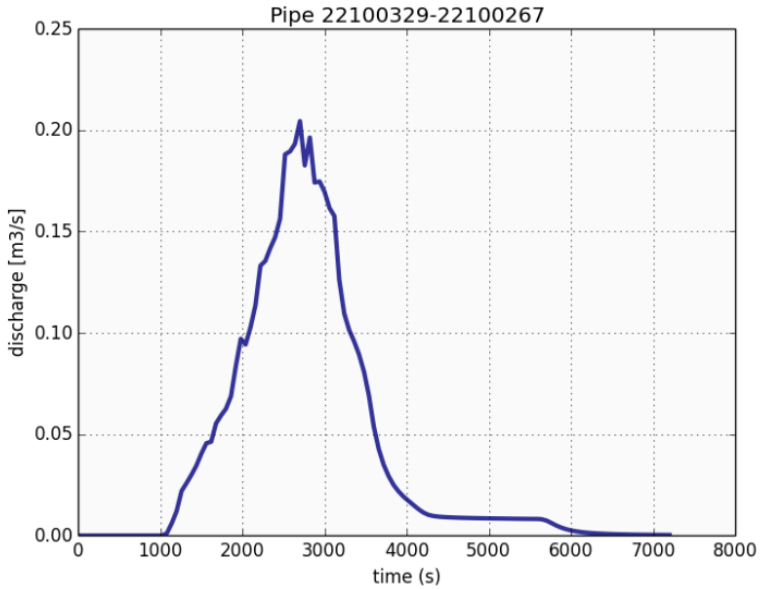

Figure 4-20: Storm sewer discharge from upslope at the Dalestraat to the flood location during scenario 1.

The amount of surface runoff from the Dalestraat and Sint Gerlachusstraat area depends on the interaction with the storm water sewer system in this area. The Figures 4-20 and 4-21 show the storm water sewer discharge from this area during scenario 1 and 2 respectively. Table 4-8 gives the dimensions of this drainage pipe. Part of the water in this area is drained by the storm water sewer. Yet, in the flood maps urban surface runoff from this area is also visible.

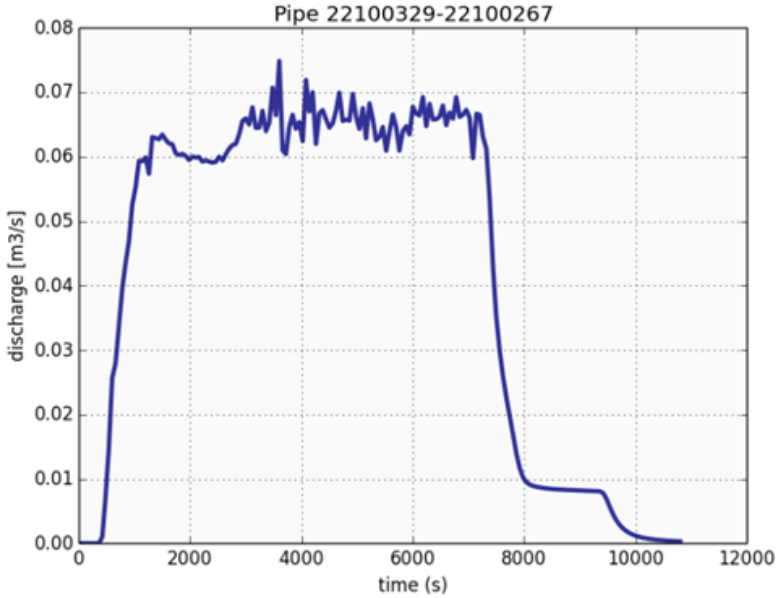

Figure 4-21: Storm sewer discharge from upslope at the Dalestraat to the flood location during scenario 2.

Table 4-8: Dimensions of the storm water pipe corresponding to the Figures 4-20 and 4-21.

Code	Length [m]	Area [m^2]	Invert level start point [m NAP]	Invert level end point [m NAP]
_22100329-_22100267	40	0.13	172.4	170.98

Surface runoff from the Bergstraat area contributes to flooding left and right of the speedbump at the Dalestraat. Right of the speedbump, it flows towards the culvert to enter the Banholtergrub stream. Left of the speed bump, water flows alongside a house, Dalestraat 51, towards the Banholtergrub stream. During both extreme scenarios, the depth of flooding at the Dalestraat is so large that the speedbump is not really an obstacle because the water level exceeds the elevation of the speed bump. During less severe flood conditions this will not be the case.

At the Dalestraat, the discharge capacities of the surface water structures of the Banholtergrub are too small for the total amount of receiving rainwater. In particular, runoff from the Banholtergrub stream and the Dalestraat/Sint Gerlachusstraat area contribute to flooding at the Dalestraat.

With the current model validation it is unknown how accurate the flood depth calculations at the Dalestraat are. Due to the significant contribution of open channel flow from the Banholtergrub stream and urban surface runoff from the Dalestraat and Sint Gerlachusstraat to flooding at the Dalestraat, flooding at this location is caused by flows comparable to the Dorpsstraat flood location in Mheer. Because of these similarities in contributing surface flows it is expected that the model overestimates the flood depth and extent at the Dalestraat.

4.3.4 Location 4: Pastoor Engelenstraat, Banholt

The Pastoor Engelenstraat in Banholt has a small storm water sewer system that drains towards the nearby located Banholtergrub stream (Figure 4-22). Also, at this flood location there is an external overflow from the wastewater to the storm water sewer.

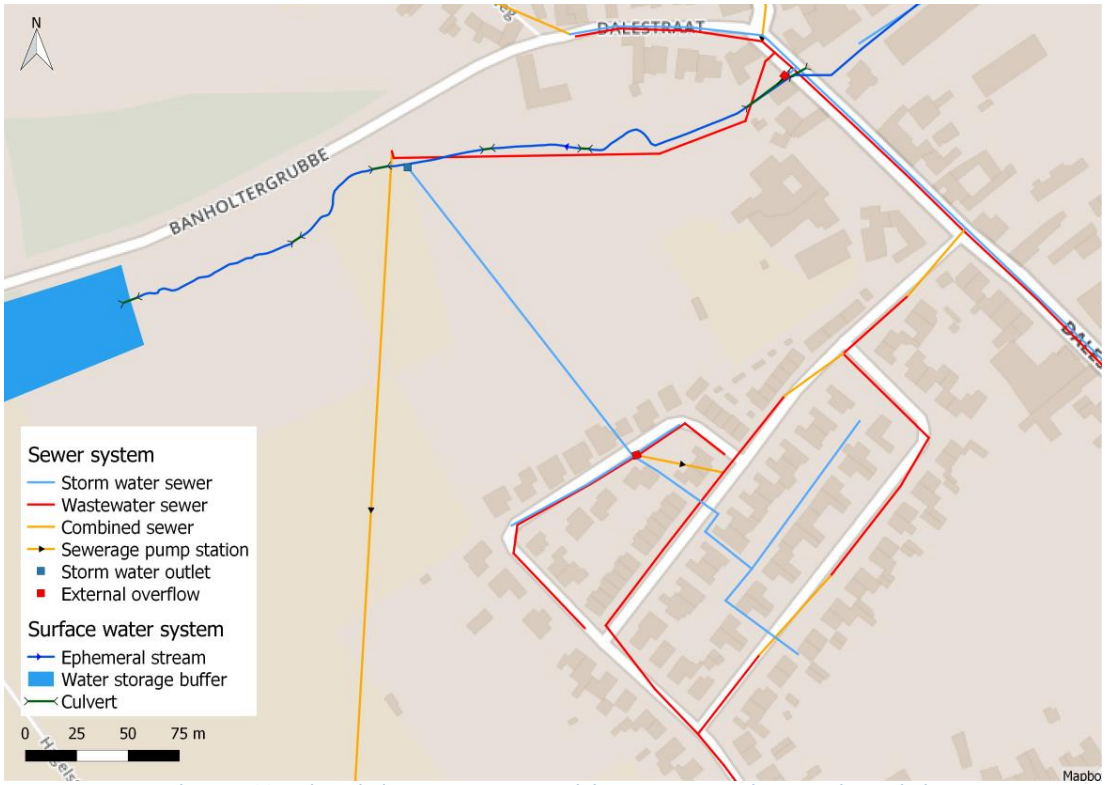

Figure 4-22: Urban drainage system around the Pastoor Engelenstraat in Banholt.

Flood depth and duration

Table 4-9 gives the maximum average flood depths calculated at the Pastoor Engelenstraat corresponding to scenario 1 and 2. Moreover, Figures 4-23 and 4-24 give the corresponding flood maps of scenario 1 and 2 respectively. The flood depth and extent of scenario 1 are, again, larger than the depth and extent of scenario 2.

The calculated times to flood (Table 4-9) are significantly larger at the Pastoor Engelenstraat compared to the other flood locations in the research area. At the end of the model simulation average flood depth is 3 centimetres. Considering that the street has a sidewalk which is about 5 to 10 centimetres higher than the road, a flood depth of 3 centimetres can be considered as the end of flooding. Therefore, the flood durations given in Table 4-9 represent the total flood durations calculated with the 3Di model.

Table 4-9: Flood depths and durations at the Pastoor Engelenstraat corresponding to both rainfall scenarios.

	Maximum average flood depth [m]	Simulation time [min]	Time to flood [hrs]	Flood duration [hrs]	Water depth at the end of simulation [m]
Rainfall scenario 1	0.43	45	0:55	1:05	0.03
Rainfall scenario 2	0.37	120	0:41	2:19	0.03

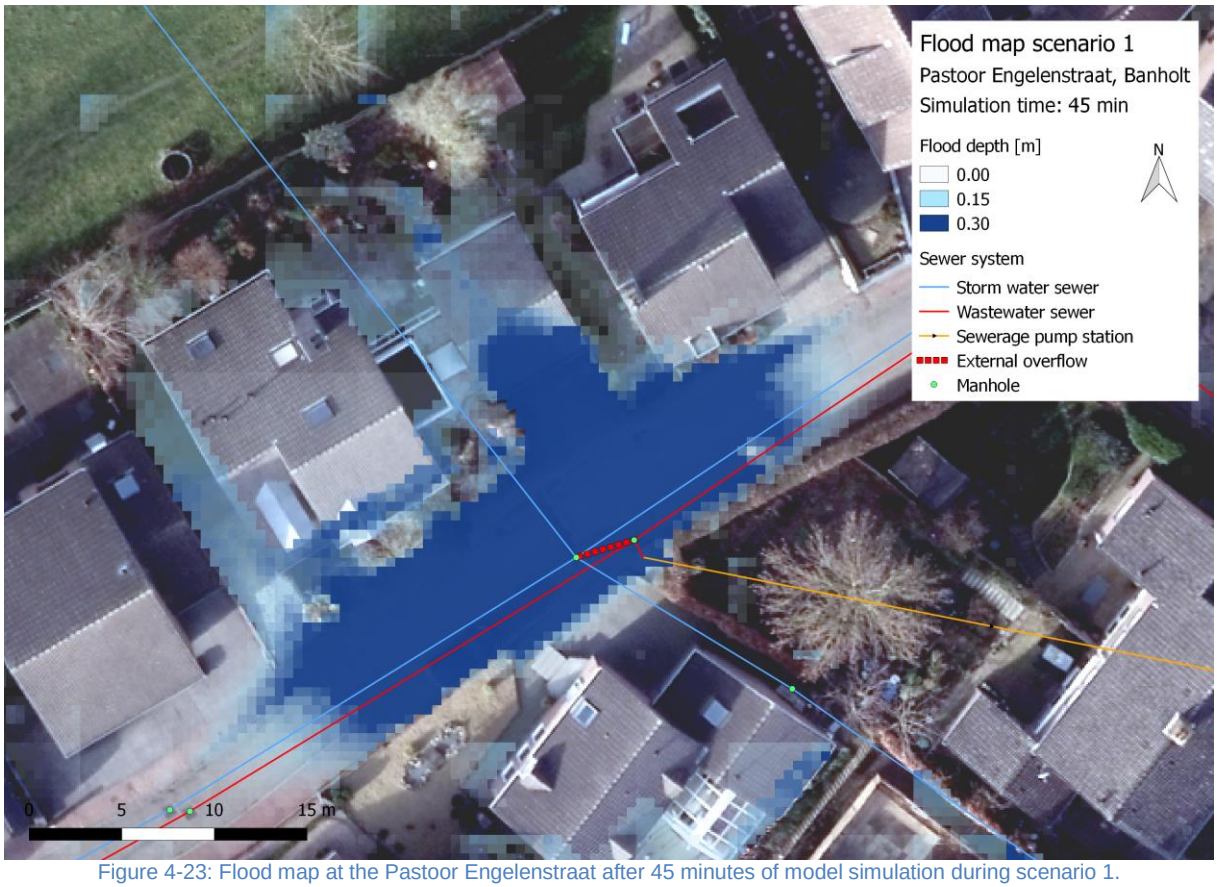

Figure 4-23: Flood map at the Pastoor Engelenstraat after 45 minutes of model simulation during scenario 1.

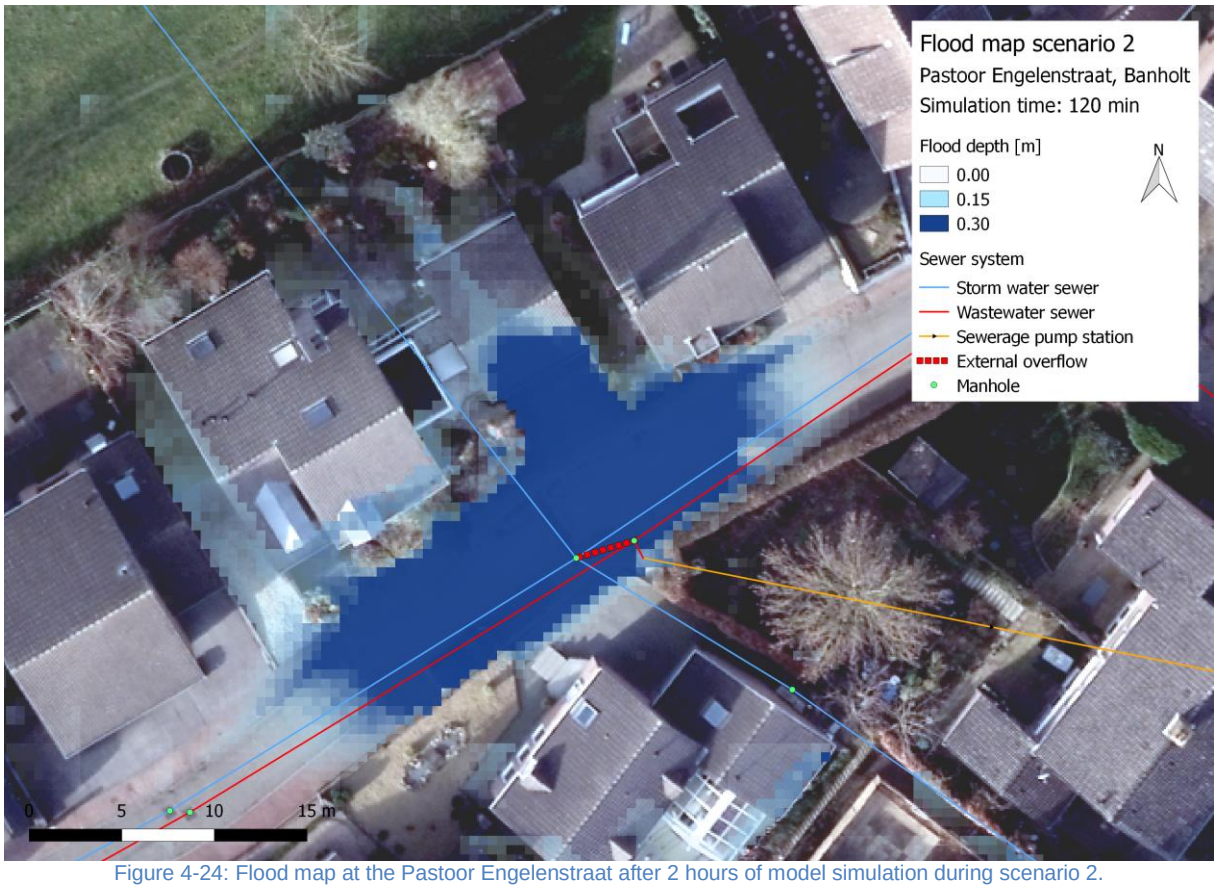

Figure 4-24: Flood map at the Pastoor Engelenstraat after 2 hours of model simulation during scenario 2.

Causes of flooding

The DEM in Figure 4-25 shows that the flood location at the Pastoor Engelenstraat coincides with a local depression. Rainwater outflow from this depression is only possible through the storm water outlet that drains towards the Banholtergrub stream.

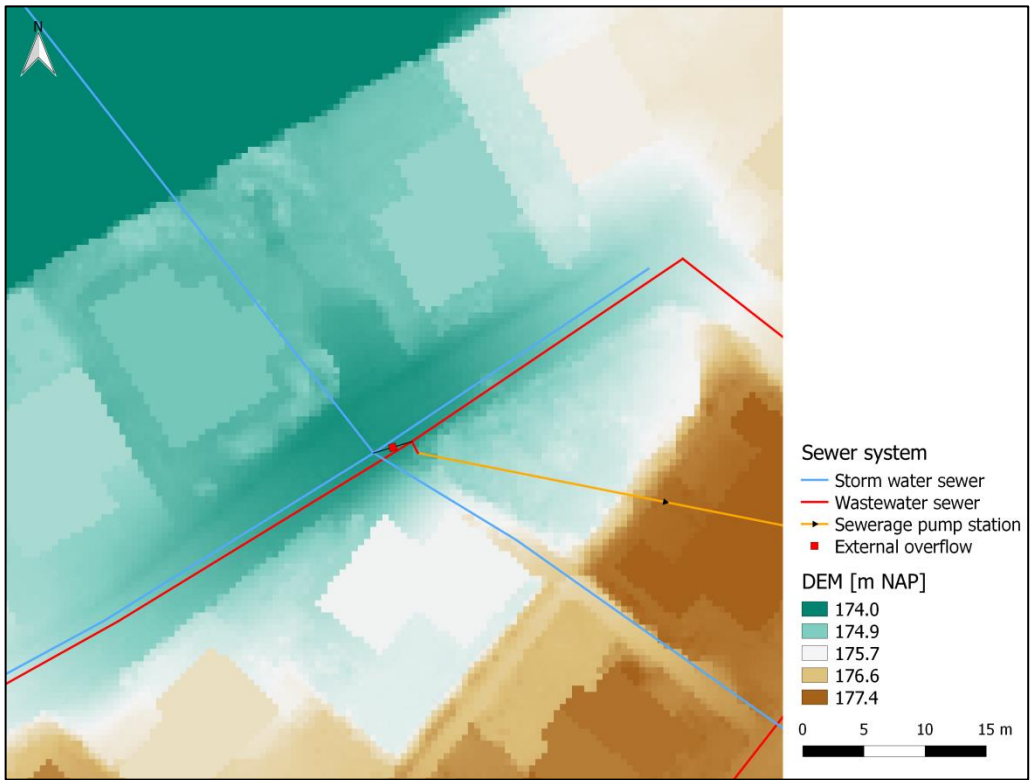

Figure 4-25: Plot of the DEM shows the local depression at the Pastoor Engelenstraat in Banholt.

Figure 4-26 shows the discharge through the storm water outlet during rainfall scenario 1. Correspondingly, Table 4-10 describes the outlet dimensions. Since the depression fills up with water, it is possible to state that the inflow towards the location is larger than the outflow capacity of the storm water outlet. As the outlet is the only outflow location, this can be regarded as the bottleneck.

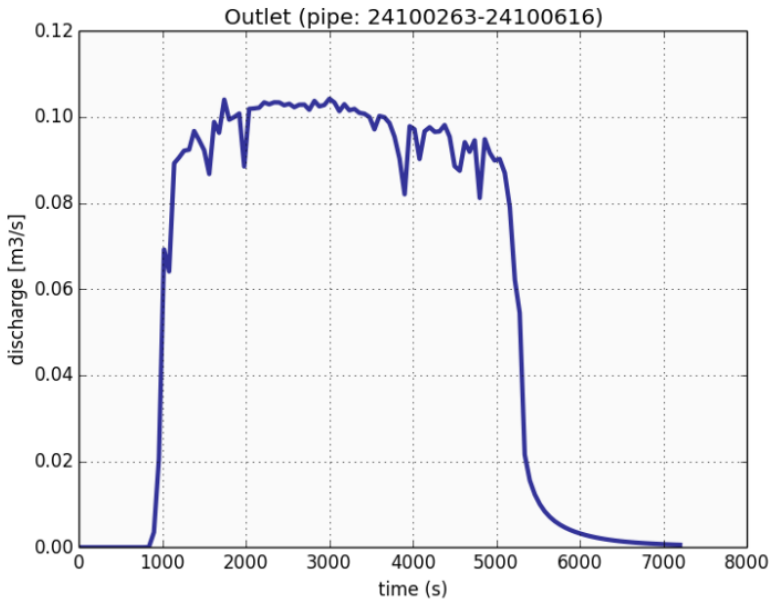

Figure 4-26: Discharge through the outlet at the Pastoor Engelenstraat during rainfall scenario 1.

Table 4-10: Dimensions of the storm water outlet that drains towards the Banholtergrub.

Code	Length [m]	Area [m^2]	Invert level start point [m NAP]	Invert level end point [m NAP]
_24100263-_24100616	178.20	0.07	172.04	166.16

Water can flow towards the Pastoor Engelenstraat either as urban surface runoff or as storm sewer flow. The water levels in the storm sewer manholes at and directly around the flood location are equal, which shows that the discharge through the sewer towards the flood location is very small to zero.

Also, the external wastewater overflow is in operation, which means that rainwater from the wastewater sewer flows over to the storm water sewer. During both scenarios the overflow is in operation with an average discharge of 0.0025 m^3/s. With this small amount the overflow does not contribute significantly to flooding at the Pastoor Engelenstraat. Yet, may cause health issues when taking into account wastewater discharge.

This means that urban surface runoff is the main contributor to flooding at the Pastoor Engelenstraat. Urban surface runoff towards the local depression indeed occurs during both scenarios. It is estimated that surface runoff contributes to flooding at the Pastoor Engelenstraat by at least 95 per cent. Most of the rainwater follows the street profiles (Figure 4-27). Only at the height of Sint Gerlachusstraat 23-25 water leaves the street and runs along the houses towards the local depression at the Pastoor Engelenstraat.

With the current model validation it is unknown how accurate the flood depth calculation at the Pastoor Engelenstraat is. Different than at other locations flooding at the Pastoor Engelenstraat is merely fed by urban runoff. Also, the time to flood is significantly longer at this location than the other flood locations.

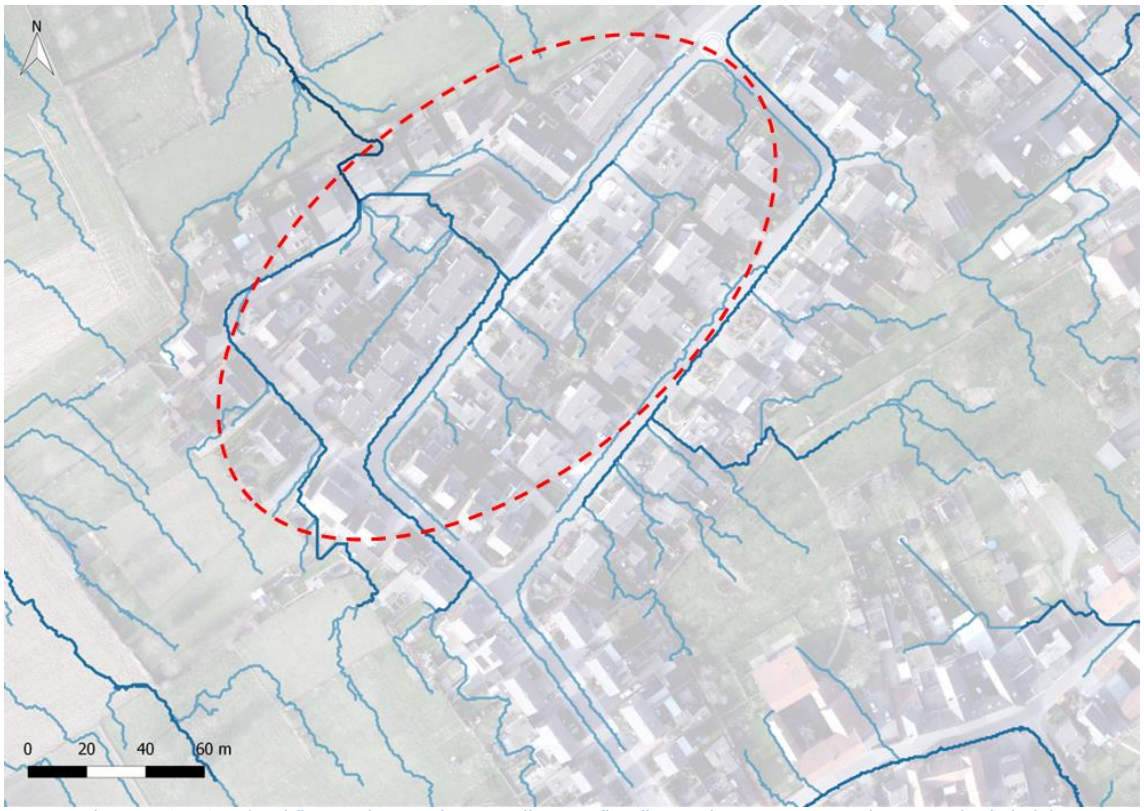

Figure 4-27: Overland flow pathways that contribute to flooding at the Pastoor Engelenstraat (red circle).

5. Discussion

5.1 Model performance and assumptions

5.1.1 Rainfall runoff distribution

The percentage of runoff simulated with our models is probably on the high side; the 3Di model calculates percentages of 60 and 50 per cent for respectively scenario 1 and 2. According to the water authority, surface runoff percentages in the area would typically lie in the range of 20 to 30 per cent, with a maximum of 50 per cent during extreme rainfall. The Limburg Soil and Erosion Model (Lisem) simulates a runoff coefficient of 18 per cent for a T25 event, and 34 per cent for a T100 event. The rainfall characteristics of a T100 event would be in line with scenario 1 and 2. Yet, the runoff coefficient calculated with Lisem is lower than the coefficients calculated with 3Di. However, comparison of the 3Di and Lisem percentages is difficult as they both represent different model flows. The 3Di runoff percentage represents all the surface and sewer flows present in the model, including temporary stored water. While the Lisem runoff coefficient represents merely surface runoff from a sub-catchment towards a storage buffer, retrieved with a model of a single buffer and contributing catchment. This could partly explain the higher 3Di runoff percentages.

In the model, infiltration is accounted for with a constant infiltration capacity without any saturation limit. However, the influence on the model results is limited, because of the short simulation times. Also, the chosen infiltration capacity of 480 mm/day is arguable. Experts from the water authority estimate that 240 mm/day would be a more appropriate value. As a result, infiltration is overestimated during rainfall. However, because the subgrid technique assumes one water level per calculation cell, the infiltration rate is underestimated during the last dry hour of model simulation. This could contribute to the overestimation of the calculated runoff percentages. Yet, there is no data available to examine this further.

The 3Di model calculates an initial interception of 6 per cent and 3 per cent for respectively scenario 1 and 2. According to (Gerrits 2009), about 20 to 40 per cent of rainfall is intercepted. Yet, this is an average annual percentage that does not represent extreme rainfall events well. During extreme storm events especially in sloping areas, the interception percentage will be lower. How well 3 to 6 per cent represents the interception flux is uncertain.

5.1.2 Urban flood locations

The flood locations that emerge during model simulation correspond well with historical observations. The urban locations presented in Chapter 4 are well known by the municipality as flood prone. During both extreme scenarios flooding also emerged at the Herkenradergrubbe. This is comparable to the experience of 18 August 2011. This location (Figure E-2) is excluded from the urban flood analysis due to its rural location. Nevertheless, the emergence of flooding at this location is correct.

Evaluation of the model results combined with the model performance would imply that the maximum average flood depths at the Dorpsstraat and Dalestraat are significant overestimations. Here, flood depths are overestimated with at least a factor two. These overestimations are the result of overestimations in surface runoff discharges. At the Steegstraat model calculations result in flood depths comparable to reality. However, this is probably caused by incorrect upslope water storage and inaccurate runoff routing towards the Horstergrub stream.

The time to flood is significantly longer at the Pastoor Engelenstraat compared to the other flood locations. It is expected that runoff routing and velocities are more accurate in the urban areas due to a combination of smaller calculation cells and on average smaller slopes in the streets of the villages. This would suggest a flood depth in a more correct order of magnitude at the Pastoor Engelenstraat, as this location is purely fed by urban surface runoff.

5.1.3 Rainfall runoff routing

For surface runoff routing 3Di solves the momentum equation in two dimensions for each time step. The subgrid method 3Di uses to solve these equations efficiently, has an impact on the flow pathways and runoff dynamics.

Flow pathways

The main flow paths calculated with 3Di seem reasonable, based on the emerging flood locations. However, local deviations occur, as a result of the way 3Di calculates discharges between calculation cells. Due to the subgrid technique small obstacles located within one calculation cell, such as houses or street curbs, can be passed over. For example, at the Steegstraat it is observed that water not only flows towards the flood location, but is also stored upslope in local depressions near buildings. Moreover, due to the assumption used to represent the floor levels of buildings in the DEM, rainwater flows over houses, causing deviations in the flow paths. This results in less runoff towards the Steegstraat flood location and more towards the Horstergrub stream.

Runoff dynamics

At the Dorpsstraat in Mheer and Dalestraat in Banholt there are significant deviations in observed and simulated flood depths. The overestimation of the simulated flood depths is significantly influenced by discharge from the Horstergrub and Banholtergrub streams. In rural areas, including these streams, too much water travels downslope too fast during model simulation.

The overestimation of the volumetric overland flow rate (Q) is caused by an overestimation of the flow through cross-section at the border between the calculation cells. This overestimation in cross-section emerges, because 3Di assumes one water level per calculation cell. By solving the momentum equations 3Di determines the amount of Q that can flow between cells. Per time step, water can flow from one calculation cell to the next. The amount of water that can flow from one cell to the next is calculated by the velocity times the cross-section of the calculation cell. Or shortly: $Q = u * \Delta h * B$.

The depth (Δh) of the cross-section can be heavily overestimated during 3Di calculations in sloping areas, as can be seen in Figure 5-1. Also, the steeper the slope in one calculation cell, the larger the flow-through surface becomes hence the larger the overestimation in runoff discharge.

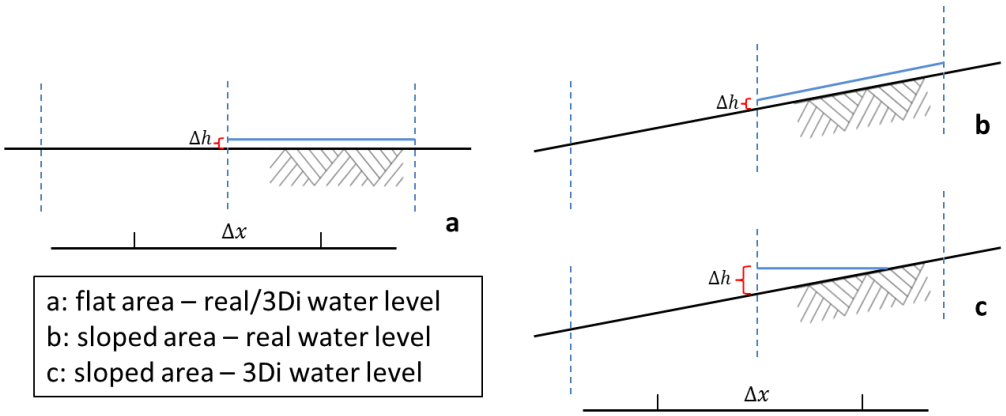

Figure 5-1: Water levels in flat and sloping areas with corresponding cross-section depths (Δh).

5.1.4 Surface-sewer interaction

At three of the four urban flood locations the sewer system plays an important role, both for the flood magnitude and flood duration. Consequently, taking into account the surface-sewer interaction is of added value for accuracy of the urban flood analysis results.

Flow exchange is assumed between the sewer manholes and the surface, however in reality this exchange occurs predominantly through sewer inlets. This assumption is regularly applied in 1D-2D urban drainage analyses because this reduces the number of calculation points (e.g. Mark et al. 2004; Hsu et al. 2000). Moreover, data about the sewer inlets was not available. Therefore, exchange through the manholes was the best possible option.

Rainwater can flow past sewer inlets due to high flow velocities, especially in sloping areas. In the model this can also occur because the location of inlets and manholes can differ within calculation

cells. Inlets are usually located at the lowest point of a street profile, while manholes are usually located in the middle of a street. The impact of this differentiation will be larger in sloping areas compared to flat ones.

In reality, part of the buiding roofs in the research area drain directly to the wastewater sewer. In total this is an area of 38,834 m^2 of impervious surface, which is 11 per cent of all the paved surfaces in the research area. In the model, these buildings drain onto the surface. This assumption might have a small impact on the model results.

5.2 Model calibration and validation

The model results are associated with a high level of uncertainty, since the model is not calibrated and limitedly validated. According to the water authority, the amount of runoff is too high. Yet, whether this is correct and means that infiltration or interception, or both, are underestimated is uncertain. This uncertainty is caused by a lack of field data. Calibration and validation of the rainfall runoff fluxes is required for an increase in reliability of the model results.

According to scholars, a lack of calibration and validation data is one of the main obstacles of 1D-2D dual drainage modelling (e.g. Chen et al. 2009; van Dijk et al. 2014; Mignot et al. 2006). For calibration, such models require data on in-sewer water levels and discharges, and data from overland flooding events (ten Veldhuis 2010). Yet, overland flow occurs infrequent and especially for sloping areas it is difficult to predict discharges of rural areas, specifically for extreme events (van Dijk et al. 2014; ten Veldhuis 2010). Additionally discharge measurements of open channel streams can be used for calibration and in this research area the water levels in the water storage buffers.

Due to this lack of data, knowledge of the model's sensitivity to change in important parameters is of added value. The overestimation in overland flow discharge has the largest impact on the model results. Therefore, model parameters that could reduce this overestimation should be analysed. Based on the momentum equation, this analysis should focus on the calculation grid size ($\partial x \; and \; \partial y$) in relation to time step size (∂t), and the surface roughness coefficient (c_f).

The calculation grid is not a calibration parameter, but the combination of calculation grid cells and time step size is of impact on the speed of hillslope runoff. There are various options possible to improve the current model performance by altering the calculation grid. For example, model performance will probably be improved if the calculation grid is refined at the surface water streams comparable to studies by Dahm et al. (2014) and Verhoeven (2013). Also, grid refinement based on a maximum allowed bathymetry difference per calculation cell could result in a calculation grid that improves the model performance. Yet, because water can only flow from one calculation cell to the next, it is also important that the calculation cells are not too small in relation to the flow velocities and time step size.

Surface roughness impacts the runoff velocity, and can be used for model calibration. However, for significant reduction of the water level in a storage buffer and a delay in surface runoff, friction values might have to be increased with a factor 10 to 50. When applied uniformly to the research area, this would yield an unrealistically high time to peak.

To improve the model performance by roughness calibration a non-uniform friction layer would be required. This layer should have high friction values at the steep rims and open channel roughness values at the location of the surface water streams. Another improvement option would be to include the surface water system as a 1D component in the model. This way, the calibration of open channel flow and hillslope runoff can be separated.

5.3 Research scope and limitations

For sloping areas in the Netherlands and abroad, 3Di can be of added value as a decision support tool. Yet, up till now the suitability of the 3Di modelling toolbox for urban pluvial flood modelling in sloping areas is only based on the case study performed during this research. This case study demonstrates the applicability of the 3Di toolbox in moderate to strongly sloping catchments with an ephemeral character. Furthermore, the research area comprises of two small villages in a larger rural

contributing catchment. The combination of these aspects is very site specific for the south of Limburg. In a rural catchment hydrological processes have a bigger role than in a fully urbanized and paved catchment. Therefore, these characteristics have an impact on the modelling choices made during this research.

Also, in this research 3Di is only used to analyse the impact of flood in time and space. Eventually, the municipality and water authority are interested in a modelling tool that can predict the magnitude of flooding, corresponding consequences and the impact of possible measures. The 3Di toolbox is capable of this. Nonetheless, it is outside of the scope of this research.

In this research the surface water system is of ephemeral character and therefore included in the 2D flow component of the model. In case of perennial streams it would not be possible to account for the surface water system in the 2D component of the model. Then the surface water system has to be included as a 1D system. An advantage of one-dimensional inclusion of the surface water is easier inclusion of the surface water structures compared to two-dimensional representation of the surface water system.

Moreover, the relatively small bottom slope condition of De Saint Venant equations is not fully met in sloping areas. Yet, two pilot projects, one in Taiwan and one in Singapore showed that the rainfall runoff distribution of 3Di can provide acceptable results in moderately sloping urban catchments after model calibration (see Dahm et al. 2014; Verhoeven 2013).

This research focuses on storm events with high intensity and short durations. Moderately long storm events have a completely different impact on the research area. During moderately long storm events subsurface flow could play a role in the rural runoff dynamics. Therefore, the current model cannot be used to analyse this type of extreme rainfall.

6. Conclusion & recommendations

6.1 Conclusion

This thesis presents an urban flood analysis of the contributing catchments of Banholt and Mheer, with a 1D-2D dual drainage 3Di model. The theoretical background in Chapter two provides an overview of the hydrological and hydraulic processes that play a role during extreme storm events. Moreover, this chapter explains how 3Di accounts for these processes. Chapter 4 gives an overview of the urban flood locations in Banholt and Mheer. Also, this chapter describes the magnitude and the causes of flooding at these locations, and provides insight in the contributing overland flow pathways. Based on the results in Chapter 4 and the discussion of the results in Chapter 5, this chapter provides an answer to the main research question:

What is the hydraulic behaviour of storm water in sloping areas during extreme rainfall, and how can the 3Di modelling toolbox contribute to assess the causes of urban pluvial flooding?

In the research area, a large part of the rain that falls during the rainfall scenarios 1 and 2 becomes surface runoff. The pathways and amount of runoff depend on catchment characteristics and rainfall patterns. From the model results it can be concluded that the magnitude of flooding has a strong relationship with rainfall intensity. Still, interception and infiltration are hydrological processes that should be taken into account during the urban flood analysis.

In Banholt and Mheer, a location appeared to be flood prone by a combination of its location and the surface water or storm water sewer structures present. All the locations are located either in the surface water stream valleys, a local depression or have a steep upslope contributing runoff area. As a result, these areas receive significant volumes of overland flow. Combined with a sewer or surface water structure with a limited outflow capacity this results in flooding. The analysis with the 3Di model provides insight in the flood prone locations and the magnitude and causes of flooding at these locations. Hence, added value of 3Di can be found in the possibility to include both 1D sewer flow and 2D surface flow simultaneously. Inclusion of both systems, and their interaction, is of added value because most flood locations in the research area appeared to be flood prone due to a contribution of both systems.

The subgrid method of 3Di makes it possible to include the whole contributing catchments in the model without too much loss of calculation speed. Including these whole catchments showed that rural runoff and open channel flow contribute to flooding in the research area, and is therefore of added value in the urban flood analysis. Also, with the subgrid method 3Di can account for various functional land use types at a small spatial scale. This way, 3Di can account for spatial variation within a research area.

After model simulation, flood maps can be plotted of each desired time step during model simulation. These flood maps are of high-resolution because of the high spatial resolution 3Di can cope with, which is of added value for the urban drainage managers. Also, from these maps the largest contributing overland flow pathways can be derived. Insight in these pathways is required to define the causes of flooding.

3Di modelling contributes to analysing the causes of pluvial flooding by its two-dimensional surface runoff routing, and the interaction between 1D sewer flow and 2D surface flow. However, with the current model performance the volume and speed of rural surface runoff are significantly overestimated. To improve the contribution of the current 3Di model for the urban flood analysis in the area, model calibration and validation is recommended.

6.2 Recommendations

The recommendations that follow from this research are subdivided into recommendations to improve the currently existing model for the case study and recommendations that focus on the improvement of the 3Di toolbox for sloping areas.

6.2.1 Recommendations Banholt - Mheer

Most importantly, improvement of the model performance is required to increase the reliability of the results and the usability of the 3Di model for the municipality and water authority. To achieve improvement of surface runoff, the following steps are recommended:

1. Analyse the impact of the calculation grid in combination with the time step size on hillslope runoff to select a more suitable calculation grid. Consider grid refinement by a maximum allowed bathymetry difference for the rural areas.
2. Consider implementation of the surface water streams in the 1D component of the model, even though they are of an ephemeral character. This will improve the roughness calibration possibilities of the model.
3. After selection of a more suitable calculation grid, hillslope runoff should be calibrated with use of the friction parameter.

Model improvement should be seen as an iterative process. Currently there is not enough data available to fully calibrate and validate the model performance. Therefore collection of field measurements during flood events is recommended. These measurements should at least contain flood information such as location, flood depth and extent, flood duration, consequences of flooding and experienced problems. Additionally, the collection of stream discharge measurements upstream of the urban flood locations would be recommended. Also, complaints of inhabitants can be recorded in addition to field measurements.

For the municipality it is recommended to use an improved 3Di model to analyse the consequences of flooding and to assess the effectiveness of possible flood risk reduction measures. For this purpose, calibration and validation of sewer flow is recommended to ensure an accurate connection between the surface and sewer system at the flood locations. Sewer measurements, such as storm water outlet discharges, of the municipality could be used for this.

6.2.2 Recommendations for 3Di in sloping areas

In its current form 3Di is suitable for urban pluvial flood analyses in sloping areas, yet improvements are possible. The most influential aspect of 3Di on urban flood modelling in sloping areas is the use of the subgrid technique combined with the assumption that water levels could be averaged over one calculation cell. To improve the suitability of 3Di for urban flood analyses in sloping urban areas, research should focus on this aspect. More specific future research should focus on a reduction of:

1. The overestimation in runoff discharge due to an overestimation of the cross-section depth (Δh) at the calculation cell border. A reduction in the overestimation could be realised by a maximum height difference allowed per calculation cell. Or, by assigning the water level a slope parallel to the DEM slope of the calculation grid cell (situation b in Figure 5-1).

Further research is recommended for two other aspects related to the subgrid technique of 3Di since they could improve the accuracy of runoff routing in sloping areas:

2. Analyse the consequences associated with surface runoff that bypasses obstacles such as street curbs, buildings and other water retaining obstacles, in the DEM. If the consequences are significant, consider implementation of a no-flow obstacle comparable to levees with a retaining height representing either the curb height or flood level.
3. Analyse the impact of the current assumption used to buildings in the DEM subgrid layer. Reconsider the assumption used for buildings in the DEM to improve runoff routing and the flood extent. Preferably update the DEM with the actual floor levels of the buildings. Otherwise the highest bathymetry plus 15 centimetres floor level could be a solution.

Finally, in sloping areas where surface runoff dynamics play a dominant role in pluvial flood risk management, quantification and improved visualisation of the surface runoff dynamics, such as average flow velocities or volumes for the most important overland flow pathways, could be of added value.

References

3Di consortium, 2014. 3Di website - 3Di explained. , p.39. Available at: www.3di.nu [Accessed May 20, 2015].

Alkema, D., 2007. *Simulating floods: on the application of a 2D-hydraulic model for flood hazard and risk assessment*. Utrecht University.

Allitt, R. et al., 2009. Investigations into 1D-1D and 1D-2D urban flood modelling. In *WaPUG Autumn Conference (No. 25)*.

Al-Sabhan, W., Mulligan, M. & Blackburn, G. a., 2003. A real-time hydrological model for flood prediction using GIS and the WWW. *Computers, Environment and Urban Systems*, 27(1), pp.9–32.

Aronica, G.T. & Lanza, L.G., 2005. Drainage efficiency in urban areas: a case study. *Hydrological Processes*, 19(5), pp.1105–1119.

Bates, P.D. & De Roo, A.P.J., 2000. A simple raster-based model for flood inundation simulation. *Journal of Hydrology*, 236(1-2), pp.54–77.

Battany, M.C. & Grismer, M.E., 2000. Rainfall runoff and erosion in Napa Valley vineyards : effects of slope, cover and surface roughness. *Hydrological processes*, 14, pp.1289–1304.

Boyd, M.J., Bufill, M.C. & Knee, R.M., 1993. Pervious and impervious runoff in urban catchments. *Hydrological Sciences Journal*, 38(6), pp.463–478.

Butler, D. & Davies, J.W., 2011. *Urban Drainage* Third ed., London, UK: Spon Press.

Casulli, V., 2009. A high-resolution wetting and drying algorithm for free-surface hydrodynamics. *International Journal for Numerical Methods in Fluids*, 60, pp.391–408.

Casulli, V. & Stelling, G.S., 2013. A semi-implicit numerical model for urban drainage systems. *International Journal for Numerical Methods in Fluids*, 73, pp.600–614.

Chang, T., Wang, C. & Chen, A.S., 2015. A novel approach to model dynamic flow interactions between storm sewer system and overland surface for different land covers in urban areas. *Journal of Hydrology*, 524, pp.662–679.

Chen, C.F. & Liu, C.M., 2014. The definition of urban stormwater tolerance threshold and its conceptual estimation: An example from Taiwan. *Natural Hazards*, 73(2), pp.173–190.

Chen, J., Hill, A.A. & Urbano, L.D., 2009. A GIS-based model for urban flood inundation. *Journal of Hydrology*, 373(1-2), pp.184–192.

Chow, V.T., 1959. *Open-channel hydraulics*, New York, USA: McGraw-Hill Book Co.

Crowder, R.A., 2009. Hydraulic analysis and design. In *Fluvial design guide*. UK: Environment Agency, p. 44.

Dahm, R. et al., 2014. Next Generation Flood Modelling using 3Di : A Case Study in Taiwan. In *DSD International Conference*. Hong Kong, p. 11.

van Dijk, E., 2011. Anticipating urban flooding due to extreme rainfall. In *the International Water Week Amsterdam*. Amsterdam, the Netherlands, p. 11.

van Dijk, E. et al., 2014. Comparing modelling techniques for analysing urban pluvial flooding. *Water Science & Technology*, 69(2), pp.305–311.

Dingman, S.L., 1984. *Fluvial hydrology*, New York, NY USA: W.H. Freeman and Co.

Dingman, S.L., 2008. *Physical Hydrology* Second ed., Long grove, IL USA: Waveland Press, Inc.

Djordjevic, S., Prodanovic, D. & Maksimovic, C., 1999. An approach to simulation of dual drainage. *Water Science & Technology*, 39(9), pp.95–103.

Ebrahimian, M. et al., 2012. Runoff estimation in steep slope watershed with standard and slope-adjusted curve number methods. *Polish Journal of Environmental Studies*, 21(5), pp.1191–1202.

Engman, E.T., 1986. Roughness Coefficients for Routing Surface Runoff. *Journal of Irrigation and Drainage Engineering*, 112(1), pp.39–53.

Etedali, H.R., Liaghat, A. & Abbasi, F., 2012. Evaluation of the Evalue Model for Estimating Manning ’s Roughness in Furrow Irrigation. *Irrigation and Drainage*, 61, pp.410–415.

Fox, D.M. & Bryan, R.B., 1999. The relationship of soil loss by interrill erosion to slope gradient. *Catena*, 38(3), pp.211–222.

Garne, T.W. et al., 2013. *Wheather related damage in the Nordic countries - from an insurance perspective*.

Gerrits, M., 2009. Na regen komt interceptie. *Stromingen*, 15(1), pp.37–40.

Gerrits, M., 2010. *The role of interception in the hydrological cycle*. Delft University of Technology.

Google, 2009. Google maps - street view. Available at: https://www.google.nl/maps/@50.7801135,5.792079,3a,75y,99.99h,78.03t/data=!3m6!1e1!3m4!1stogrGoGoSC8bYPt0SlRSxA!2e0!7i13312!8i6656!6m1!1e1 [Accessed January 2, 2016].

Hanssen, R. et al., 2012. Hoogte in de Lage Landen: AHN3 - Technische ontwikkeling en hoogteverandering. In *AHN congres de waarde van hoogte in de Lage Landen*. Ede, the Netherlands, p. 23.

Hofierka, J. & Knutová, M., 2015. Simulating spatial aspects of a flash flood using the Monte Carlo method and GRASS GIS: a case study of the Malá Svinka Basin (Slovakia). *Open Geosciences*, 7(1), pp.118–125.

Hsu, M.H., Chen, S.H. & Chang, T.J., 2000. Inundation simulation for urban drainage basin with storm sewer system. *Journal of Hydrology*, 234(1-2), pp.21–37.

Huang, M. et al., 2006. A modification to the Soil Conservation Service curve number method for steep slopes in the Loess Plateau of China. *Hydrological Processes*, 20(3), pp.579–589.

Jak, M. & Kok, M., 2000. A database of historical flood events in the Netherlands. In *Flood issues in contemporary water management*. Springer Netherlands, pp. 139–146.

Kluck, J. & van Luijtelaar, H., 2010. Extreme neerslag in bebouwd gebied. *RIONEDnieuws*, 3, pp.1–3.

KNMI, 2014. *KNMI'14: Climate Change scenarios for the 21st Century – A Netherlands perspective* Scientific. B. van den Hurk et al., eds., De Bilt, the Netherlands: KNMI.

Leandro, J. et al., 2009. A comparison of 1D/1D and 1D/2D coupled hydraulic models for urban flood simulation. *Journal of Hydraulic Engineering*, 135(6), pp.495–504.

Lenderink, G. et al., 2011. Intensiteit van extreme neerslag in een veranderend klimaat. *Meteorologica*, 2, pp.17–20.

Lipeme Kouyi, G. et al., 2009. One-dimensional modelling of the interactions between heavy rainfall-runoff in an urban area and flooding flows from sewer networks and rivers. *Water Science and Technology*, 60(4), pp.927–34.

van Luijtelaar, H., 2014. *Ervaringen met de aanpak van regen wateroverlast in bebouwd gebied: Voorbeelden en ontwikkelingen anno 2014. RIONED reeks 18*, Ede, the Netherlands.

van Luijtelaar, H., Gastkemper, H.G. & Beenen, A.S., 2008. Heavier Rainfall Due to Climate Change: How to deal with effects in urban areas. In *11th International Conference on Urban Drainage*. Edinburgh, Scotland UK, p. 10.

Maksimović, Č. et al., 2009. Overland flow and pathway analysis for modelling of urban pluvial flooding. *Journal of Hydraulic Research*, 47(4), pp.512–523.

Mark, O. et al., 2004. Potential and limitations of 1D modelling of urban flooding. *Journal of Hydrology*, 299(3-4), pp.284–299.

Mark, O. & Parkinson, J., 2005. The future of urban stormwater management: An integrated approach. *Water*, 21(8), pp.30–32.

Mignot, E., Paquier, a. & Haider, S., 2006. Modeling floods in a dense urban area using 2D shallow water equations. *Journal of Hydrology*, 327(1-2), pp.186–199.

de Moel, H. & Aerts, J., 2011. Effect of uncertainty in land use, damage models and inundation depth on flood damage estimates. *Natural Hazards*, 58(1), pp.407–425.

Nassif, S.H. & Wilson, E.M., 1975. The influence of slope and rain intensity on runoff and infiltration. *Hydrological Sciences Bulletin*, 20, pp.539–553.

Nelen & Schuurmans, 2016. *3Di reference manual*, Utrecht, the Netherlands.

NHV, 2002. *Hydrologische woordenlijst* 5th ed. E. Moors et al., eds.

Niemczynowicz, J., 1999. Urban hydrology and water management – present and future challenges. *Urban Water*, 1(1), pp.1–14.

Ochoa-Rodriguez, S. et al., 2013. *Urban pluvial flood modelling: current theory and practice. Review document related to Work Package 3 - Action 13*.

van Oldenborgh, G.J. & Lenderink, G., 2014. Weer en klimaat Nederland: Hoe vaak komt extreme neerslag zoals op 28 juli tegenwoordig voor, en is dat anders dan vroeger? Available at: https://www.knmi.nl/kennis-en-datacentrum/achtergrond/hoe-vaak-komt-extreme-neerslag-zoals-op-28-juli-tegenwoordig-voor-en-is-dat-anders-dan-vroeger [Accessed January 10, 2016].

RIONED Foundation, 2015. *Gemeentelijke aanpak regenwateroverlast*, Ede, the Netherlands.

RIONED Foundation, 2004. *Leidraad riolering: Module C2100 Rioleringsberekeningen, hydraulisch functioneren*, Ede, the Netherlands.

RIONED Foundation, 2009. *Leidraad riolering: Module C2150 Water op straat*, Ede, the Netherlands.

RIONED Foundation, 2013. *Riolering in beeld benchmark rioleringszorg 2013*, Ede, the Netherlands.

RIONED Foundation, 2006. *Stedelijke Wateropgave: Vergelijking normen voor water op straat en inundatie*, Ede, the Netherlands.

Schmitt, T.G., Thomas, M. & Ettrich, N., 2004. Analysis and modeling of flooding in urban drainage systems. *Journal of Hydrology*, 299(3-4), pp.300–311.

Smith, M.W., Cox, N.J. & Bracken, L.J., 2007. Applying flow resistance equations to overland flows. *Progress in Physical Geography*, 31(4), pp.363–387.

Spekkers, M.H., 2015. *On rainstorm damage to building structure and content*. TU Delft.

Stelling, G.S., 2012. Quadtree flood simulations with sub-grid DEMs. *Proceedings of the ICE-Water Management*, 165(10), pp.567–580.

Sto. Domingo, N.D. et al., 2010. Flood analysis in mixed-urban areas reflecting interactions with the complete water cycle through coupled hydrologic-hydraulic modelling. *Water Science and Technology*, 62(6), pp.1386–1392.

STOWA, 2015. *Actualisatie meteogegevens voor waterbeheer 2015*, Amersfoort, the Netherlands.

TU Delft, 2008. *Riolering*, Civiele Gezondheidstechniek CT-3420. TU Delft.

van 't Veld, A.C., 2015. *Potential measures to reduce fluvial and tidal floods in the Pampanga Delta*. Delft University of Technology and National University of Singapore.

ten Veldhuis, J.A.E., 2010. *Quantitative risk analysis of urban flooding in lowland areas*. TU Delft.

Verhoeven, G., 2013. Next generation flood forecasting and flood risk management for Singapore - 3Di pilot application.

Volp, N.D., Van Prooijen, B.C. & Stelling, G.S., 2013. A finite volume approach for shallow water flow accounting for high-resolution bathymetry and roughness data. *Water Resources Research*, 49, pp.4126–4135.

Zhan, X. & Huang, M.L., 2004. ArcCN-Runoff: An ArcGIS tool for generating curve number and runoff maps. *Environmental Modelling and Software*, 19(10), pp.875–879.

Zhang, S. & Pan, B., 2014. An urban storm-inundation simulation method based on GIS. *Journal of Hydrology*, 517, pp.260–268.

Zoppou, C., 2001. Review of urban storm water models. *Environmental Modelling and Software*, 16(3), pp.195–231.

Appendices

A. Site description

The villages of Banholt and Mheer are surrounded by rural area, as can be seen in Figure A-1. In addition to the villages of Banholt and Mheer the research area comprises the two contributing watersheds of the ephemeral Horstergrub and Banholtergrub streams (Figure A-2). The boundary of the research area is equivalent to the divides of these watersheds. In total the research area covers 9.13 km^2.

The land use map (Figure A-1) is retrieved by combining several data sources:

- Basic registration of Addresses and Buildings (BAG);
- Digital topographic base file of the Netherlands' Cadastre, Land Registry and Mapping Agency[10];
- Statistics Netherlands Land use map[11] and
- Key Register Crop Plots[12].

Combining land use information from these sources results in a functional land use map with a resolution of 0.25 m^2.

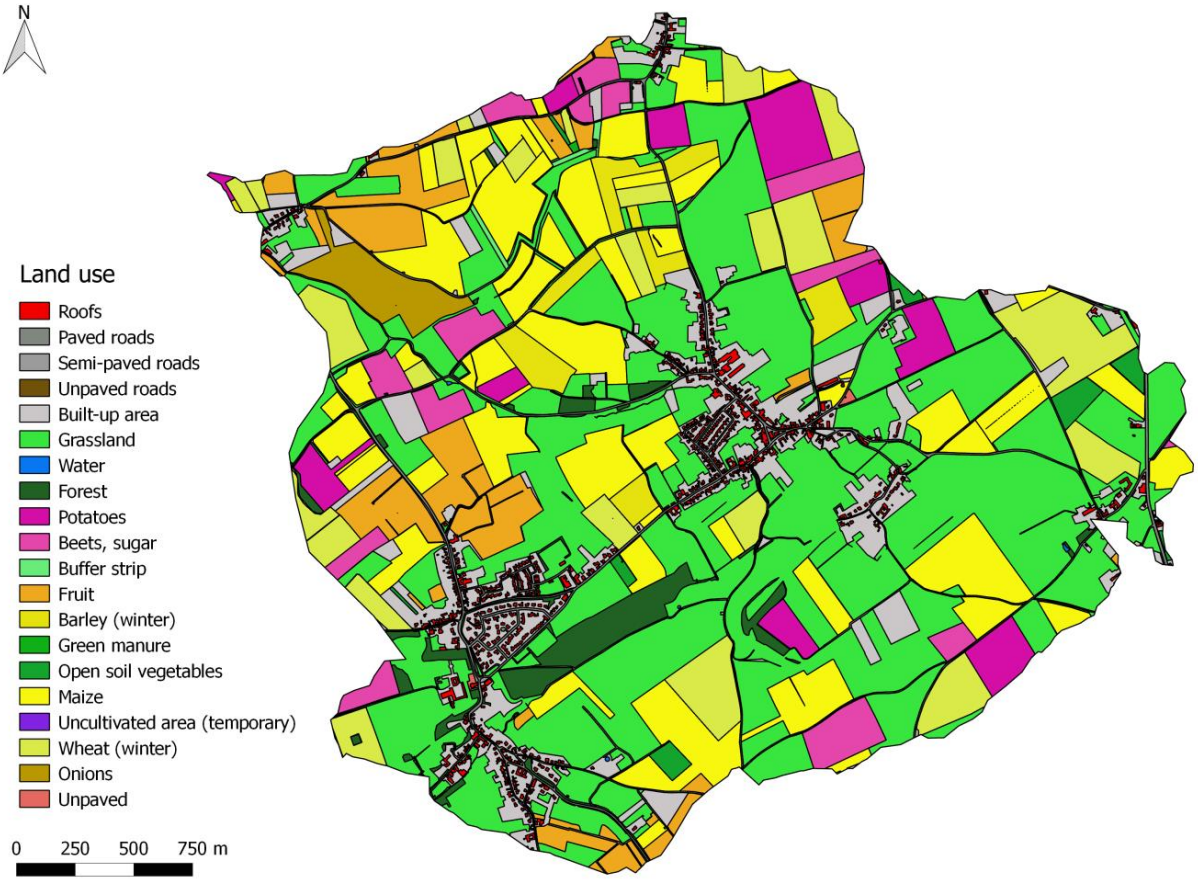

Figure A-1: Land use map of the research area.

[10] In Dutch: Top10NL
[11] In Dutch: CBS Bodemgebruik
[12] In Dutch: Basisregistratie Gewaspercelen

During excess rainfall the sloping character of the region results in surface runoff towards the Banholtergrub and Horstergrub streams. The water authority constructed fifteen water storage buffers in the area to reduce peak discharges, and to increase the surface water storage capacity of the area (Figure A-2). Due to the presence of these storage buffers the area can be divided into 15 sub-catchments (Figure A-3).

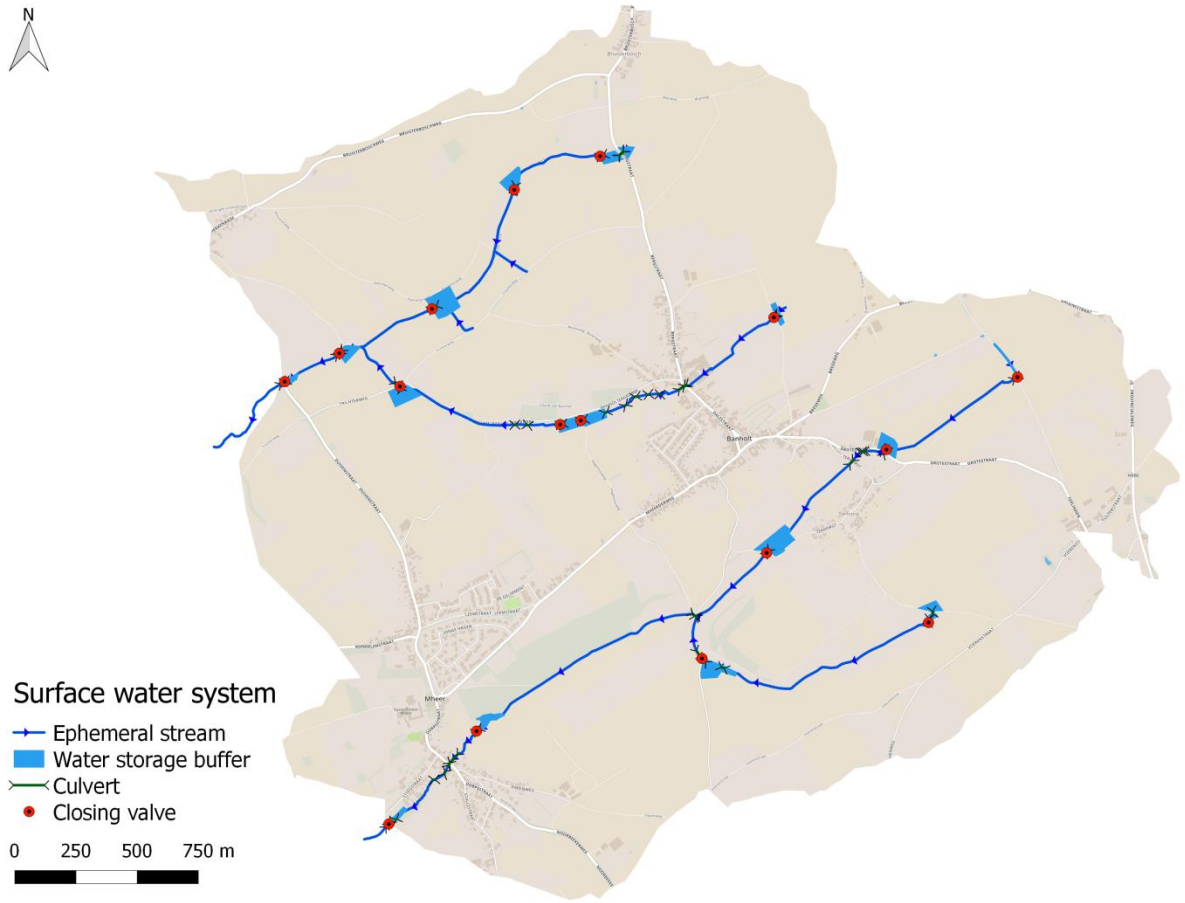

Figure A-2: Surface water system with the Horstergrub (below) and Banholtergrub stream (above).

The storage buffers are incorporated in the landscape, as can be seen in Figure A-4. Under dry conditions these buffers are, just like the Horstergrub and Banholtergrub streams, not filled with water. During storm events the buffers fill up with water, which can leave the buffers through culverts. Behind the culvert a closing valve is used to control the amount of outflow (Figure A-5, left). Furthermore, there are several culverts constructed in the streams between the buffers (Figure A-5, right). These culverts vary in length between 3 and 47 meter. They also vary in through-flow surface.

The sewer system in de villages of Banholt and Mheer consist of a separated system with a wastewater sewer and storm water sewer (Figure A-6). In reality, there are several locations where the storm water system is accidently connected to the wastewater system. The model comprises the currently existing sewer system, and therefore accounts for these wrong connections. Also, there are several locations where street gullies are connected to the wastewater system. Locations where the wastewater sewer interacts with rainwater, caused by either a wrong connection or street gully, are marked as combined sewer (Figure A-6).

In the area most of the roofs are not connected to the sewer directly, but drain onto the surface. As a result most of the rainwater is drained over the surface. However, several building roofs drain directly to the wastewater system. This is the case for 38834 m^2 of impervious surface, which represents 11 per cent of all the paved surfaces in the area.

When the wastewater sewer exceeds its capacity it flows over to the storm water sewer. In total the system has five external overflows from the wastewater sewer to the storm water sewer. The storm water sewer has ten outlet locations where it discharges the storm water to the surface water system.

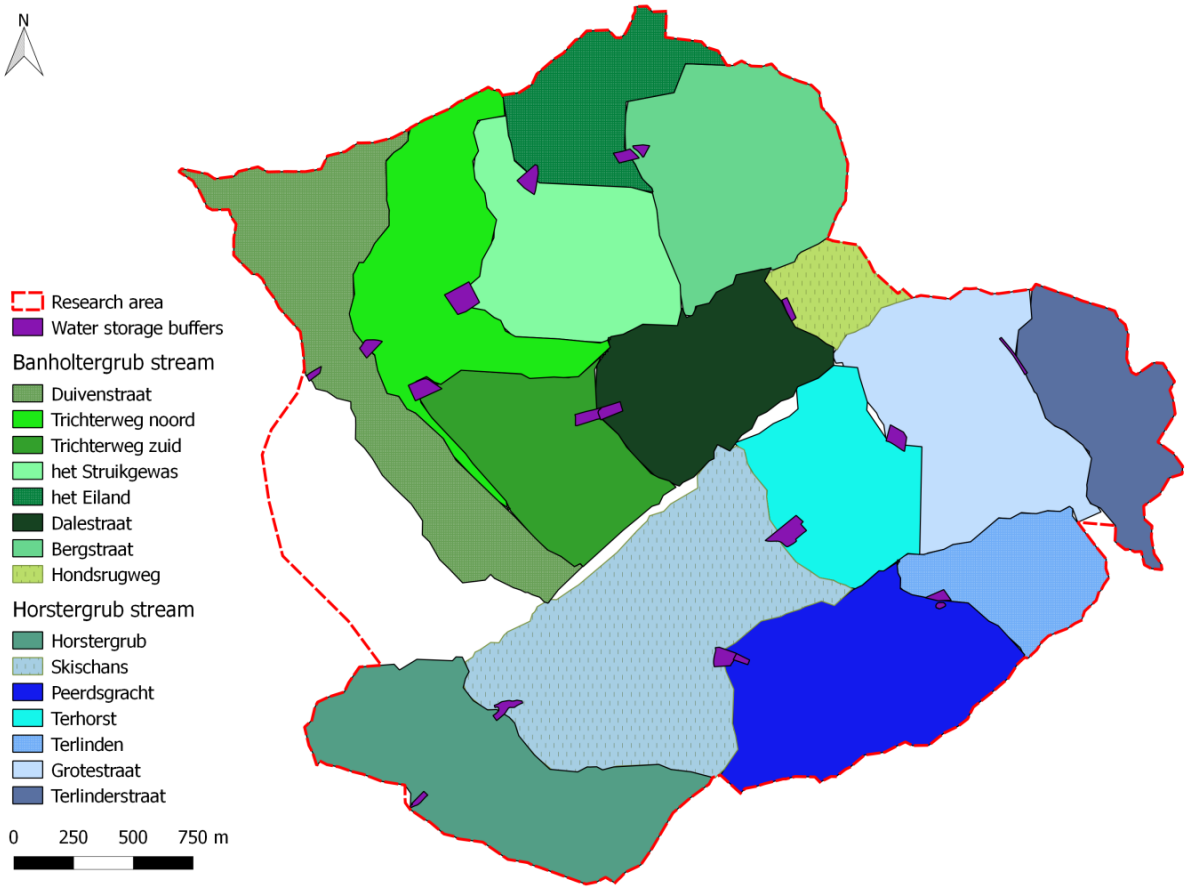

Figure A-3: Overview of sub-catchments draining to the water storage buffers in the research area.

Figure A-4: Photographs show the incorporation of the water storage buffers in the landscape.

Figure A-5: A closing valve at a buffer outlet (left) and a culvert incorporated in the landscape (right).

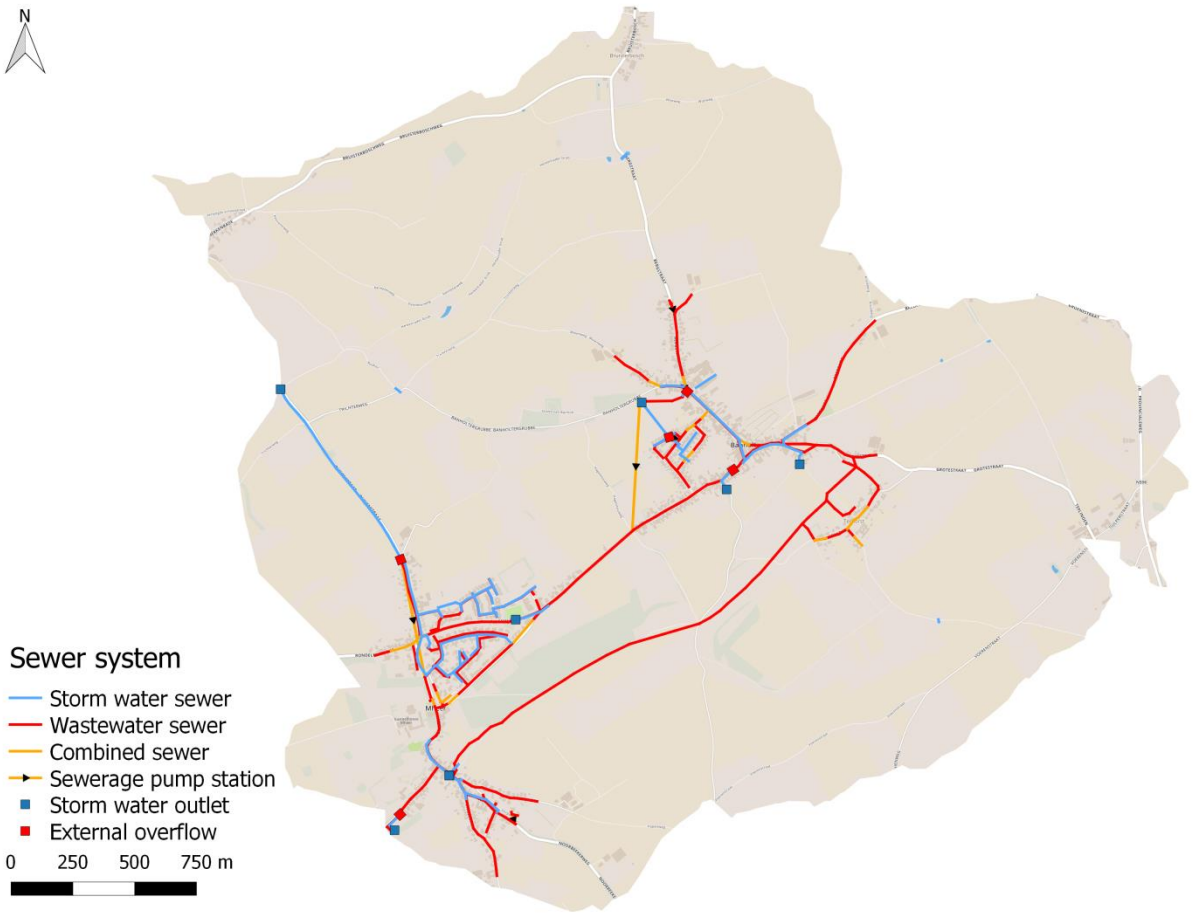

Figure A-6: Sewer system of Banholt and Mheer.

B. Subgrid layers

The 2D flow component of the model consists of three subgrid layers. Additionally an interception layer is retrieved to account for this flux initial to model simulations. All subgrid layers have a spatial resolution of 0.5 x 0.5 meter. For the whole research area one subgrid layer contains 36.6 million pixels.

B.1 DEM layer

The map with current heights of the Netherlands (AHN2) is generated in 2012 for the Province of Limburg and has a spatial resolution of 0.25 m^2. The AHN2 has an elevation precision of approximately 5 centimetres (Hanssen et al. 2012). The DEM layer is generated from a filtered AHN2. Because the filtered AHN2 is not completely filled at certain locations, e.g. houses, tunnels and surface water, it is interpolated using the following assumptions:

- *Buildings:* The location of buildings is known from the BAG. For each building from the BAG an average surface level is determined as the median of the building circumference surface levels. This value, plus 15 centimetres representing the floor level of the building, is assigned to the entire area of the building.
- *Other locations:* At other locations the AHN2 is closed by interpolation according to the Inverse Distance Weighting method.

The open channel flow is incorporated in the 2D flow component of the model. Since the surface water system of the area has an ephemeral character, the streams were dry during the time the AHN2 was generated. Therefore, the streams are accurately visible in the AHN2. The permanent earthen dams of the storage buffers are also visible in the AHN2. For a correct representation of the surface water system several adjustments are made to the DEM subgrid layer (Figure 3-3):

- Two buffers (Horstergrub and Trichterweg) were altered after generation of the AHN2 in 2012. Revision measurements of the water authority are used to implement these buffers into the DEM layer.
- Obstacles within a calculation cell are not taken into account, since water levels in calculation cells are determined with a V-h relationship. Consequently, culverts in rural area with a length shorter than the calculation cell do not have a function and are carved into the DEM.

B.2 Friction layer

The friction rainwater is subjected to during surface runoff impacts the surface runoff velocity (Hofierka & Knutová 2015). In this research Manning friction coefficients are used to account for surface roughness. The well-known and often used values for open water hydraulics of e.g. Chow (1959) are empirically derived values based on assumptions that are not applicable to surface runoff. Therefore, these values are not readily suitable to use for surface runoff dynamics (Smith et al. 2007). Yet, these values are the starting point for the determination of the friction values used in this research.

Friction values are highly uncertain due to the many factors of impact:

- Water depth.
- Surface slope.
- Land use (material and vegetation).
- Obstacles such as litter, leafs, crop ridges and roughness from tillage.
- Inflow rates.
- The impact of raindrops that fall on the surface.

For more information on the amount of impact of these factors on friction values, see e.g. Engman (1986); Etedali et al. (2012); Hofierka & Knutová (2015) and Smith et al. (2007).

Due to this high uncertainty, determination of friction values is often based on assumptions and model calibration (Hofierka & Knutová 2015). As there is no measurement data to calibrate the model, this is not possible in this research.

B.2.1 Sensitivity analysis

Friction is an important parameter since it impacts the velocity of overland flow. Therefore a sensitivity analysis is conducted with a simplified 3Di model. This simplified model consists of a 2D flow component only. The aim of the sensitivity analysis was to create insight in the impact of friction on surface runoff velocities, to support the selected model input.

The sensitivity analysis was conducted for only one storage buffer, known as the buffer Terhorst. This way, the water level hydrograph of the buffer provides insight in the average surface runoff velocities towards the buffer. The used friction values are ranged between zero friction (n=0 $s/m^{1/3}$) and large friction (n=0.5 $s/m^{1/3}$). This range is based on values found in the previously mentioned literature.

In general, the higher the friction value, the slower the rise of the water level in the buffer as a result of a deceleration in runoff velocities (Figure B-1). More specific:

- Friction values in the range of 0-0.03 $s/m^{1/3}$ do not result in any significant delays in runoff velocities.
- Between n=0.03-0.08 $s/m^{1/3}$ a delay is mostly visible in the beginning of the rainfall runoff conversion.
- With a friction value of 0.5 $s/m^{1/3}$ there is a significantly larger delay in runoff visible.

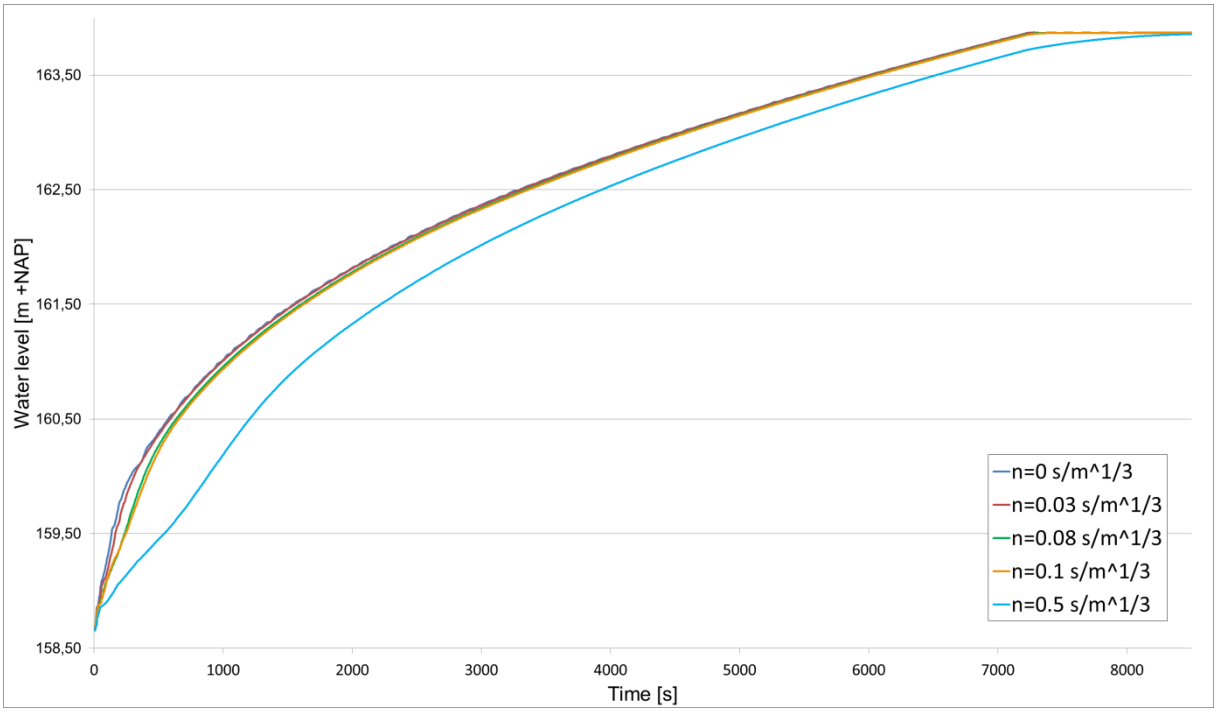

Figure B-1: The impact of various friction values on the water level rise in storage buffer Terhorst.

B.2.2 Model input

The following conclusions are drawn based on the studied literature and results from the sensitivity analysis:

- Friction is a highly uncertain parameter due to the many factors that influence surface runoff dynamics.
- Due to the space dependency of the factors that influence friction, empirically derived values from other areas are not directly applicable in this research.
- The friction values used in this research are associated with a high level of uncertainty as a result of the limited calibration possibilities.

In this research the rural unpaved sloping areas are assigned a friction value of n=0.07 $s/m^{1/3}$. The other land use types, for example built up areas and roofs are assigned commonly known friction

values of Chow (1959). Despite the high uncertainty of friction different values are used to account for the non-homogeneous land use in the research area. The friction value assigned to each land use type is given in Table B-1. Use of these values yields the friction layer for this research (Figure B-2).

Table B-1: Conversion values used to retrieve the friction, infiltration and interception subgrid layers.

Land use	Friction (Manning [s/m$^{1/3}$])	Permeability factor [-]	Interception [m]
Roofs	0.058	0	0.0025
Paved roads	0.039	0	0.0025
Semi-paved roads	0.039	0.5	0.0025
Unpaved roads	0.039	1	0.0025
Built-up area	0.058	0	0.0025
Grassland	0.06	1	0.003
Water	0.026	1	0
Forest	0.058	1	0.01
Potatoes, consumption on clay/loess soil	0.07	1	0.003
Beets, sugar	0.07	1	0.003
Buffer strips	0.06	1	0.003
Fruit	0.058	1	0.005
Barley, (winter)	0.07	1	0.003
Green manure	0.06	1	0.003
Open soil vegetables	0.07	1	0.0025
Maize	0.07	1	0.003
Uncultivated area (temporary)	0.07	1	0.01
Wheat (winter)	0.07	1	0.003
Onions	0.07	1	0.0025
Unpaved	0.058	1	0.0025

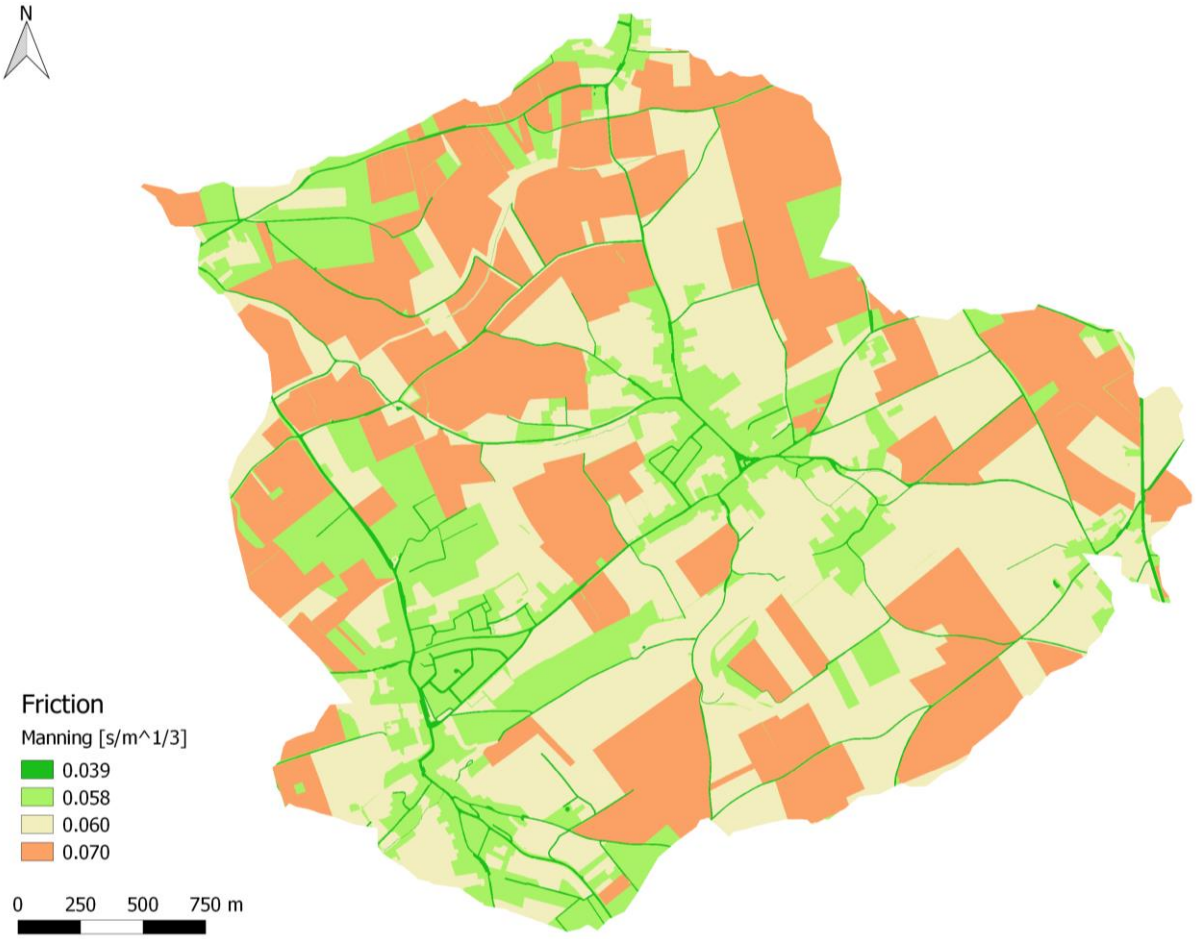

Figure B-2: Friction subgrid layer.

B.3 Infiltration layer

An infiltration layer is derived from the functional land use layer and the maximum infiltration capacity of the soil type in the area with the following steps:

- Determination of the maximum infiltration capacity of the soil. A maximum infiltration capacity of 480 mm/day is used in this research. This value is an assumption and is adopted from the soil map of Nelen & Schuurmans.
- To each land use type a permeability factor is assigned (Table B-1). The permeability factors used in this research are adopted from conversion tables Nelen & Schuurmans uses for the subgrid development of 3Di models.
- The infiltration capacity is multiplied by the permeability factor, which results in a layer with an infiltration value per pixel (Figure B-3).

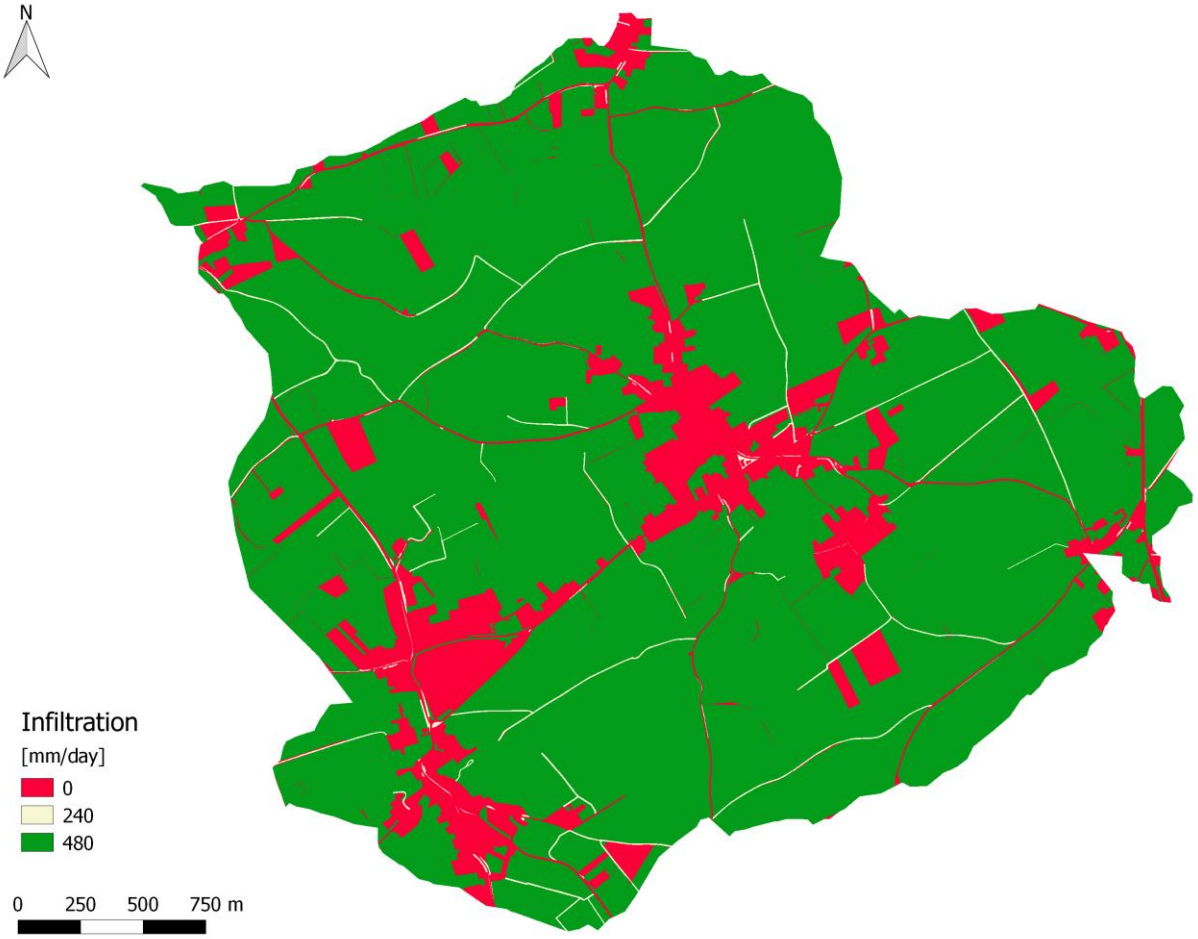

Figure B-3: Infiltration subgrid layer.

B.4 Interception layer

Even though interception cannot be inserted as a subgrid layer in an urban 3Di model, the layer is retrieved to calculate the average interception capacity of the area. An initial interception capacity is assigned to each land use type (Table B-1). The interception values used in this research are adopted from the conversion tables Nelen & Schuurmans uses for the subgrid development of 3Di models. This results in the interception layer shown in Figure B-4. Based on this layer, the total amount of interception initially subtracted from the rainfall input scenario calculations is 3.2 mm/m^2.

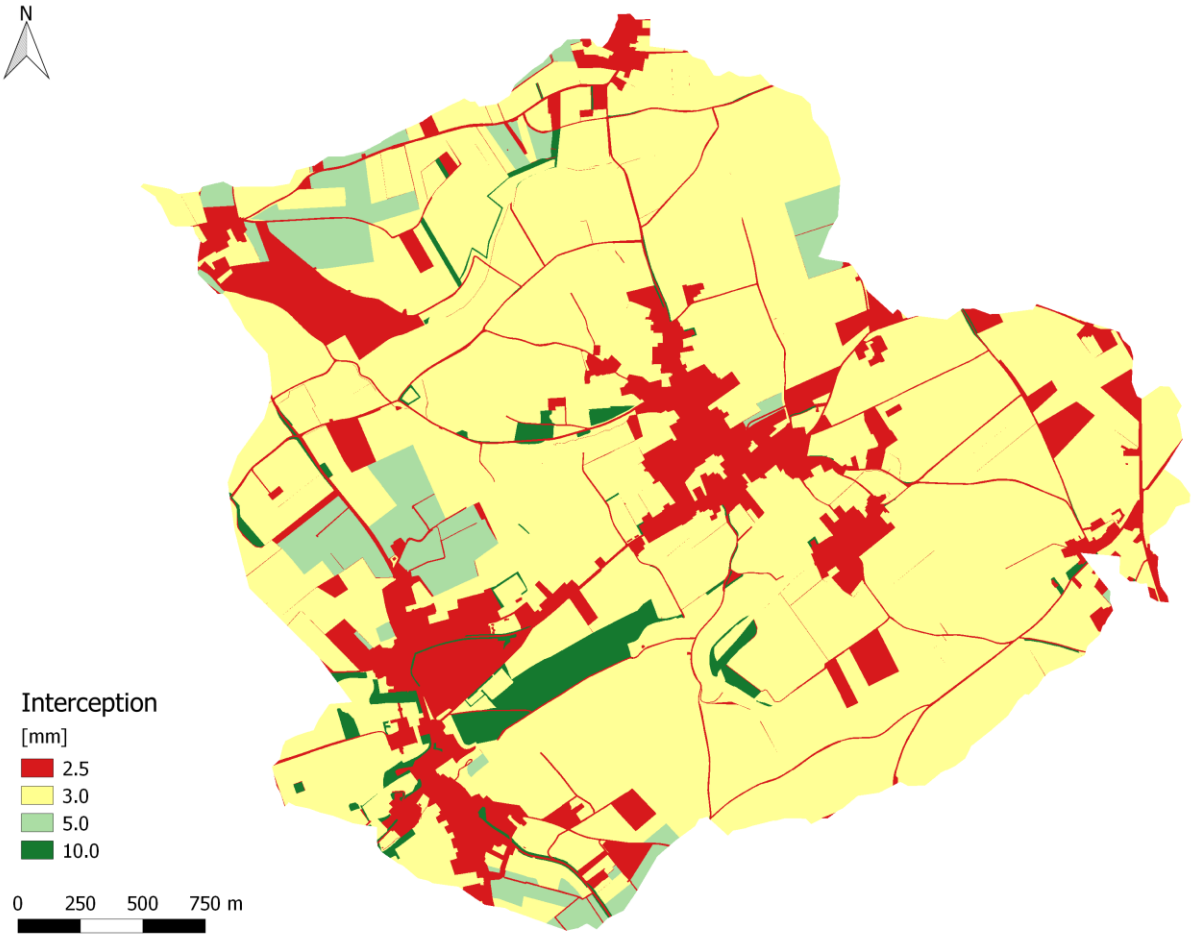

Figure B-4: Interception layer.

C. 1D elements

The sewer system, the surface water structures and applied boundary conditions are all represented by 1D elements. The 1D flow component is built up of nodes and branches, with additional input parameters that depend on the element the node or branch represents (Nelen & Schuurmans 2016).

C.1 Sewer system

The wastewater load of the sewer system is small compared to the flows caused by extreme rainfall. Therefore, the wastewater load is neglected during this research.

To translate the received sewer data into a 3Di model, numerous checks on quality and completeness are conducted. The results of these checks are communicated with the municipality, and where necessary data improvements or assumptions are made. Table C-1 gives an overview of the input parameters required to represent the 1D flow component of the 3Di model. Figure A-6 shows the sewer system incorporated in the 3Di model.

Table C-1: Overview of the 1D model elements and the required input parameters.

1D element	Input parameters
Manhole	• Drainage level (in this research equal to surface level) • Surface level, must be equal to the DEM subgrid layer • Bottom level • Manhole area • Connection type (isolated, embedded, connected)
Pipeline	• Sewerage type (combined, wastewater or storm water) • Invert level start point and invert level end point • Start manhole and end manhole • Pipeline area • Friction value and friction type (Manning in this research)
External overflow (weir)	• Crest width and crest level • Crest type and discharge coefficient • Start manhole and end manhole • Allowed flow direction between start and end manhole • Friction value and friction type (Manning in this research)
Storm water outlet	• See the input parameters of a manhole • Open water level (if present, in this research not the case)
Sewerage pump station	• Pump capacity [l/s] • Start manhole and end manhole (only start manhole when the water is pumped out of the area) • Start level suction side and end level suction side
Orifice	• Initial opening height [m NAP] • Opening width and height • Crest type and discharge coefficient • Start manhole and end manhole • Allowed flow direction between start and end manhole • Friction value and friction type (Manning in this research)

C.2 Surface water structures

The surface water structures present in the research area (Figure A-2) can be subdivided into culverts with closing valves and culverts without closing valves.

In 3Di every pipeline, hence also culverts, require a manhole start and end node. Culverts without closing valves are schematized as a pipeline with a start and end manhole (Figure C-1). Therefore, they require the same input parameters as sewer manholes and pipelines.

Figure C-1: Schematization of a culvert and outlet of a water storage buffer in 3Di.

Culverts with closing valves, located at the storage buffers, are schematized as an orifice with a start and end manhole (Figure C-1). In 3Di, an orifice can only be of rectangular shape (Figure C-2). The, in reality, round outlet constructions have to be translated into rectangular shaped orifices. To achieve this translation, the flow-through area created by the opening height of the closing valves is calculated. Subsequently, this flow-through area is used to calculate the dimensions of the orifice (width x height).

Table C-1 shows the input parameters required for the manholes, pipelines and orifices used in the schematization of the surface water structures.

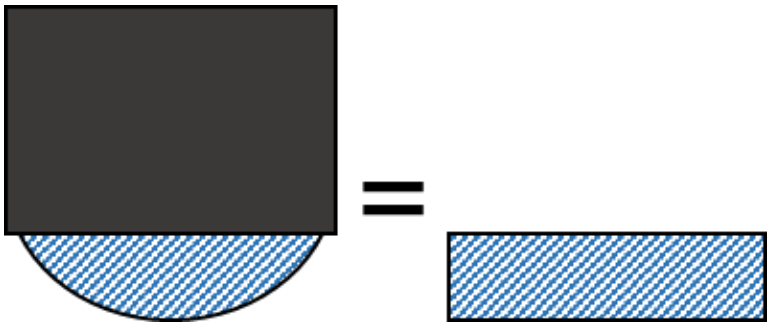

Figure C-2: A buffer outlet (left) is translated into an orifice with a rectangular cross-section.

C.3 Boundary pumps

Because the boundary of the research area coincides with the divides of the Horstergrub and Banholtergrub watersheds, only downstream boundary conditions are required. At the outflow locations of both streams boundary conditions are applied to create free water outflow (Figure C-3).

This is achieved by adding pumps to the 1D component of the model with capacities large enough to pump all the water present at these locations, out of the model.

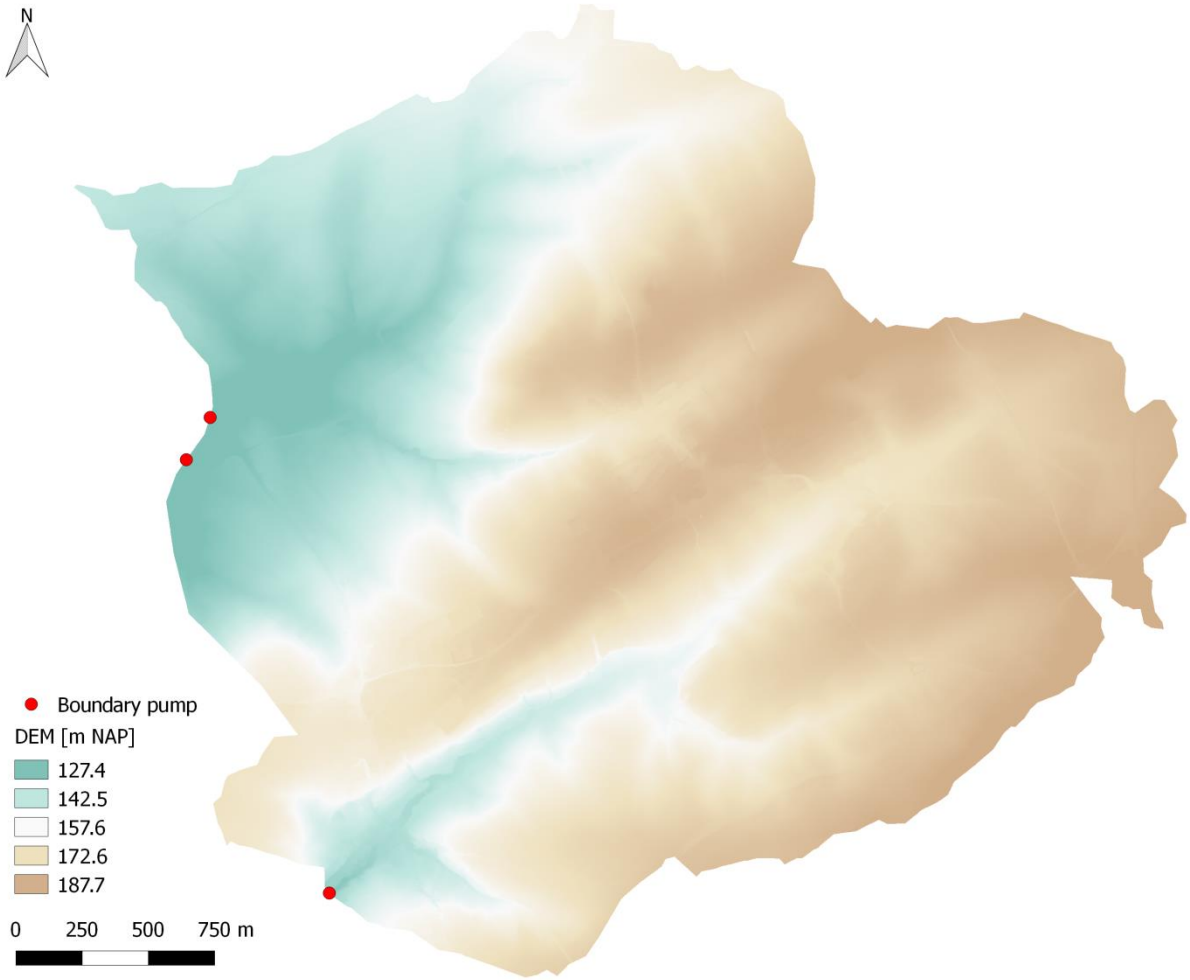

Figure C-3: locations of the downstream boundary conditions used in the 3Di model.

D. Calculation grid

Derivation of the calculation grid is an important modelling choice. In principle, the amount of calculation cells in a model is unlimited. In practice, the model performance decreases when the amount of calculation cells becomes more than 100,000 (Nelen & Schuurmans 2016).

A calculation cell must contain a minimum of four subgrid pixels. There is no limit to the amount of subgrid pixels in one calculation cell. The size of calculation cells depend on the spatial level of detail required at a specific area. Urban areas require a high level of detail due to local constraints and surface characteristics such as street gradients, sidewalks and speed bumps (Niemczynowicz 1999; Schmitt et al. 2004). Areas that require more detail should have a grid size of 10 x 10 meter or less (Crowder 2009).

During this research a non-uniform calculation grid is used. With exclusion of the rainwater storage buffers, the calculation grid in the rural area has a resolution of 20 x 20 meters. Figure D-1 show the calculation grid for the whole research area.

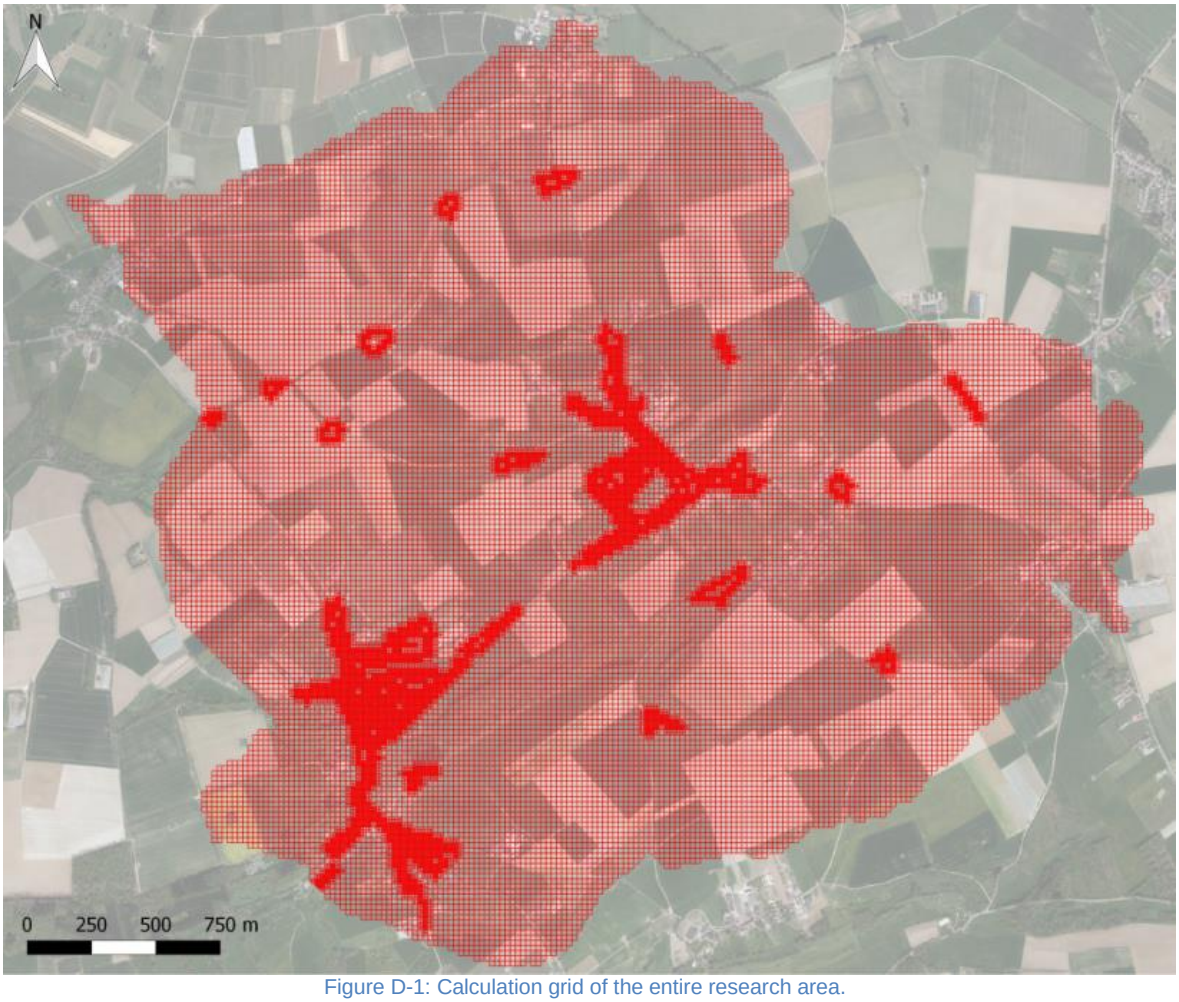

Figure D-1: Calculation grid of the entire research area.

The quadtree calculation grid consists of several resolutions for a balance between calculation speed and the required level of detail to simulate overland flow. The highest resolution of the grid is 5 x 5 meters. This resolution is assigned to the areas of interest during the analysis:

- The rainwater storage buffers.
- The urban areas of Banholt and Mheer.

Figure D-2 show the calculation grid at a part of Banholt and water storage buffer het Struikgewas respectively.

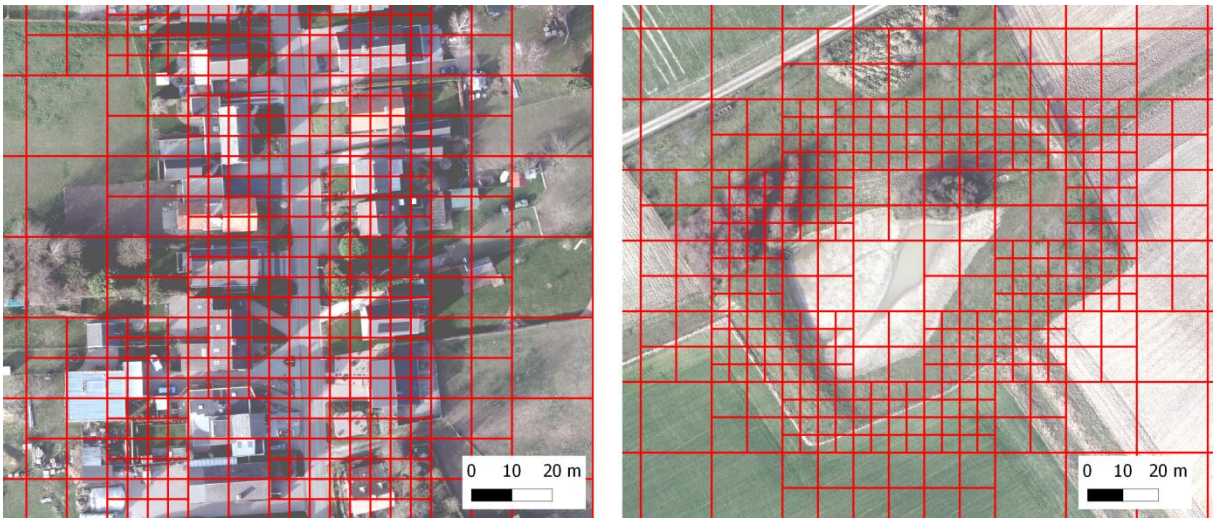

Figure D-2: Close up of the calculation grid in North-Banholt (left) and at storage buffer 'het Struikgewas' (right).

Following from the quadtree technique this means that the calculation grid contains calculation cells of 5 x 5 meters, 10 x 10 meters and 20 x 20 meters. With this calculation grid the total amount of pixel cells of the subgrid layers (36.6 million) are merged into 45,529 calculation cells.

E. Model validation

The model performance is analysed with the historical rainfall event of 18 August 2011. The model results are compared with photographs at several flood locations and with expert judgement of the municipality and water authority.

E.1 Rainfall scenario

On 18 August 2011 a total of 32 mm of rain fell between 18:40 and 20:20 hours. Figure E-1 shows the temporal distribution of this event, retreived from the Dutch national rainfall radar. The rainfall event was distributed homogeneously over the whole research area.

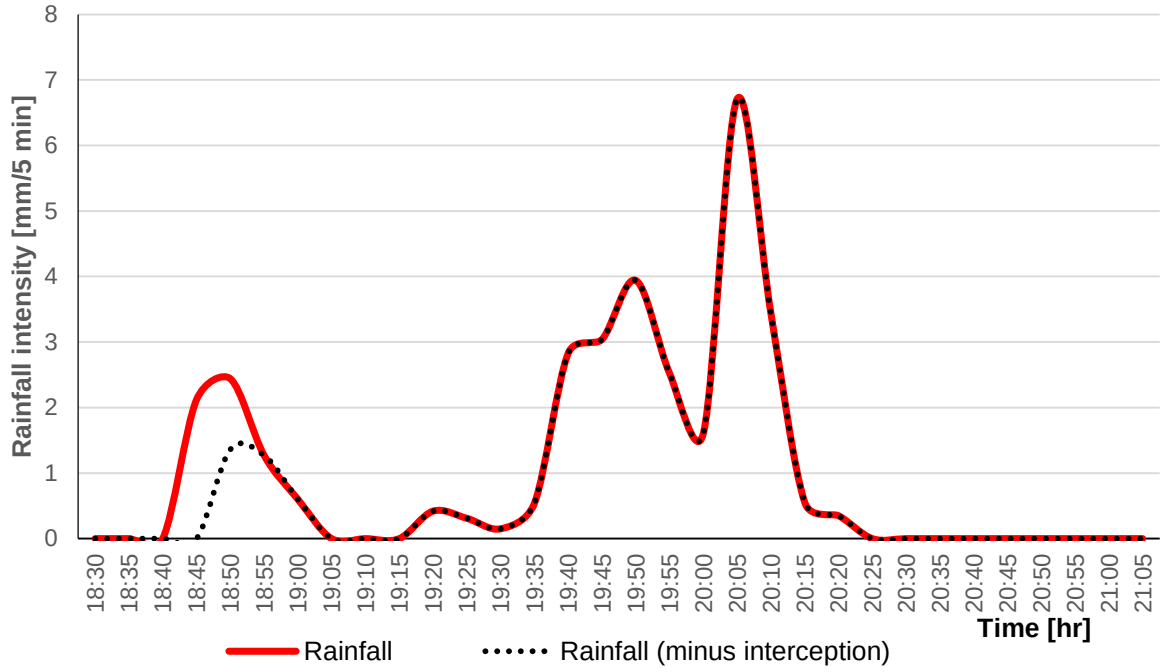

Figure E-1: Temporal rainfall scenario of 18 August 2011, extracted from the Dutch national rainfall radar.

E.2 Model results, observations and expert judgement

Table E-1 gives an overview of the fluxes calculated after model simulation. In total 39 per cent of the total rainfall becomes runoff. This percentage represents all the water in the model, including surface runoff, water storage in the buffers and sewer flow.

According to the water authority runoff percentages lies in the range of 20 to 30 per cent under normal rainfall conditions, with a maximum runoff percentage of 50 per cent. The runoff coefficients of a Limburg Soil and Erosion Model (LISEM) are 18 per cent for a T25 event and 34 per cent for a T100 event. These values are not fully comparable with the percentage calculated with 3Di, because they represent surface runoff towards a water storage buffer and the 3Di percentage represents all the water present in the model.

Table E-1: Interception, infiltration and runoff fluxes calculated after model simulation of 18 August 2011.

	Volume [m^3]	Percentage [%]
Total rainfall	300748	100
Interception	29648	10
Infiltration	154680	51
Runoff	116420	39

E.2.1 Flood locations

In total five flood locations emerge during model simulation (Figure E-2). Photographs taken during the event of 18 August 2011 at the Dorpsstraat, Steegstraat and Herkenradergrubbe locations are available for comparison.

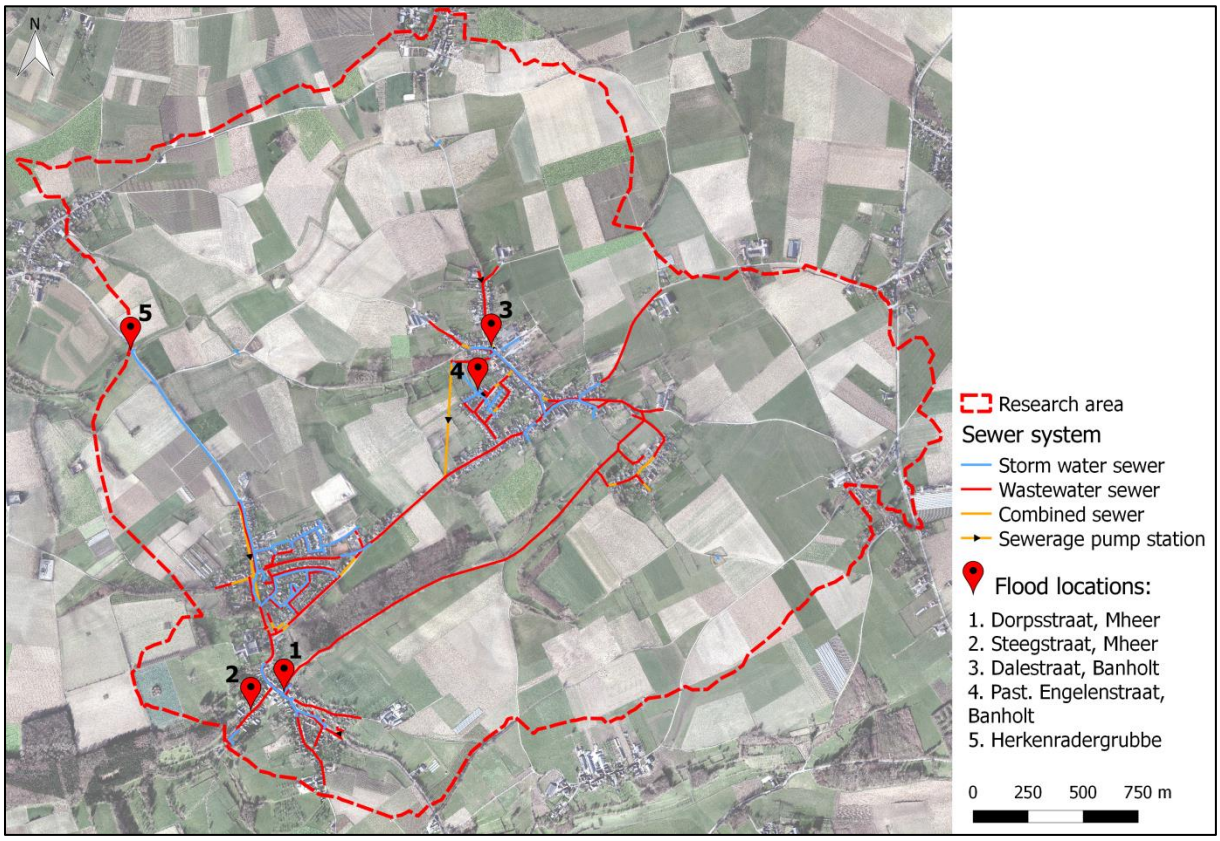

Figure E-2: Flood locations that emerged during model simulation of the rainfall event of 18 August 2011.

Dorpsstraat, Mheer

On 18 August the extent of flooding at the Dorpsstraat ranged between the two locations marked in Figure E-3: from the crossroad with the Horstergrub stream, to restaurant Taverne de Smidse. The photographs of the flooding (Figure E-4) were taken at 20:15. From the photographs, the flood depth is estimated to range between 5 and 15 centimeters with an average of about 10 centimeters.

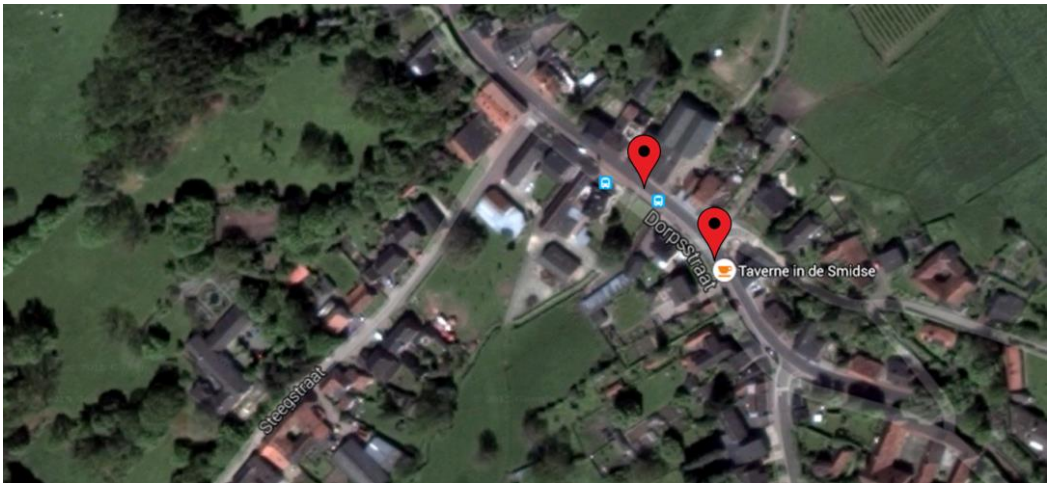

Figure E-3: Map marking the flood location at the Dorpsstraat in Mheer ranging between the two pins.

Figure E-4: Photographs of flooding at the crossroad with the Horstergrub stream (left) and at restaurant Taverne de Smidse.

Figure E-5 shows a flood map of the model results. Compared with the photographs the model overestimates the flood extent and flood depth at the Dorpsstraat. The average flood depth in the simulation is 20 centimeters. Also, in the simulation the street is flooded over its whole profile, while in the photographs part of the steet profile is dry and part is flooded.

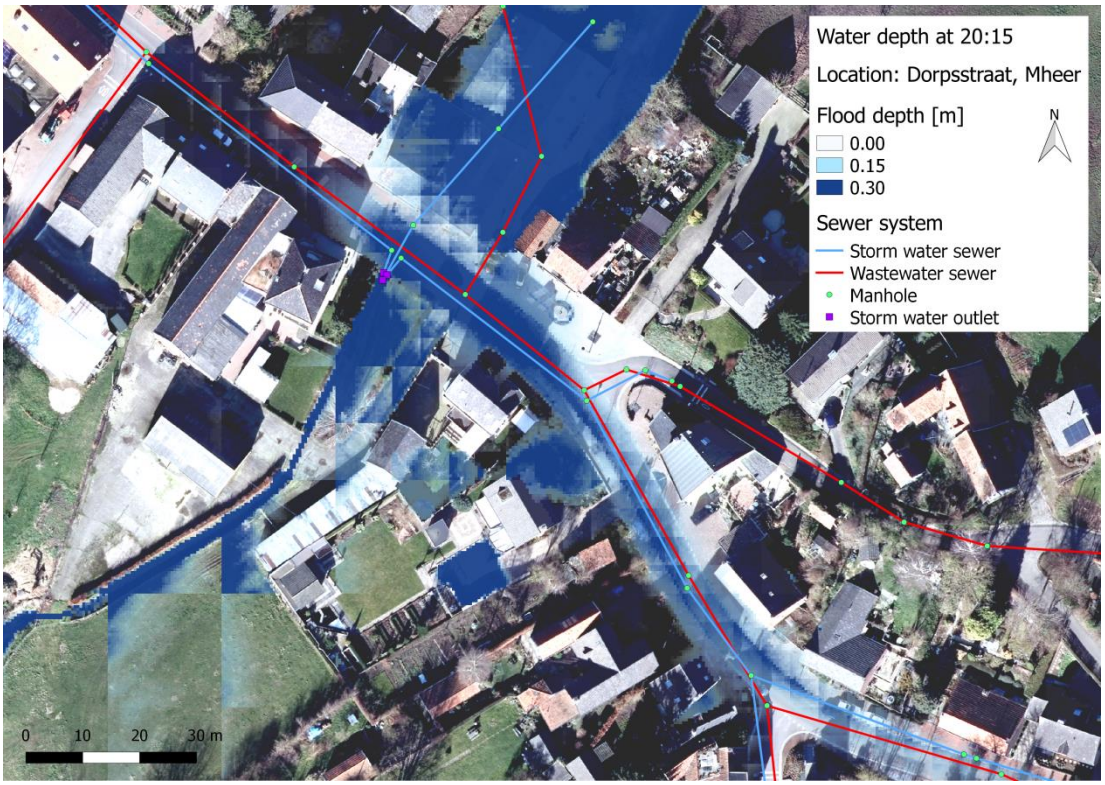

Figure E-5: Flood map of the Dorpsstraat flood location after simulation of the rainfall event of 18 August 2011.

Steegstraat, Mheer

The Steegstraat is defined as a flood location because here water enters the driveways up to the front door of houses. Figure E-6 shows the location and photographs of flooding at Steegstraat house number 9 in Mheer. The photographs were taken at 20:10 (left) and 19:50 (right). From the photographs the average water level is estimated to be about 5 centimeters.

The results of the model simulation (Figure E-7) show an average flood depth of 6 centimeters. This is comparable to the water level retrieved from the photographs.

Yet, the flood map also shows that there is flooding located on top of buildings. This is the result of the assumption used to represent houses in the DEM layer. The rainwater is placed on top of these houses because they are the lowest location in a calculation cell. However, as a result this water is not placed on the street where it should actually be routed to. Moreover, rainwater seems to be held in local depressions near buildings.

Figure E-6: Map marking the flood location and photographs of flooding at the Steegstraat in Mheer.

Figure E-7: Flood map of the Steegstraat flood location after simulation of the rainfall event of 18 August 2011.

Dalestraat, Banholt

At the Dalestraat in Banholt (Figure E-8) flooding emerged during the model simulation. The average flood depth is about 25 centimeters (Figure E-9). According to the municipality, this location is known to be prone to flooding. So, that flooding emerged at this location can be correct. However, no judgement can be given about the emergence and magnitude of flooding in the model simulation, because it is unknow whether flooding emerged during the event of 18 August 2011.

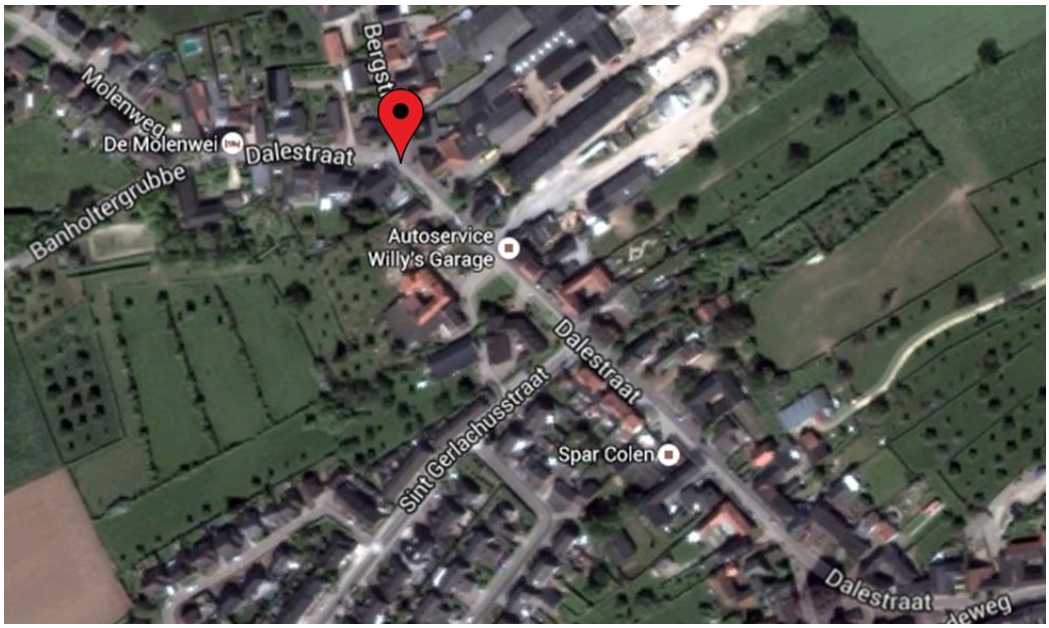

Figure E-8: Map marking the flood location at the Dalestraat in Banholt.

Due to an error in the model rainwater entered the wastewater sewer through the external overflow at this location. This external overflow is equipped with a return valve, so in reality rainwater cannot enter the wastewater sewer. Due to the connection settings of the manholes there is no flow exchange between the wastewater sewer and surface. So, this modelling error does not impact flooding at the Dalestraat. The impact of the error downstream in the wastewater sewer seems also mildly.

Figure E-9: Flood map of the Dalestraat flood location after simulation of the rainfall event of 18 August 2011.

Pastoor Engelenstraat, Banholt

At the Pastoor Engelenstraat in Banholt (Figure E-10) flooding, with an average depth of 35 centimeters, emerged during model simulation (Figure E-11). The municipality confirmed that the Pastoor Engelenstraat is known as a flood prone location. However, there is noting known about flooding during 18 August 2011. So, whether the emergence of flooding during model simulation is corrent is uncertain.

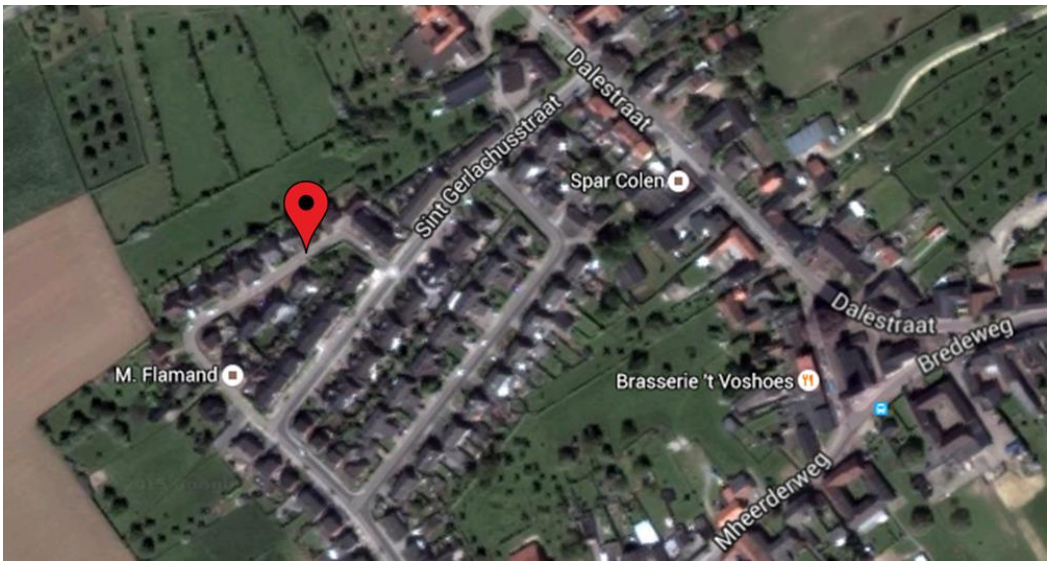

Figure E-10: Map marking the flood location at the Pastoor Engelenstraat in Banholt.

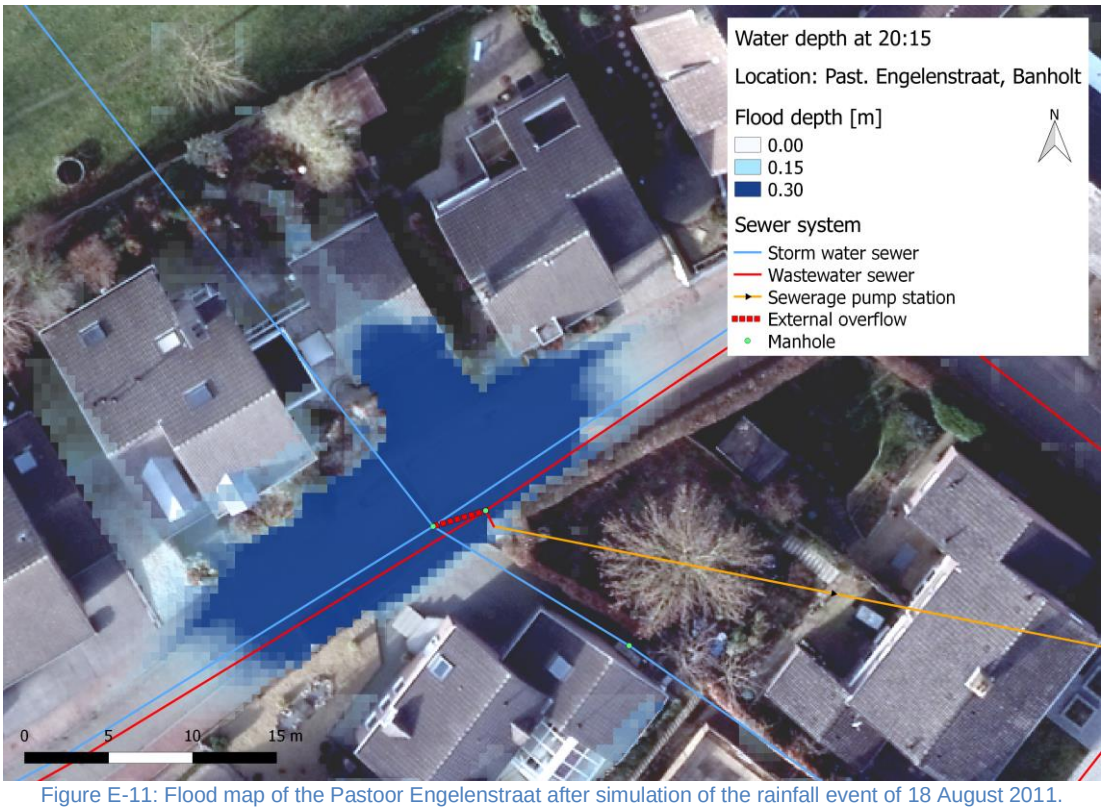

Figure E-11: Flood map of the Pastoor Engelenstraat after simulation of the rainfall event of 18 August 2011.

Herkenradergrubbe

By observing the photographs of the Herkenradergrubbe (Figure E-12) closely one can see that the water on the street has a different water level than the water in the Banholtergrub stream, both upstream and downstream.

The photograph on the right shows that rainwater flows from the street, into the pit behind the orifice of the upstream water buffer. In the plotted flood map, Figure E-13, this pit is not visible. This can be explained by the assumption that the water level is uniform in one calculation cell. Because the water level is uniform the pit is filled during model simulation.

Figure E-12: Map marking the Herkenradergrubbe flood location and photographs available for validation.

The photographs are taken at 20:30 hours on 18 August 2011. Even though it was dry at that time, in the left photograph upslope, a small amount of runoff is still visible on the road. In the model simulation there is also still a small amount of runoff at this time. The water depth on the street is estimated to be around 15 to 20 centimeters.

The average water depth calculated with the model is about 15 centimeters. Which seems to be correct to a little small. Especially when taking into account that in the model this location only receives runoff from the direction of Mheer and not from the road in the direction of Herkenrade/Sint Geertruid, since this area is excluded from the research area.

In the model simulation the Duivenstraat water storage buffer is full and overflowing. In the right photograph it is visible that there is some water at the surface behind the Duivestraat storage buffer. In comparision with the photograph, the model overestimates the water level in the buffer.

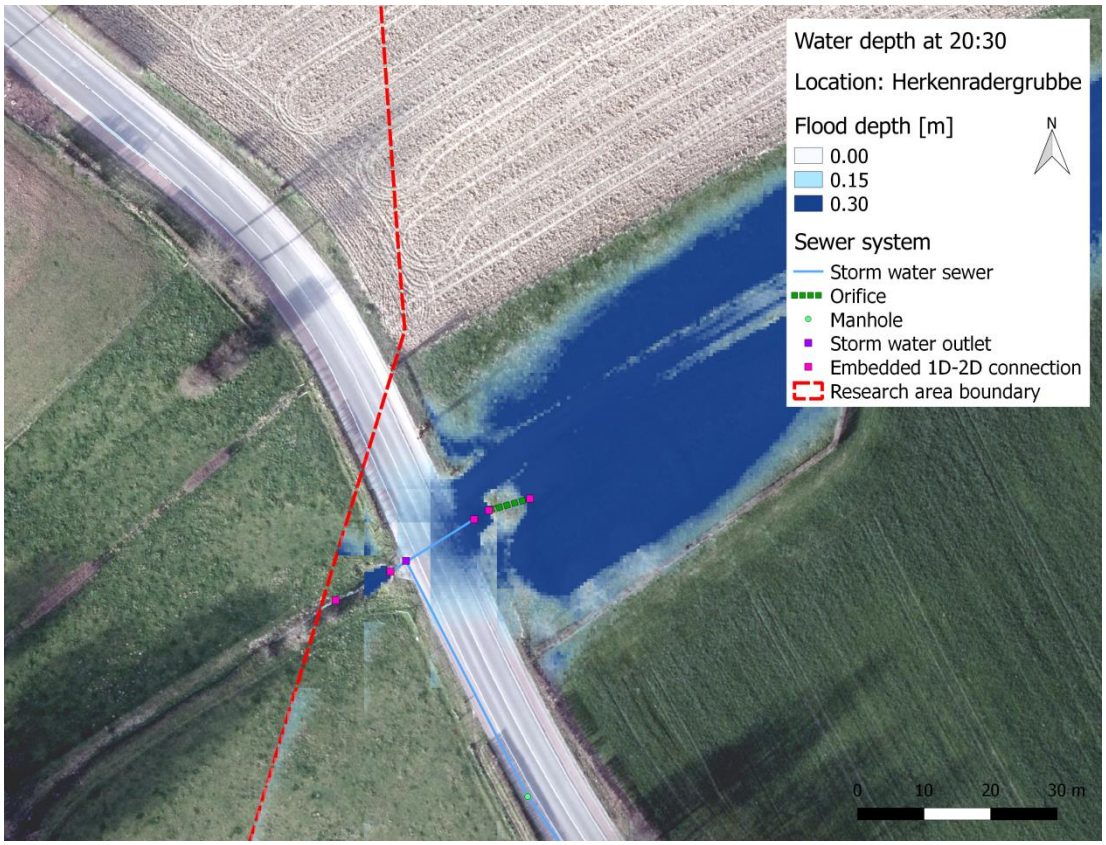

Figure E-13: Flood map of the Herkenradergrubbe after simulation of the rainfall event of 18 August 2011.

Buildings

During model simulation flooding emerged in local depressions near several buildings. Figure E-15 gives an overview of these buildings. Most of these houses have a paved driveway, sloping towards a garage - partly - below surface level (Figure E-14), with the Dorpsstraat 7 and 30 as exceptions. At Dorpsstraat 7 the entrance of the house is located at a local depression compared to street level (Figure E-16). At Dorpsstraat 30 the depression is located in the backyard of the house. These locations are of interest, because they might result in rainwater entering buildings.


Figure E-14: The sloping driveway at the Burgemeester Beckersweg 43, Mheer (Google 2009).

At all the locations there is a sidewalk between the street and the flood location near the houses. Figure E-17 shows the flood map at Michiels Kessenichstraat 13 in Mheer. Here it is visible that there is merely water located adjacent to the house, in a local depression in the DEM. According to the municipality, water problems or flooding are never mentioned by the building owners of these houses. Only the Burgemeerster Beckersweg 55 could experience flooding due to water retention by a speed bump close to this house. Although it is not sure whether actual flooding at this house ever occurred.

3Di overestimates the flood depths adjacent to the buildings significantly due to the V-h relationship it uses for water level calculations. As a result, runoff at the streets is not retrained by the sidewalk, but

placed in the local depressions adjacent to the buildings. In reality only the rainwater that falls directly on the sloping driveways will runoff towards the houses.

Figure E-15: Map showing the locations where flooding occurs in local depressions adjacent to buildings.

Figure E-16: The entrance of Dorpsstraat 7 in Mheer forms a local depression (Google 2009).

Figure E-17: Flood map at the Michiels Kessenichstraat 13, Mheer shows flooding at the sloping driveway.

E.2.2 Rural runoff

There are no rural runoff observations or measurements available in the research area. Yet, the water authority is interested in the simulated rural runoff dynamics. To evaluate the model performance the water levels in the water storage buffers are used to determine whether buffers flow over during simulation of the rainfall event of 18 August 2011.

It is assumed that when the water level in the storage buffer is higher than the retaining heigt of the buffer, overflow occurs (see Table E-2). The water retaining height of the storage buffers is defined based on the DEM subgrid layer and can therefore slightly alter from the heights known by the water authority.

At some buffers the difference between the calculated maximum water level and retaining height is unrealistically large. This can be caused by an alteration in the location of buffer overflow, and thus the determined retaining heigth value, and the location of measuring the water level in the buffer (Figure E-18).

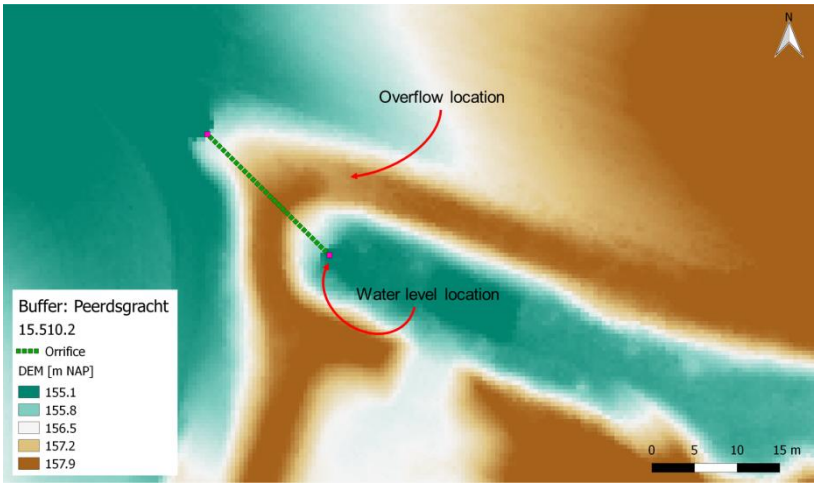

Figure E-18: Different locations of measuring the water level and the retaining height of buffer Peerdsgracht.

Moreover, the overflow durations are determined by estimating how long the water levels in the buffer are higher than the retaining heights (Table E-2).

Based on the results presented in Table E-2, and judgement of these results by the water authority, the model seems to overestimate the amount of buffers with overflow. The water authority does not know whether, and if so, at which buffers overflow occurred. Also, due to the lack of knowledge and data it is not possible to judge the overflow durations in any way.

There are several possible causes for the deviation between the model results and the expectations of the water authority:

- The volumes of the buffers in the model alter from reality. If the storage volume in the model is smaller due to alterations between the bottom level and the water retaining height of the buffer in the DEM layer compared to reality, this can result in unexpected overflow of a buffer.
- A discharge reduction of the orrifice of a buffer, as for example the result at the Herkenradergrubbe flood location can result in an overestimation of the water level in a buffer. At the Herkenradergrubbe flood location the discharge of the buffer reduces during model simulation because the water level in the pit directly behind the orifice rises. This causes a head difference reduction and with that a reduction of the buffer discharge ($\Delta h \sim Q^2$). In reality the head difference is expeted to be larger. If the model underestimates the outflow discharge of a buffer, this can result in an overestimation of water level.
- Finally, the overestimation of the water levels in the buffers can also be caused by the concepts applied in the calculation core of 3Di.

Table E-2: Calculated maximum water levels and overflow durations at the water storage buffers.

Storage buffer	Retaining height [m NAP]	Maximum water level [m NAP]	Overflow [h_{max}>$h_{retaining}$]	Start overflow [hrs]	Overflow duration [hrs]
Duivenstraat	119.95	120.57	yes	19:54	1:36*
Trichterweg Noord	123.25	123.51	yes	20:06	1:00
Trichterweg Zuid	130.85	130.97	yes	20:12	0:24
Het Struikgewas	128.85	130.05	yes	19:48	1:42*
Het Eiland	140.65	140.92	yes	20:06	1:24*
Bergstraat 1	151.30	151.40	yes	20:12	0:06
Bergstraat 2	151.15	151.39	yes	20:12	0:24
Dalestraat 1	156.95	157.14	yes	20:06	0:18
Dalestraat 2	154.05	154.27	yes	20:06	0:24
Hondsrugweg	180.35	179.39	no		
Terlinderstraat	176.75	176.88	yes	20:06	0:24
Grotestraat	170.85	170.98	yes	20:18	1:12
Terlinden 1	177.25	176.62	no		
Terlinden 2	177.20	176.55	no		
Terhorst	160.45	160.65	yes	20:06	1:12
Peerdsgracht 1	158.60	157.62	no		
Peerdsgracht 2	157.60	157.72	yes	**	**
Skischans	140.30	140.63	yes	20:00	1:30
Horstergrub	131.75	132.09	yes	19:54	1:00

* This buffer still flows over at the end of the model simulation. So, the given overflow durations are only until the end of the model simulation.
** The start of overflow and overflow duration of buffer Peerdsgracht 2 could not be determined.

F. Extreme rainfall scenarios

In this research the added value of 3Di model for urban flood analyses in sloping areas is analysed with use of two extreme rainfall scenarios. There are no Dutch standard rainfall scenarios developed for the hydraulic analyses of urban drainage systems during extreme precipitation (RIONED Foundation 2015). Therefore, the rainfall input required for this research is developed in this section.

The following conditions apply to both rainfall scenarios:

- The rainfall scenario must exceed the total of 50 millimetres of rain according to the definition of the KNMI.
- The storm events have a short duration.
- The spatial distribution of rainfall is assumed homogeneous for the whole research area.
- Interception is initially subtracted from the rainfall input scenario before start of the model simulation.
- After the storm event ends, the model will run dry for another hour which is included in the temporal distribution of the storm events.

F.1 Rainfall scenario 1

The total amount of rainfall for this event, is retrieved from the newest statistics of the Foundation for Applied Water Research (STOWA). STOWA makes a distinction between annual, summer and winter amounts of precipitation. Extreme events with a short duration are most likely to occur during the summer months (Lenderink et al. 2011). According to these statistics, a total of 56.8 mm of rain falls during an event with a return period of 100 years (T100) and a duration of 2 hours during the summer months (STOWA 2015, p.58).

So, a total of 56.8 millimetres of rain is selected as the starting point of rainfall scenario 1. Yet, the STOWA statistics do not include a temporal distribution of rainfall events. Therefore, the temporal distribution of the T08 event of RIONED is applied to the total amount of rainfall. The T08 event of RIONED is an event that statistically occurs every 2 years. The duration of this event is 1 hour with a peak intensity at the back of the event (RIONED Foundation 2004).

The temporal distribution of input scenario 1, with a total of 56.8 mm of rain falling in 1 hour and an additional dry hour of simulation time, is shown in Figure 3-5.

F.2 Rainfall scenario 2

As a second rainfall scenario an extreme event, previously used by Nelen & Schuurmans as an extreme scenario for urban flood analyses, is adopted for this research. Nelen & Schuurmans uses this extreme scenario for a so called climate stress test of cities. During a climate stress test, it is analysed how the drainage systems of cities cope with extreme precipitation.

In this scenario 100 millimetres of rain falls in 2 hours. Even though this is an extreme scenario it occurs almost annually somewhere in the Netherlands. The probability of the occurrence of such an event in the research area is approximately once every 100 years.

With an additional dry hour after the two hours of constant rainfall, the temporal distribution of rainfall input scenario 2, with 2 hours of constant rainfall and an additional dry hour, is given Figure 3-6.